THE SPACE-TIME CHARACTERISTICS OF MINIMUM AND MAXIMUM TEMPERATURE VALUES OVER THE TROPICAL EASTERN AFRICA REGION

By Stephen Mutua King'uyu

A thesis submitted in part-fulfillment for the Degree of Master of Science in Meteorology of the University of Nairobi.

August, 1994

DECLARATION.

This thesis is my original work and has not been presented for a degree in any other university.

Signed........................ 19-08-94 ....

STEPHEN MUTUA KING'UYU.

This thesis has been submitted for examination with our approval as University supervisors.

Signed.................................... 29/8/94 ....

PROF. L.A.J. OGALLO.

Signed.................................... 22/8/94 ....

DR. E.K. ANYAMBA.

Department of Meteorology,

University of Nairobi,

P.O. Box 30197,

Nairobi.

TABLE OF CONTENTS

CHAPTER THREE

LIST OF FIGURES

LIST OF TABLES

ABSTRACT

This study examined the space-time characteristics of minimum and maximum temperature values over the Tropical Eastern Africa region in order to delineate any significant changes in the traditional space-time temperature characteristics over the region. The temporal characteristics investigated in the study included the inter-annual patterns of the trend, seasonal and cyclical variations at the individual stations.

Both graphical and statistical methods were used in the trend analysis. In the graphical approach, visual examination of the inter-annual trend was used whilst analysis of variance (ANOVA) and non-parametric methods were used in the statistical approach. The recurrences of low/high inter-annual temperature values were examined using the maximum entropy method (MEM) of spectral analysis.

The last part of the study attempted to provide some insight into the potential causes of the observed inter-annual variability in the temperature characteristics. **El-Niño**/Southern oscillation (ENSO), the Quasi-Biennial Oscillation (QBO), cloudiness, and OLR data were used in the study to quantify the regional/global scale systems that may be associated with the observed temperature characteristics. Relationships between these systems and the observed temperature characteristics were investigated using Simple correlation analysis. χ^2 -tests were used in case of grouped minimum and maximum temperature observations.

The data used in the study was from 53 stations with record lengths of 24 and 53 years. All the data were quality-controlled before they were used in any analysis. Results of the quality-control analysis declared most of the temperature records within Tropical Eastern Africa to be homogeneous as most of the mass curves were linear. Instrumental records world-wide have been affected by changes in instrument types,

changes in observational schedules and methods, and changes in the station environment.

The inter-annual minimum and maximum temperature patterns showed distinct decadal variability signals in the observed minimum and maximum temperature records. The 1980's decade was generally the warmest in record at most of the locations The late 1970's and the early 1990's were also relatively warm periods in most areas. These patterns were however reversed at maritime and lake areas

The warming/cooling observed at some locations in recent years introduced significant linear trends when the records were subjected to trend analysis. The observed minimum and maximum temperature trend patterns however showed a lot of geographical and seasonal variations. Some locations did not indicate any significant trend signals.

Recurrences of extremely high/low values were the commonest feature of the inter-annual variability patterns of the minimum and temperature records. Results of the spectral analysis showed recurrences of extremely high/low temperature values centred around four major spectral peaks namely, 2-2.9 years, 3-4 years, 4.5-6.5 years, and 10-12.5 years. Few spectral peaks also appeared with longer periods of recurrence. The long-period cycles were however not statistically significant at most of the locations.

The 2-2.9 years spectral peak was associated with the QBO whilst the 3-4 and 4.5-6.5 years peaks were associated with the inter-annual variability in ENSO characteristics. The 10-12.5 years cycle was associated with the solar variability cycle. These quasi-periodic oscillations have also been observed in many other Climatic parameters over the region. They however explained a very small proportion of the total inter-annual temperature variation

Results of the Simple correlation analysis indicated that both morning and afternoon cloudiness were negatively correlated with the observed minimum and maximum temperature values and the subsequent temperature range. Maximum temperature values were also found to be significantly correlated with QBO phases. Statistically significant correlations were also found between the minimum and maximum temperature values and the Southern Oscillation Index (SOI), especially for time-lagged temperature values

It may be concluded from this study that the period starting from the 1970's to the early 1990's was relatively warm at a number of locations in the study region. Relative cooling or no temperature change at all was observed at most maritime locations within the same period Large variations were however evident in the space-time characteristics of the warming/cooling trends The observed warming/cooling trends may have been reflective of inter-decadal temperature variability. To determine whether these trends were actually signals of new inter-decadal variability in the minimum and maximum temperature records, the temperature observations of the 1990's will be central Although no comprehensive analysis was carried out to delineate urbanisation effects in the study, preliminary examination showed that a larger scale phenomenon may be responsible for the observed minimum and maximum temperature trends. A more elaborate study will however be required to delineate with certainty the role played by urbanisation in the observed warming/cooling signals

The findings of this study are of utmost importance especially at this time when much political, scientific, and socio-economic attention has been focused on human-induced Climate issues. Temperature is an important parameter in the determination of the space-time distribution of natural resources, and life in general These findings will therefore be useful to planners and managers of food, agriculture, water, socio-economic, and many other natural resources that are Climate-dependent. The findings will complement the current global search for models that can incorporate climate change and variability at the regional and local levels.

CHAPTER ONE

1.0 INTRODUCTION AND LITERATURE REVIEW

This chapter gives the general information on the basic concepts addressed in the thesis. A brief review of some of the relevant literature is also presented in the chapter, together with the major objectives of the study.

1.1 INTRODUCTION

The space-time distribution of global water, food, ecological, and many other natural resources are largely controlled by the space-time distribution of climate. Climatic anomalies and especially the extreme events like droughts, floods, frost occurrence, and other anomalous climate variabilities have therefore been linked to loss of life and property, famine, migrations, and other socio-economic miseries Ecosystems have however been able to adapt to the inter-annual anomalies of the local environment using survival lessons learnt from their ancestors.

Most climatic studies have been based on (i) Instrumental records, (ii) Proxy records which are derived from climate related parameters, and (iii) Climate simulations based on General Circulation Models (GCM's). Most of the available instrumental records generally do not show any significant long-term trends in the mean climate patterns, although recurrences of anomalous climatic events have been common. The space-time characteristics of the recurrence patterns have varied significantly at the global, regional, and local levels. Some of the variability patterns have been presented by the Intergovernmental Panel on Climate Change, IPCC (1990a, 1992a, 1992b) among many others. The IPCC assessment has indicated that an increase of about 0.3-0.6 °C has been observed in the global mean surface temperatures over the last 100 years from instrumental records. The observed temperature patterns have been marked by many geographical and seasonal variations. Such variations have never the less been found to lie within natural climate variability and also to conform with model predictions. The IPCC assessment has also noted that similar or even higher order global temperature increases have also been common from the geological and proxy records of the planet earth

Recent climate records have revealed some unique anomalies in the global surface temperature. These records have shown the 1980's decade to have been the warmest in record, although only slightly warmer than the 1940's. The records have also shown the 1990/91 period to have been the warmest in recent years' record (WMO, 1992b, 1993). Evidence from the available temperature records have shown warming signals in minimum (night-time) temperature over various parts of the world. Such signals have been relatively negligible in the maximum (day-time) temperature series in some locations. The warming tendency has been more pronounced in the middle latitude regions of the Northern hemisphere. Tendency towards higher lower-atmospheric temperatures has also been observed from radiosonde data (IPCC, 1992; Kukla and Karl, 1992a, 1992b; Karl *et al*, 1991; Stouffer *et al*, 1989). Some of the observed patterns are shown **Figure 1**. Volcanic eruptions like that of Mt. Pinatubo in June 1991, coupled with other natural forces, have been associated with the recently observed surface and tropospheric cooling, and stratospheric warming (Christy and McNider, 1994).

Man's impacts on the environment have increased year after year since the 'Industrial age'. Man's degradation of the environment has added a new dimension to the processes which may affect the conditions of the future climate. The recent WMO (1992) release, indicating that Ozone levels over the Antarctica have reached an all time low (30 - 35% lower than pre-Ozone hole levels) is of concern. It is however, still not possible to separate the natural and the human-induced climate components using the current trends of climate variability.

A lot Of scientific and political attention has been given to the human-induced global warming potentials in recent years, culminating in the signing of the 'Vienna Convention' for the protection of the Ozone layer in 1985. The 'Montreal protocol' for the regulation of the industrial use of CFC's and other Ozone depleting substances was signed in 1987 and ratified in 1989 by several countries. Another recent global effort has been the WMO/UNEP coordinated Inter-governmental Panel on Climate Change, IPCC (1990, 1992a, 1992b), a brain child of the United Nations General Assembly. The IPCC is charged with the responsibility of examining the science of global climate, assessing

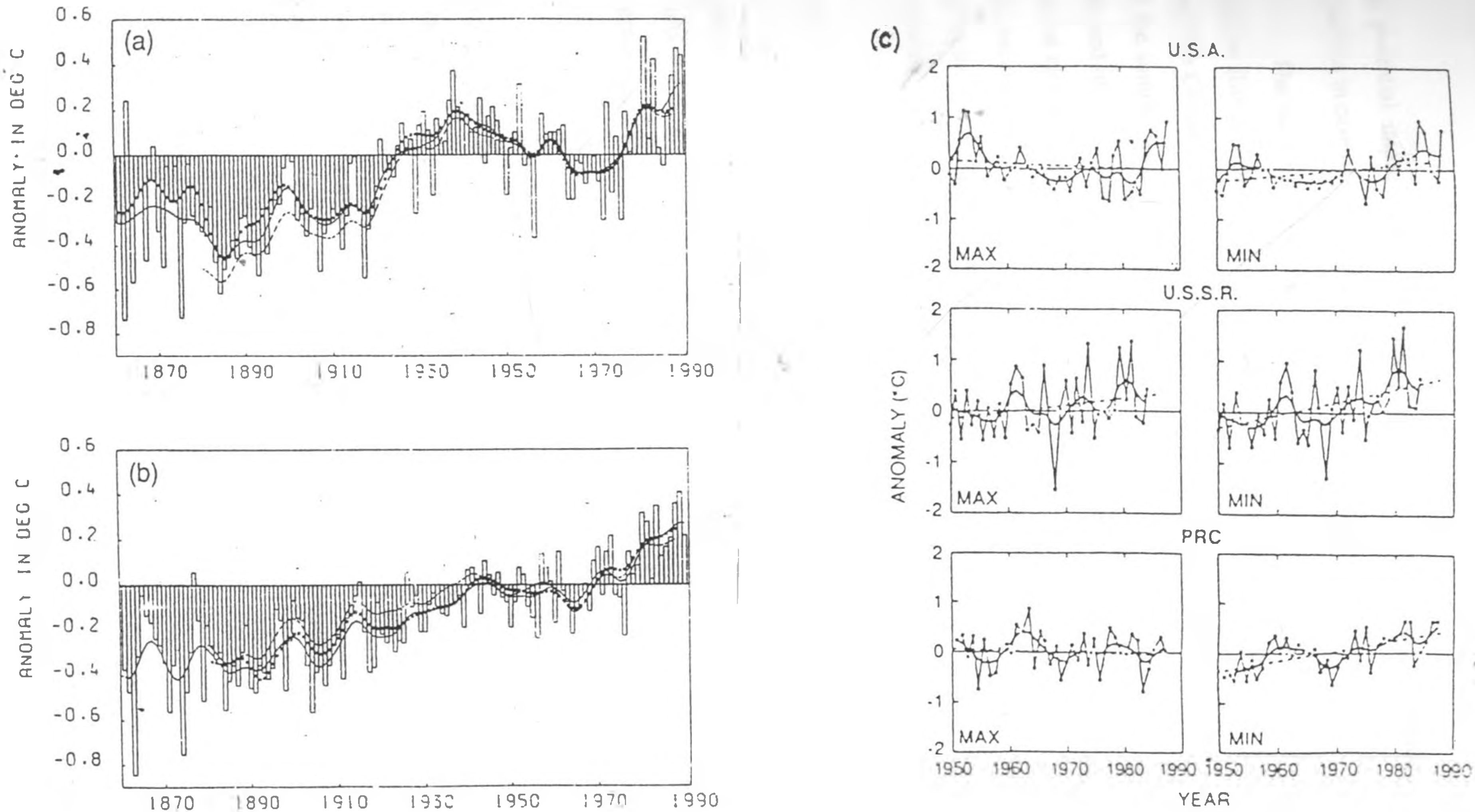

Figure 1: Observed temperature change patterns: (a) Northern hemisphere, (b) Southern hemisphere land-air temperatures expressed as anomalies relative 1951-1980. Annual values from P.D. Jones - smoothed curves; P.D. Jones 1861-1989 values - solid lines; Hansen and Lebedeff 1880-1987 values - dashed lines; Vinnikov *et al* - dotted; adopted from IPCC (1992a); (c) Variations of mean annual maximum and minimum temperature since 1951: Adopted from Kukla and Karl (1992).

the potential impacts of any climate change, and formulation of mitigation policy strategies in case of climate change.

The most historic global Climate policy forum was the 'Earth Summit' of June 1992 in Rio de Jeneiro, which was attended by over 100 Heads of states and at which both the Climate and Bio-diversity conventions were adopted. Another recommendation at the summit was the preparation of a desertification convention to be ready towards the end of 1994 The IPCC was also mandated to continuously review the status of the global climate. The next IPCC report is expected to be out towards the end of 1995. All the recommendations of the 'Earth Summit' are summed up in the 'Agenda 21' which gives the action plans and programmes for sustainable use of the environment and socio-economic development into the next century

The general concepts of climate change are still masked by several uncertainties which include the role of sulphate aerosols, the role of clouds, Ozone, and other atmospheric pollutants, together with the complex nature of atmospheric chemistry and feedback processes Due to the long residence periods of some of the gases introduced into the atmosphere by man's activities, there has also been some fear that the atmospheric forcings may trigger off larger anthropogenic greenhouse warming which is not likely to be detected for a decade or more (IPCC, 1992).

This study will investigate the space-time patterns of the minimum and maximum temperature values which have been observed over Tropical Eastern Africa in order to delineate any significant changes in the traditional space-time temperature characteristics over the region The potential causes of any observed temperature trends will also be examined in the study Details of the objectives will be presented in section 1.3. A brief literature review of some of the relevant work is presented in the next section.

1.2 LITERATURE REVIEW

There has been a number of studies on the space-time characteristics of various meteorological parameters. Amongst the oldest in record are studies on the space-time characteristics of global temperature and precipitation data. Callander (1938) found a slight increasing trend in the temperature series fore some 200 global stations. He associated this with increased anthropogenic carbon-dioxide production. In a later study using data for 400 global meteorological stations, Callander (1961), found a rising trend in temperature from the Arctic to 45° S. The trend was however quite small in most regions equator-ward of 35° N, and not quite apparent in some.

Landsberg (1959) found periodicities of 1.8-2.7 years, and greater than 50 years in the temperature series for Woodstock college, Maryland, for the period 1870 onwards. The 11 year sunspot cycle and its second harmonic (5.6 years) were discernible in the temperature series at the 99.9% and 95% confidence levels respectively under the 'null white noise' spectrum hypothesis.

Polowchak (1968) defined a "rhythm" index which quantitatively characterised the temperature rhythm variations in various North American regions using the daily temperature series for some 17 North American stations.

Joseph (1973a) found the auto-correlation coefficient for most of the annual mean, minimum, and maximum temperature series for five American stations to be significant. A study of the daily minimum and maximum temperature series on the East slope of Colorado Front Range revealed strong annual oscillations and high correlations between different spatially separated stations (Joseph, 1973b).

Three different studies (Jones, 1986, Hansen and Lebedeff, 1987, 1988; Vinnikov *et al*, 1987, 1990) have shown globally averaged land temperatures for the last decade to have been the highest in the past 100-140 years. Inter-decadal and geographical variations are however common, with some locations showing cooling or no significant temperature change during some decades. Inter-hemispheric variations in the temperature patterns have also been observed. Temperature changes in the northern hemisphere have for example been found to be abrupt and irregular over land. The early 1920's are shown to have warmed by about 0.3°C. Generally, however, the land surface temperatures are found to have oscillated about a stationary mean trend through out most of the 19th and early 20th centuries A steady increase in temperature is seen to have occurred just before 1970.

Karl *et al* (1988) detected urban effects for towns with small populations of about 10,000 people using temperature records from 1219 stations across the United States of America (U S A.) for the period 1901-1984. They found that urbanisation decreases the daily maximum temperature in all seasons except winter and the temperature range in all seasons, whilst increasing the diurnal minima and the daily means in all seasons In a related study, Karl *et al* (1991) found no significant increase in the mean maximum temperature series for the U S., the U S S R , and the People's Republic of China as opposed to significant trends in the mean minimum temperature series. They concluded that climate models may have underestimated increases in the minimum temperature relative to those of the maximum temperature and that other factors (in addition to greenhouse warming) may have contributed to the warming in the N.H. land-mass Their results were confirmed by those of Kukla and Karl (1992a, 1992b).

Global rainfall characteristics have too been the subject of various studies. Winstanley (1973) predicted a decrease to a minimum in global rainfall around 2030 A D using data for Africa, the Middle East, and India Parthasarathy (1973) found significant cycles of 8 5-12.0 years in arid and semi-arid regions and 2.0-3.5 years over the majority of the Indian subcontinent from the rainfall series of 31 meteorological stations whilst Jagannathan (1973) found Indian monsoon rainfall to be related to sunspot cycle oscillations No significant trends have been observed in the all Indian rainfall records from recent studies (Sontakke *et al,* 1993; Pant *et al,* 1993).

Various studies have used climate models to examine the potential impacts of any climate change on the physical environment Climate model results have shown that the mean global temperatures are likely to rise by 1.5-4.5°C by the year 2030, if man continues with business as usual in the degradation of the environment. Around this time, the atmospheric concentrations of the greenhouse gases are expected to have an equal effect to that of a doubling of the current carbon-dioxide atmospheric levels (UNEP, 1987, IPCC, 1992). The magnitude, onset, duration, and rate of change, are likely to be different at regional and local levels. Some locations may even cool down or experience no change at all (IPCC, 1992).

Some recent studies have observed that Micro-wave Sounding Unit (MSU) records provide the best estimate of the mean global temperature in view of their spatial coverage and accuracy (Christy and McNider, 1994). Gordon (1994) observed that human-induced warming signals can be delineated from MSU temperature records even for very short time scales. Using the daily MSU temperature records for the period 1979-1993, he observed a weekly temperature warming anomaly peak at the mid-week in the Northern hemisphere He also found a slight decreasing trend in the mean global temperature in recent years, attributable to the Mt Pinatubo volcanic eruption. After removing the effects of ENSO and volcanic eruptions however, Christy and McNider (1994) found a positive trend in the mean global temperature records. MSU techniques have also been used to provide a global coverage of ocean precipitation estimates (Spencer, 1993).

Any changes in the space-time characteristics of the global climate will have severe impacts on the space-time weather variability and the characteristics of extreme climate events like the frequency of intense rainfall, frost occurrence, ENSO events, floods, droughts, strong winds, thunderstorms/lighting, and strong ocean currents. Some synoptic phenomena like tropical cyclones, their frequency of occurrence, and their tracks may also change (Simpson and Riehl, 1951; Anthes, 1982; Glantz, 1992; IPCC, 1990, 1992).

Spatial coverage of polar ice and mountain glacier may also be reduced through melting. IPCC (1990a, 1990b, 1992a, 1992b) has observed that this melting, coupled with thermal expansion of sea water may lead to a sea-level rise of about 20±10 cm by the year 2030 Changes in the traditional patterns of the natural climate variability could also accentuate those of large-scale natural events like droughts, floods, cyclones, and other weather related calamities Arid and semi-arid regions and humid areas where water demand and pollution have led to water scarcity will experience the greatest impacts on hydrological and water resources (IPCC, 1990a, 1990b, 1992a, 1992b).

Special attention has also been given to the unique vulnerability of the coastal areas, river valleys, and small islands, to any sea-level rise. Most of the world's populations are concentrated in these areas. It is in these areas therefore, that human settlement patterns would be most affected by sea-level rise and climate related calamities Any changes in the climate variability will therefore have far-reaching ecological and socio-economic implications Details of these may be found in IPCC (1990b) and many other references.

Some of the weaknesses of the current information on climate variability and change include:

(i) Poor understanding of the global climate system and the complex interactions between the various forces that control climate

(ii) Inability of the existing models to represent the coupled regional/local climate systems, especially over the tropics, where weather is controlled by mainly small-scale, and non-linear systems that change rapidly (IPCC, 1990, 1992; Alusa and Allen, 1991).

(iii) Poor space-time distribution of climatological data that may be used to detect the climate change signals, attributable to an equally poor and sparse observational network, especially over tropical areas Causes of the poor temporal distribution of data are that many stations have very short climatological records whilst others have many data gaps and other discontinuities, the latter due to changes in instrument types (Parker, 1990), changes in observational schedules and methods (Karl *et al*, 1986; Parker, 1990), and relocation of station sites and other changes in the station environment (Okoola, 1979; Salinger, 1981; Jones, 1986a, 1986b).

(iv) Poor understanding of the adaptive capability of the ecosystems and other natural systems to any climate change.

(v) Poor understanding of the total earth system involving the atmosphere, land, ocean, and the biosphere

(vi) Unavailability of climate change scenarios at the regional and local levels.

(vii) Consistency of the statistical methods that have been adopted for use in various analyses has been questioned by some authors (Basset, 1992; Solow and Broadus, 1989). Recent studies have observed that changes in the inter-annual climate variability are more important than changes in the mean climate (Katz and Brown, 1992; Tarleton and Katz, 1993).

A lot of studies have also examined the temporal characteristics of rainfall over Africa. No significant trends have been discerned from most of the studies. Oscillations with periods of 2.0-2.5 years, 3.0-3.7 years, 4.0-6.0 years, 10-12.5 years, and 16-20 years, have however, been found in most of the studies (Tyson *et al*, 1975; Ogallo, 1977). Wood and Lovett (1974) found the rainfall series for Addis-Ababa to be related to the sunspot number for Zurich. The former led the latter by some 1.3 years. The effect of solar activity on rainfall over South Africa is believed to be modulated by the QBO (Tyson, 1993). There is also evidence of an oscillation in sea surface temperatures in the Indian ocean similar to the QBO.

The prolonged Sahelian drought of 1968-1973 has also been the subject of various studies (Bunting, 1975; Druyan, 1988; Semazzi *et al*, 1988; Wolter, 1989; Nicholson, 1989; Folland *et al*, 1986; Drought, 1993; WMO, 1993). This drought, although more severe and persistent than any other in the history of the Sahel, has been found to lie within expected climate variability and may occur 3-4 times each century. The drought, coupled with ENSO events, overgrazing, and other human-induced degradation of the environment, have been blamed for the expansion of desert-like conditions over the Sahel and the Eastern Africa region (Drought, 1993; WMO, 1993). The normalised precipitation anomalies for the Sahel, the U.S.S.R., East Africa, and the All India monsoon are shown in **Figure 2**. Results of the Tropical Oceans and Global Atmosphere (TOGA) Coupled Ocean-Atmosphere Response Experiment (COARSE), under way in warm pool of the Pacific, are expected to lead to the development of the theory which will help clarify aspects of ENSO not fully understood previously. This will be a big step in the long-term forecasting of the global (and in particular tropical) climate variability. There is however, need for the understanding of an observed, although weak, north-south oscillation in the global atmospheric circulation (Morel, 1993; Moura, 1993).

Various studies have examined the space-time characteristics of rainfall over Eastern Africa (Masaya, 1975; Rodhe and Virji, 1976; Ogallo, 1980, 1983; Ogallo and Aliba, 1994; Nyenzi, 1988, 1992). No significant trends have been found in the rainfall series apart from a slight increasing trend over the dry belt (Rodhe and Virji, 1976; Ogallo, 1980). Cycles with periods centred at 2.0-2.5, 3.0-3.7, 4.8-6.0, and 10.0-12.5 years have been found in most of the rainfall series. No evidence of any significant shift

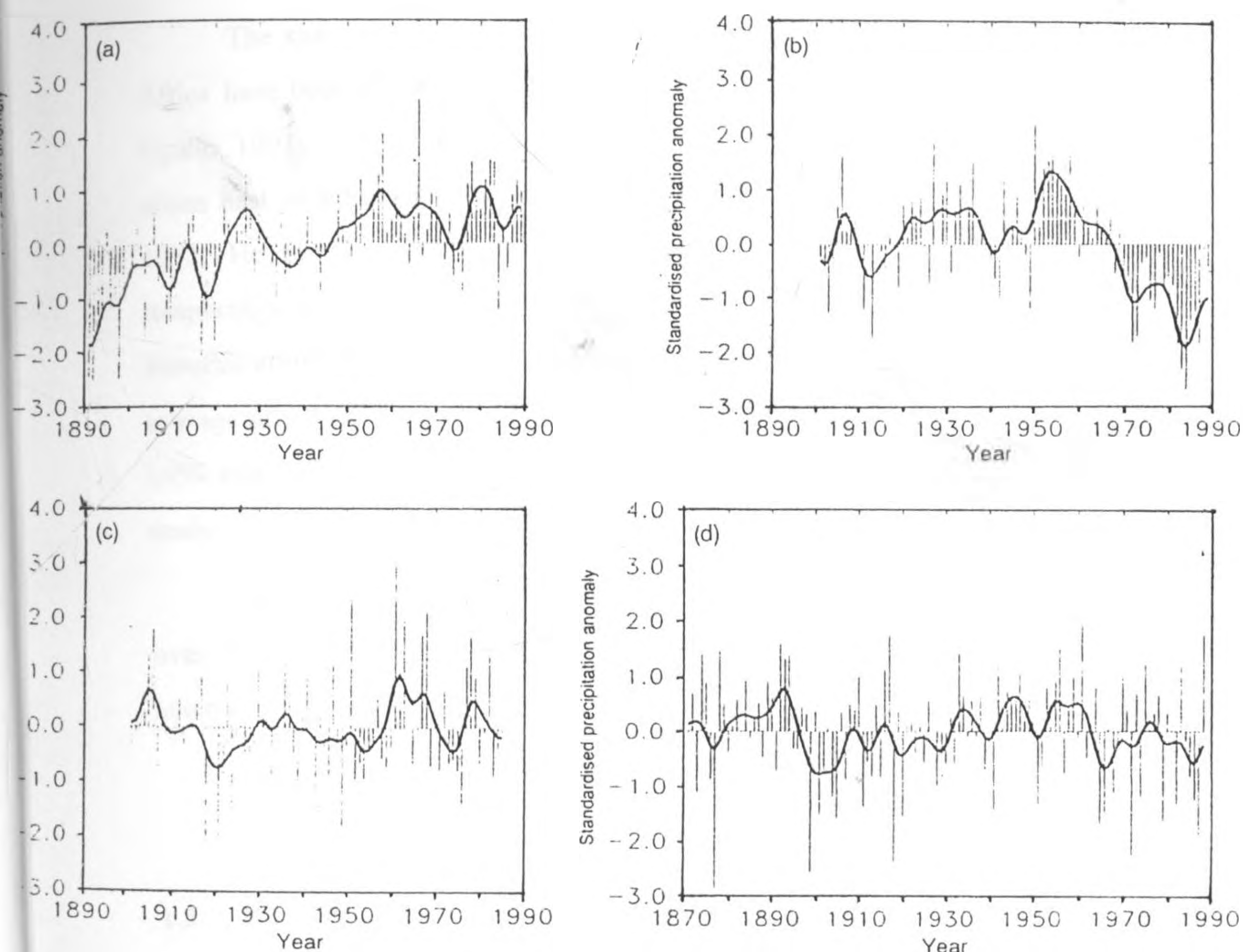

Figure 2: Standardised regional precipitation anomalies: (a) USSR, (b) Sahel, (c) East Africa, (d) All - India monsoon. Adopted from IPCC (1990a)

in the seasonal rainfall patterns has been found based on the amplitude and phase angle at the 95% confidence level (Ogallo, 1983).

A study of the past and present history of the Lewis glacier on Mt. Kenya and other mountain glaciers over tropical Eastern Africa has revealed a general recession of mountain glaciers over the tropics (Hastenrath, 1983). This recession has been attributed to a drastic precipitation decrease over the last two decades of the 19th century, although the general circulation causes are obscure

The space-time characteristics of temperature and the zonal wind over eastern Africa have been the subject of various studies (Okoola, 1979; Kinuthia *et al,* 1991; Ogallo, 1993a, 1993b,). Okoola (1979) examined the temporal behaviour of the Nairobi urban heat island using time series of extreme temperature data for the period 1969-1977 He found a strong seasonal component for both minimum and maximum temperature series and a slight increasing trend in the city heat island On the other hand, Kinuthia *et al* (1991) found surface air temperatures over Kenya to have increased by an average of 0.45°C between 1965 and 1973 compared to a decrease of 0.35°C between 1959 and 1964 No urbanisation effects were removed from the records used in their study.

Ogallo (1993a, 1993b) found that most of the extreme temperature anomalies over Eastern Africa can be explained in terms of ENSO and other Climate system anomalies

The following section highlights the importance of the current study.

1.2.1 JUSTIFICATION OF THE STUDY

Most of the studies that have been carried out on Climate change and variability have been rather global in nature Very little of such work been carried out within the Tropical Eastern Africa region

Temperature is an important parameter in the determination of the space-time distribution of natural and other Climate-dependent resources. The present study is therefore devoted to the space-time characteristics of minimum and maximum temperatures over tropical Eastern Africa. Details of the objectives are presented in the following section.

1.3 OBJECTIVES OF THE STUDY

The objectives of this study are:-

(i) To examine the space-time characteristics of minimum and maximum temperature records over the tropical Eastern Africa region in order to determine any regional surface warming/cooling signals

(ii) To delineate the global/regional climate systems that may be associated with any observed extreme temperature variability. This involves the examination of any association between the observed space-time extreme temperature anomalies and the synoptic/regional climate trends as reflected in the rainfall, cloudiness, QBO, and ENSO. A description of the area of study follows in the next section.

1.4 DESCRIPTION OF THE AREA OF STUDY

The term tropical Eastern Africa will be used here to imply East, Central, and Southern Africa. The countries which were used in this study are Angola, Botswana, Burundi, Comoros, Djibouti, Ethiopia, Kenya, Lesotho, Malagasy, Malawi, Mauritius, Mozambique, Rwanda, Seychelles, Somalia, Sudan, Swaziland, Tanzania, Uganda, Zambia, and Zimbabwe (**Figure 3**). A brief description of the climate of the region is presented below.

1.4.1 THE CLIMATE OF TROPICAL AFRICA

Unlike the higher latitudes, whose climate patterns are marked by high seasonal variability of temperature and other climatic parameters, the climatic parameter with the highest variability in the tropics is rainfall. The subtropical high pressure cells generally separate the higher latitude climate conditions from those of the tropical zone.

Within the tropical zone, seasonal temperature changes are relatively small due to insignificant seasonal changes in the solar radiation. It is for this reason that tropical climatology is often described in terms of seasonal rainfall variation than with temperature. Temperature however, becomes an important parameter over the highlands and as one moves towards the tropics from the Equator. The range between the temperature of the warmest and the coldest months is about 10°C close to the subtropical belt.

The climates of Eastern Africa are controlled by various synoptic features which are briefly discussed in the following subsections. These include the Inter-Tropical Convergence Zone (I.T.C.Z.), monsoon winds and ocean currents, jet-streams, easterly waves, tropical cyclones, the sub-tropical anticyclones, and teleconnections

1.4.1.1 THE INTER-TROPICAL CONVERGENCE ZONE (I.T.C.Z.)

The ITCZ is a zone characterised by low and medium level convergence and upper level divergence. It is therefore marked by severe thunderstorms and showers over most areas. Generally, air-streams from the northern and southern hemispheres converge here, but over Africa, this generality is broken, as the ITCZ breaks into two

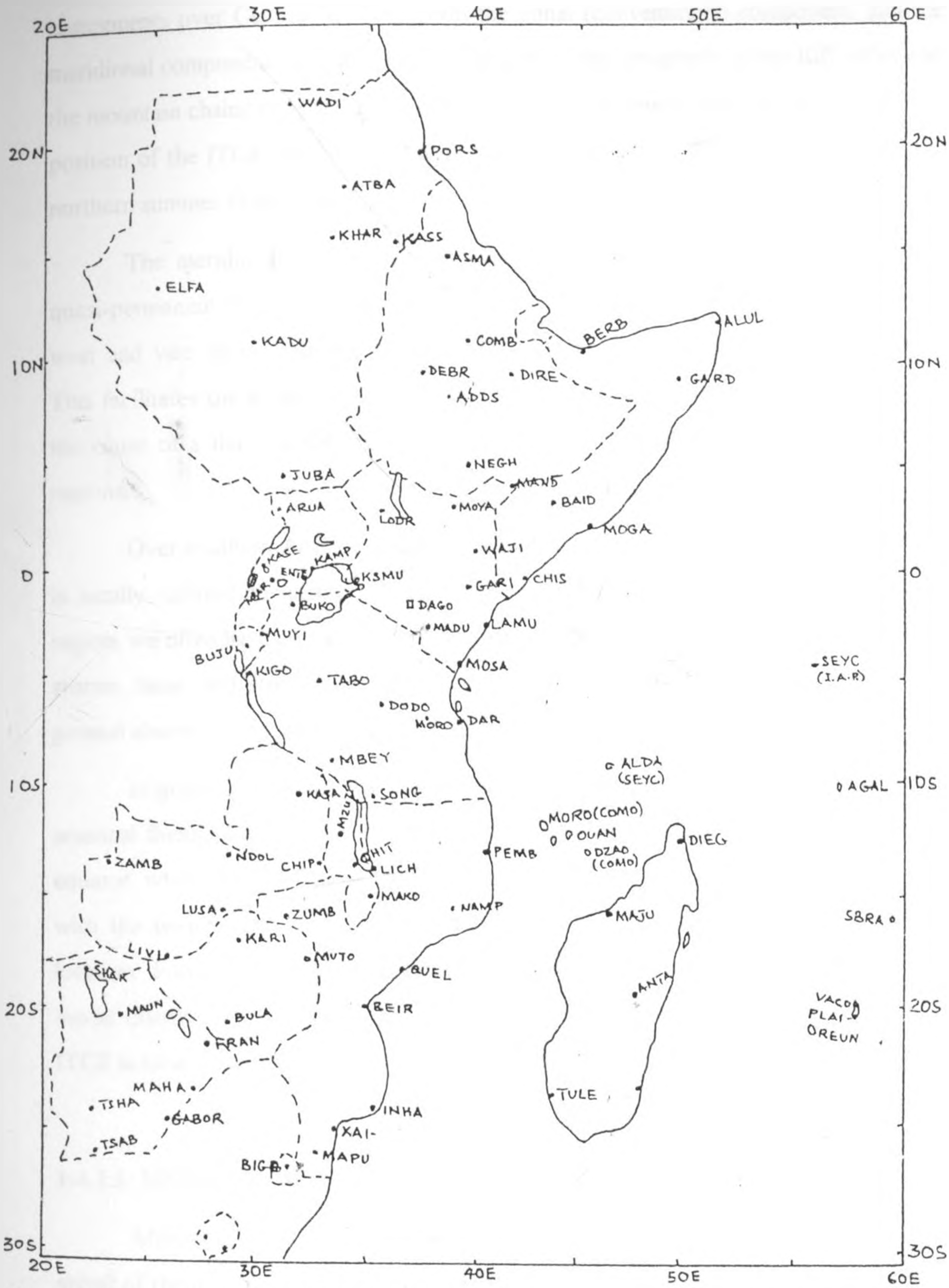

Figure 3: Map of the study area and data network

components over Central Africa to form the zonal (conventional) component, and the meridional component. This division is attributed to the geography of the Rift valley and the mountain chains of East Africa. **Figure 4** shows the mean pressure patterns and the position of the ITCZ over Africa during the northern winter (January) season, and the northern summer (July) season.

The meridional arm has a north-south orientation and can be observed as a quasi-permanent low over the central African region. This arm fluctuates from east to west and vice versa, with the most eastern/northern extent occurring in July-August. This facilitates the penetration of westerly winds more eastward, and is believed to be the cause of a third rainfall peak observed in parts of Uganda and the neighbouring regions

Over southern Africa exists large-scale hemispheric air-mass convergence which is locally referred to as the Congo Air Boundary (CAB). Over the Kalahari desert region, we often have convergence of hemispheric winds which are associated with dust-storms, haze, and strong turbulence, imposing severe aviation problems. Due to the general absence of moisture, the ITCZ in this region is often called the "dry line".

In general, the zonal arm fluctuates north and south with the over-head sun. The seasonal fluctuation generally delineates the regional seasonal characteristics. Near the equator, where the ITCZ passes twice each year, we have a bi-modal rainfall distribution with the two rainfall peaks associated with the seasonal passage of ITCZ over the location. Further away from the Equator, we have only one rainfall season, i.e. uni-modal distribution, with peak rainfall during the hemispheric summer season when the ITCZ is located over the respective hemisphere

1.4.1.2 MONSOON WINDS AND OCEAN CURRENTS

Monsoon winds and ocean currents provide the mode of moisture transfer. The speed of the monsoon winds determines how far they will penetrate inland, whilst their direction determines whether they will be moisture laden or dry. The north easterly monsoon current attains maximum intensity in January. Over northern Kenya, the current breaks into two, one branch flowing west-wards into the interior of Africa, and

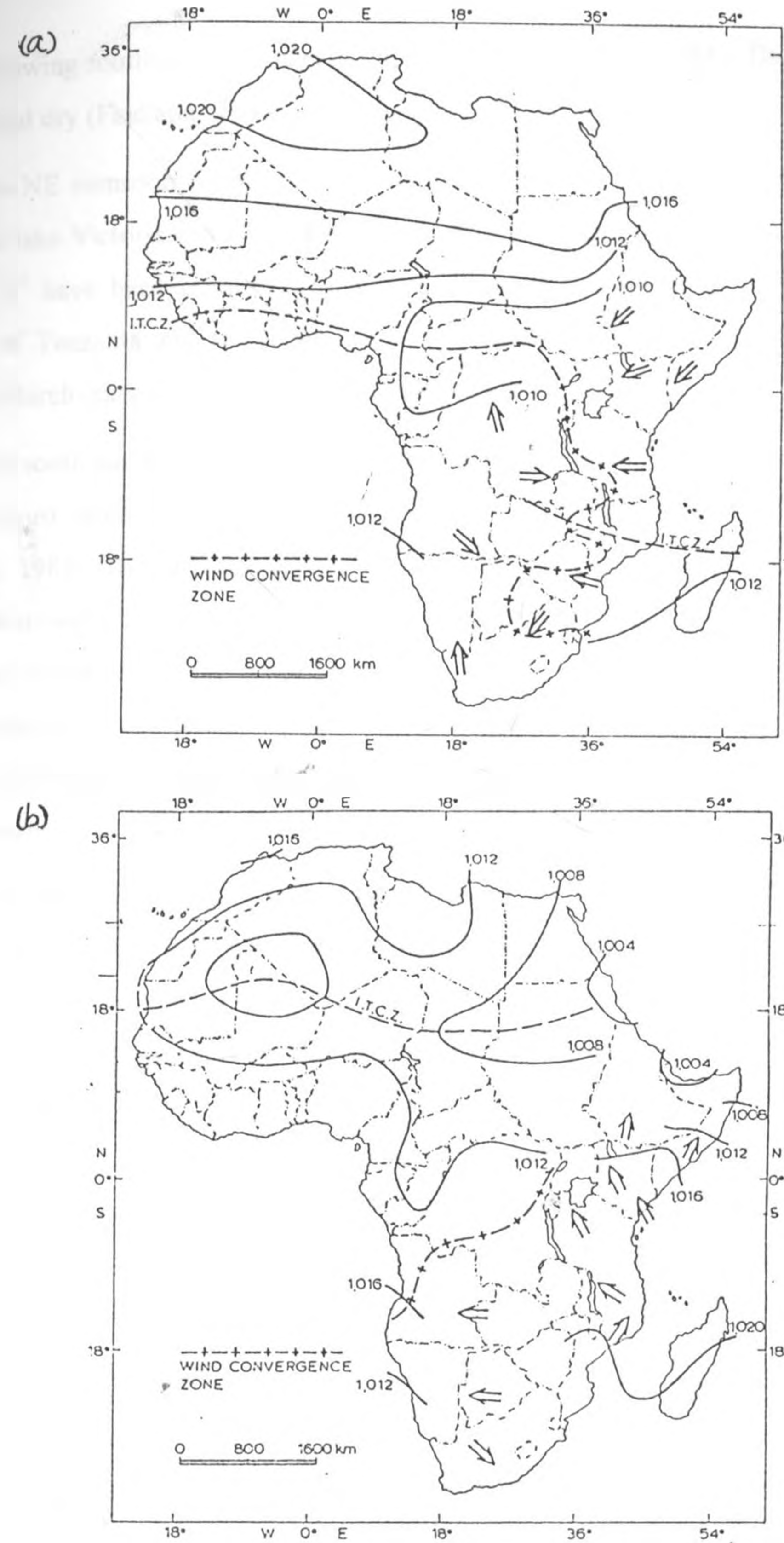

Figure 4: Mean pressure patterns over Africa showing the position of the I.T.C.Z. during: (a) Northern hemispheric winter, January; (b) Northern hemispheric summer, July. Adopted from Griffiths (1972)

the other flowing south-wards parallel to the coast line (Anyamba, 1983). This current is often hot and dry (Findlater, 1968)

The NE monsoon current is highly diffluent over most of eastern Africa, except around the lake Victoria and Uganda regions, where maximum convergence values of $1 \times 10^{-5}\ S^{-1}$ have been observed Maximum divergence is observed in the eastern lowlands of Tanzania and Kenya in February (Anyamba, 1983) The retreat of this current in March marks the start of the long rainy season

The south easterly/south westerly monsoon current attains its maximum intensity in July-August season with peak wind speeds of 13.5 mS^{-1} at the 850 mb level (Anyamba, 1983) The current branches into two over coastal Tanzania with one branch flowing west-wards between the Hanang-Ngorongoro mountains to the north, and the Kapengere mountains to the south (Anyamba, 1983). Anyamba (1983) observed yet another branching over northern Kenya, where one branch flows in a south easterly to easterly direction into Uganda and southern Sudan. The other branch becomes a south westerly current flowing over north eastern Kenya and Somali.

Anyamba (1983) observed that the SE/SW monsoon current influences weather over East Africa for a longer period than the NE monsoons It is also more intense, albeit being shallower, extending to only 3 km above mean sea level This current is diffluent over the eastern lowlands of East Africa Elsewhere, it is confluent at low levels, and diffluent aloft It is the cause of cyclonic flow associated with weather over western Kenya and Uganda in July-August Anyamba (1983) also observed an anticyclonic diffluent flow over the eastern Kenya highlands during the SE/SW monsoon season The retreat of the SE/SW monsoons in September marks the start of the short rainy season **Figure 5** shows the mean wind field over East Africa during the months of May, June, July, and August

The major regional ocean currents include the Mozambique, Benguela, Somali, and Canary The Mozambique current is warm, and flows from NE to SW, with maximum strength during the southern hemispheric summer season, due to the influence of the North-easterly monsoon winds This current helps reduce the diurnal and annual temperature ranges around the eastern coast of southern Africa and keeps the diurnal

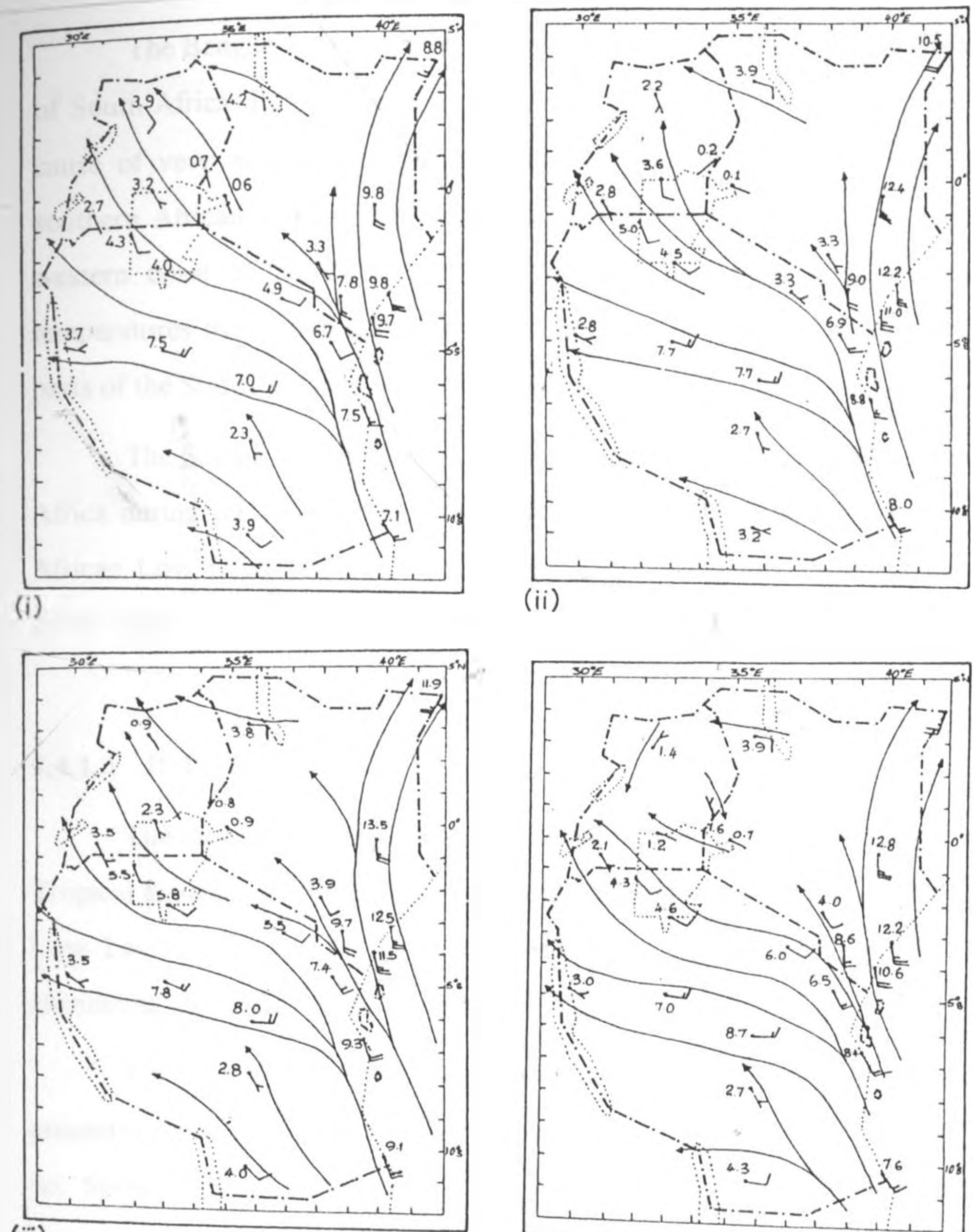

Figure 5: Mean wind field over East Africa in (i) May, (ii) June, (iii) July, and (iv) August at 1.5 km a.m.s.l. Adopted from Anyamba and Kiangi (1985)

temperature maxima high (Griffiths, 1972). It is known as the Agulhas current south of Lourenco-Marques

The Benguela cold current flows from the Atlantic ocean along the western coast of South Africa Its effect and that of the Mozambique current are thought to be the cause of very high surface temperature anomalies (+8°C) over broad areas of the southern African interior (Griffiths, 1972) The Canary cold current blows along the western coast of North Africa. It is believed to be cause of decreased summer temperatures over some north African countries and increased cloud cover over some parts of the Sudan in January (Griffiths, 1972)

The Somali current flows along the eastern coast of East Africa and the Horn of Africa during the northern summer season This is also the peak season of the East African Low Level Jet, EALLJ (Bunker, 1965, Findlater, 1969; Krishnamurti *et al*, 1976; Ngara, 1977)

1.4.1.3 JET STREAMS

The major jet streams over tropical Africa are the African Easterly Jet (AEJ), the Tropical Easterly Jet (TEJ), the Sub-Tropical Jet streams (STJ's), and the East African Low Level Jet (EALLJ). There are also other smaller scale jets due to mountain channeling, like the Marsabit/Turkana jet (Kinuthia, 1991)

The AEJ is a mid-tropospheric northern summer feature, whose jet-core is found around the 650 mb level Maximum intensities are July. It is also called the West African Jet Strong cyclonic wind shears to the south of the jet core have been associated with Easterly waves, that propagate westward into the Atlantic ocean. Their formation is due to the combined barotropic/baroclinic instabilities due to the presence of the jet.

The TEJ over Africa is an extension of the Indian TEJ during the northern summer season Maximum intensity is attained in July and August, and with the jet core being found between 200 mb and 100 mb levels It is thus an upper tropospheric feature, with core speeds of 35 mS^{-1} Maximum intensities are found between 9-15°N, and the jet core is found to be very steady in its direction, which is strictly easterly (Okoola, 1983).

The EALLJ is a lower tropospheric jet stream, observed during the northern summer season Details of its observational and other aspects have been given by Bunker (1965), Findlater (1966, 1977, 1978), Krishnamurti *et al* (1976), Ngara (1977), and Anyamba and Kiangi (1985) The EALLJ is embedded in the SE/SW monsoon currents, with the jet core being found around 1.5 km above mean sea level Core speeds of 13 mS^{-1} in July and August are common (Ngara, 1977)

The EALLJ is found to be very steady in direction, maintaining a SE/SW flow south and north of the equator respectively. It is found to be most intense at night and the early morning, getting rather diluted in the afternoon due to the action of thermal eddies redistributing energy within the jet The highlands of Eastern Africa and Malagasy are thought to play an important role in the evolution of the jet, confining it to a narrow zone.

This jet is unique as it is the only known cross-equatorial jet. All others are zonal and confined to one hemisphere. It therefore plays an important role in the transfer of mass and momentum from the southern to the northern hemispheres It is found to transport almost half of the total mass transported across the Equator from the southern to the northern hemisphere (Cadet and Reverdin, 1981).

The Turkana jet in the Turkana channel of Kenya is formed due to the channeling of winds between the Ethiopian highlands and the mountain chains of East Africa. The vortices generated by this jet are thought to contribute to the development of easterly waves and to affect the easterly mid-tropospheric African Easterly Jet in West Africa (Kinuthia, 1991)

1.4.1.4 EASTERLY WAVES

Easterly waves are not well documented over Eastern Africa and the Indian ocean, mainly due to their feeble nature. This makes them not easily discernible on synoptic charts, a problem also aggravated by scarcity of data over the region Mention of westward moving wave-like disturbances was first done during the world war II (Forsdyke, 1960) Zangvil (1975) also found westward moving waves over the Indian ocean between latitudes 5-15° both north and south of the Equator These had a period of 5 days.

Cadet and Olory-Togbe (1977) observed weak Easterly disturbances south of the equator and westerly ones north of the equator over the Indian ocean Other reports of westward propagating waves over the eastern Africa region include Thomson (1957), Gichuiya (1970), Fremming (1970), and Njau (1982). Njau (1982) presented evidence that Easterly waves penetrate even as far inland as Nairobi and Entebbe

The observed general characteristics of these waves include a period of 3.5-7 days, a wavelength of 2000-2500 km, and a phase speed of 7-9 mS^{-1} Deep cumulus convection and heavy rains and/or showers accompany them Their axes are either vertical or slightly tilted to the west Maximum wind speeds are found at about the 550 mb level

Similar wave disturbances have also been observed over central and west Africa These have been detected from the highland region around Khartoum and Ft Lamy, 15°E (Burpee, 1972, 1974) They have periods of 3-5 days, a mean wavelength of about 2000 km, and maximum wind speeds of 1-2 mS^{-1}, near the 700 mb level Their formation is due to baroclinic/barotropic instability in the neighbourhood of the mid-tropospheric African Easterly Jet (AEJ) and latent heat release by convective systems organised by the waves (Norquist *et al*, 1977) They have been associated with the development of tropical cyclones over the Atlantic ocean (Burpee, 1972, 1974).

Westerly wave-disturbances, which produce rainy weather, are also known to exist over the Eastern Africa region Details of these waves are found in Johnson and Morth (1960), Nakamura (1967), Cadet and Olory-Togbe (1977), and Njau (1982)

1.4.1.5 TROPICAL CYCLONES

These are vortices with a closed circulation which develop from the shallower tropical depressions Due to the extremely low pressures at the 'eye' of the cyclone, cyclones may decrease weather or increase it over a region, depending on their relative position by interfering with the normal flow of winds If they hit the coast, or sometimes just approach it, they may cause wanton destruction of structures and loss of life This is due to the intense showers and thunderstorms associated with tropical cyclones, flooding of coastal lowlands, and the high winds that accompany them

East Africa is usually not directly hit by tropical cyclones although their approach plays to regulate weather over this region The most prone region to cyclone attack over Eastern Africa is the eastern coast of southern Africa, and the neighbouring Indian ocean islands

1.4.1.6 THE SUBTROPICAL ANTICYCLONES

The anticyclones that affect weather over Eastern Africa are the Azores to the north-west of Africa, the Arabian over the Arabian subcontinent, the St Hellena in the southern Atlantic, and the Mascarene in the southern Indian ocean Depending on their relative locations. strength and spatial orientation, anticyclones will either pump in moist air or dry air, or even cause mass diffluence if they are directly over a region

The Azores anticyclone is more prominent during northern hemispheric winter (January) and is the cause of subsidence and heated desiccated air over the Sahara and neighbouring regions Prominent during the same season is the Arabian anticyclone, which is the cause of dry continental north-easterly flow over most of Eastern Africa (Griffiths, 1972)

The Mascarene anticyclone generally determines the characteristics of the moist south-easterly monsoon flow over the Indian ocean which influences rainfall over most of Eastern Africa The relative position and intensity of the St. Hellena anticyclone determines the position and depth of the Quasi-permanent low pressure centre over central Africa, and hence the intensity of weather associated with it and how far to the east this weather will penetrate The relative strength and position of all these anticyclones will further determine the position and intensity of the ITCZ and the associated weather systems.

1.4.1.7 TELECONNECTIONS

Tropical Eastern African weather characteristics have been observed to be teleconnected with many anomalies in the general circulation outside the region. The large-scale systems include the **El-Niño**/Southern Oscillation (ENSO), the Quasi-Biennial Oscillation (QBO), and intra-seasonal waves, amongst many others

One of the global climate systems that is teleconnected with weather over many parts of the world is ENSO (Troup, 1965, Pan and Oort, 1983; Nichols, 1984, IPCC, 1990, 1992; UNEP, 1991, 1992b). This is associated with a zonal circulation with a recurrence period of 3-7 years Details of ENSO may be obtained from Rasmusson and Carpenter (1982), Pan and Oort (1983), Nicholson and Entekhabi (1986), and Tyson (1993), amongst many others Pan and Oort (1983) found global mean temperatures to be highly correlated with ENSO with maximum global temperatures occurring 3-6 months after the peak warmth of the **El-Niño** This is because the heat stored in the warm tropical Western Pacific is transferred either directly or indirectly to many other parts of tropical oceans There is then a loss of heat from these oceans to the global atmosphere, thereby warming the latter ENSO has also been associated with anomalies in the regional rainfall and many other weather parameters (Gray, 1984; Nichols, 1984; Emmanuel, 1987; Wolter, 1989, Rapper, 1990, IPCC, 1990a, 1992, Tyson, 1993; Valadon, 1992).

Tropical Eastern Africa is amongst global areas where ENSO impacts have been reflected in both precipitation and temperature anomalies (UNEP, 1991, 1992a, 1992b, Ogallo, 1988, 1989, 1992; Ogallo and Aliba, 1994). During a warm ENSO phase (low SOI), exceptionally high temperature departures and drought have been evident over southern Africa, especially Zimbabwe, Botswana, Southern Namibia, South Africa, Zambia, and Mozambique Some authors have associated ENSO with the prolonged Sahelian drought (Druyan, 1988; Semazzi *et al*, 1988, Wolter, 1989; Nicholson, 1989b; Folland *et al*, 1986, UNEP, 1992a; Drought, 1993; WMO, 1993)

Another system often associated with many climate anomalies is the Quasi-Biennial Oscillation (QBO) The QBO has an average period of period of 23-33 months (Landsberg, 1963). This is in sympathy with stratospheric wind oscillations over the tropical atmosphere, being westerly at one phase, and reversing to easterly at the other phase Angell (1963) discerned the QBO in both the global zonal wind and temperature records He discovered a downward progression of warming with time which he attributed to small-scale eddy fluxes in the tropical latitudes Evidence of the presence of the QBO in the variability of climate over Eastern Africa have been presented by Ogallo (1992), Ogallo *et al* (1994), Nyenzi (1992), and Tyson (1984, 1993), amongst others

Another significant climate system over the region of study is the 30-60 day wave. These waves are sometimes referred to as the "intra-seasonal waves", as their period is less than one season. They are strong over eastern and southern Africa but almost non-existent over central Africa (Anyamba, 1990). Yasunari (1980) and other authors have reported an observed meridional propagation of the wave. This wave shows marked spatial and temporal variability in its period, with two distinct peaks centred around 20-30 days and 40-50 days respectively. Anyamba (1992) observed that there appears to be some amplification of both peaks during ENSO events when the behaviour of the two peaks is similar. Attempts have been made by Cadet and Daniel (1988) amongst others to use the intra-seasonal (40-50 day) wave in long range forecasting in those areas where it has regular and significant influence

Other systems that have been associated with Tropical weather include unique regional systems associated with topography, large water bodies, and other thermally induced systems. There are the air-streams like the Congo air, and the dry Sahelian Hammattans. There is too, a spill-over from the middle latitude disturbances, and troughs in the upper-level westerlies (Anyamba, 1983).

The next chapter will present the various methods that were adopted in this study together with the data used

CHAPTER TWO

2.0 DATA AND METHODOLOGY

This chapter is devoted to the data and methodologies which were used to achieve the various objectives of the study.

2.1 DATA

The data used in this study were the daily maximum and minimum temperature records. There are generally four distinct seasons of the year namely, the long rains of March-May, the SE monsoon season of June-August, the short rainy season of September-November, and the NE monsoon season of December- February The four mid-season months of January, April, July, and November were chosen to represent the respective seasons.

The daily minimum and maximum temperature records were used to derive monthly time series of the extreme temperature records These records were used to study the space-time characteristics of extreme temperatures over the study region

One of the major factors that may be closely associated with temperature anomaly is radiation and cloudiness Outgoing long wave radiation (OLR) records were also used in this study to examine the relationship between the observed temperature trends and the corresponding cloudiness patterns Actual prevailing cloudiness data for Dagoretti Corner in Nairobi, and Lamu were also used The Southern Oscillation Index (SOI) and the phases of upper air winds over Nairobi were further used to examine the relationship between the observed extreme temperatures and the regional/global circulation anomalies.

Normalised pressure difference between Tahiti and Darwin were used as SOI. These records were obtained from the Climate Analysis Centre, Washington Inter-annual QBO characteristics over the region were quantified using the Nairobi stratospheric wind records (Ogallo *et al*, 1994). The large spatial variability of the QBO has, however been discussed by Jury and Pathack (1991) among many others

The study area and the network of stations used were shown in Fig.3. The data were quality-controlled before they were subjected to any analysis in order to ensure homogeneity in the temperature records. Few data gaps were however, filled up before the data were quality controlled. The methods that were used to estimate the missing records are discussed in the following section

2.2 ESTIMATION OF MISSING RECORDS

Various methods have been recommended for the estimation of missing records in Meteorological time series by WMO (1967) and WMO (1986). Below is a brief description of the most commonly used methods

2.2.1 ISOPLETH METHOD

In this method, missing records are estimated using information from neighbouring stations. The first step involves the mapping of all available records for the period with a missing record at some location. Isopleths are then drawn and the missing values extrapolated from the magnitudes of two isopleths, one on either side of the station with the missing record.

The disadvantages of this method are that it requires a dense network of stations, which is not always available, and that it is very tedious and time consuming. The method will also be more accurate over regions with homogeneous surface topography and within areas with similar climatic conditions.

It however has an advantage in that it is possible to include knowledge of physiographic relations, storm-tracks, storm types, and other factors when drawing the isopleths (Basalirwa, 1991).

2.2.2 REMOTE SENSING TECHNIQUES FOR ESTIMATING TEMPERATURE

The basic principle of estimating temperature through remote sensing is the application of different forms of the radiative transfer equation. A basic requirement is the choice of a spectral window region where the radiation from the surface rises almost un-attenuated to the satellite level. For the estimation of sea surface temperature (SST), the simplified form of the radiative transfer equation is:

$$I(v) = B(T_s, v)Z(P_s, v) - \int_{Z(P_s,v)}^{1} B(T_p, v)dZ(p, v) \text{ .... } \textbf{(1)}$$

where, I(v) is the radiance reaching the satellite, v the wave number, T_s the SST, T_p the temperature of atmosphere, and $Z(P_s,v)$ the transmittance between the satellite and the sea-surface. I(v) is measured by the satellite, whilst $B(T_p,v)$ and dz(v,p) are functions of the atmospheric temperature and water vapour profiles respectively. For operational purposes, $B(T_p,v)$ and dz(v,p) are calibrated from empirical and statistical methods. By substituting for all the known components, equation (1) may then be translated into sea surface temperature.

The major problem of sea surface temperature estimation is cirrus cloud contamination which makes it hard to differentiate between radiation from the sea surface and that from the top of the cloud. This problem has since been solved by the use of micro-wave sensors. Micro-wave radiation has a large spectral window near 1.0 cm, which is free from cloud contamination as long as the clouds are not precipitating. This makes it possible for one to estimate the temperature of surfaces below the cloud level without contamination from the clouds. The Planck's function for micro-waves is almost linear, hence errors in the estimation are further are minimised.

A disadvantage of micro-wave sensors is that the emissivity of micro-waves varies a lot from one surface to the other. Hence these sensors are mainly used for sea surface temperature estimation where spatial variation of emissivity is limited. Another disadvantage of this approach is that micro-waves require much bigger (and often heavier) antennae and larger fields of view (FOV).

Details of the various methods used are given in Smith *et al* (1970), Brower *et al* (1976), McClaim *et al* (1982), and Jianping *et al* (1990) among others.

2.2.3 CORRELATION METHODS

In this method, two aspects may be considered, namely temporal correlation, and spatial correlation In temporal correlation, we try to establish if the variable with a missing record may be correlated with some other variable at the same locality over time, whilst in spatial correlation we seek to establish if the variable may be correlated to other variables at other locations

Once such a relationship has been established, regression analysis is then used to derive mathematical functions that can describe the relationship. The derived functions may then be used to estimate the missing records.

Simple linear relationships between the variable with missing records, X_t, and a related parameter, Y_t , may be expressed as

$$Y_t = a\,X_t + b \quad \text{.............................} \quad \mathbf{(2)}$$

where a and b are coefficients to be estimated from the available data The next step involves the use of equation (2) to estimate X_t using Y_t values.

An other simple approach based on correlation is the arithmetic mean method Under this method, the ratio of the long-term averages for two correlated locations is used to estimate the missing record using expressions of the form:

$$X_t = \frac{\overline{X}}{\overline{Y}} \; x \; Y_t \quad \text{..} \quad \mathbf{(3)}$$

where $\overline{X}, \overline{Y}$ *are the long - term means of* X_t *and* Y_t *respectively,*

X_t is the series with missing data and Y_t a related series with no data gaps. The method assumes that due to the high correlation between the pair of points (variables), the ratio of the long-term averages will be reflected at any time scale. This may however, not be true over locations with unique local/ regional climate anomalies.

An advantage of this method is that the significance of the estimated records can be tested using standard statistical tests. A disadvantage of the method is that different locations may have unique characteristics that may not be easily accounted for by the simple mathematical functions derived. Another disadvantage is that the calibration of those models based on spatial correlation requires a good base network, which is often lacking and that each model may be applicable only for particular time scales.

In this study correlation methods were used for the estimation of missing minimum and maximum temperature records. All the data were quality-controlled before they were used in any analysis.

2.3 DATA QUALITY CONTROL

Quality control is important in order to detect any discontinuities in the data that may have occurred from non- natural influences like changes in observational schedules and methods, instrumental changes, shifting of station sites, urbanisation, and other human processes (WMO, 1966, Basalirwa, 1979) Heterogeneity makes records not strictly comparable over long time periods and between different stations.

It is therefore important to ascertain the homogeneity of any meteorological data before such data can be used in any study. Recommended homogeneity tests can be found in WMO (1966) for both relative and absolute homogeneity. A brief description of some of the most commonly used methods for data quality control follows below

2.3.1 CORRELATION AND REGRESSION METHODS OF QUALITY CONTROL

These methods use correlation and functional relationships between the variable, X_t, being tested for homogeneity and another variable, Y_t, which is known to be homogeneous. We first establish the degree of relationship between X_t and Y_t using simple correlation analysis. The simple correlation coefficient, r, is given by:

$$r = \frac{\Sigma(X_t - \overline{X})(Y_t - \overline{Y})}{\sqrt{\Sigma(X_t - \overline{X})^2 \Sigma(Y_t - \overline{Y})^2}} \qquad \text{..........(4)}$$

If r is statistically significant and subsets of observations X_t and Y_t are known to be homogeneous, then for the homogeneous period, Y_t may be expressed as a function of X_t using a linear relationship as in equation (2) The equation may then be used to compute values of Y_t for known values of X_t The observed and computed values of Y_t are then used to test the quality of the observations.

This method has one major disadvantage in that high correlations may not always lead to meaningful results as they might be due to seasonal effects playing down on both X_t and Y_t. Once the seasonal effects are removed, there may not be any significant correlation between X_t and Y_t (WMO, 1986). The method also assumes that samples of quality data are available for the development of the equation.

2.3.2 WALD-WALFOWITZ ONE SAMPLE RUNS TEST

This is a non-parametric (distribution-free) method which is especially useful for testing the homogeneity of data against an alternative of trend, bias, drift, oscillation, or a combination of these. This test does not require the data to be normally distributed and is based on the mean and variance of the distribution as calculated from the means and variance of different samples of the same distribution. Details of the method can be found in Siegel (1956) and WMO (1966, 1986).

Other non-parametric tests for homogeneity include the Von-Neuman's ratio, the Mann-Whitney rank test, the Kolmogrov-Sminov test, the Kruskal-Wallis test, and the Akaike's Information Criterion. Detailed descriptions of these methods may be found in WMO (1986).

2.3.3 MASS CURVES

Cumulative records or deviations from the mean are plotted against time for mass curves and residual mass curves respectively. A strictly homogeneous record would be indicated by a straight line whilst heterogeneity would be indicated by significant deviations of some of the plots from the straight line.

Two approaches have been recommended by the WMO (1966), specifically for temperature records. These methods and others based on the concept of mass and residual mass curves are briefly discussed below.

2.3.4 RELATIVE HOMOGENEITY TEST

Temporal "differences" between the series to be tested for homogeneity and other time series which are known to be homogeneous, are first computed. The resulting temporal differences series are then plotted together on linear graph paper. If any of the time series contains "sizeable" errors, they are revealed as "spikes" on the same dates at least for most of the time series. This method is used to determine inter- compatibility in different time series.

Alternatively, the actual temperature series for each station are plotted together after smoothing using five term, or any other appropriate successive (or moving) averages. This method is not as clear as the difference method.

2.3.5 ABSOLUTE HOMOGENEITY TEST

This involves comparing the differences between the series under test with only one other homogeneous series. The latter series will be a suitably derived average of the series for the individual surrounding stations. This way, evidence of relative heterogeneity can be translated directly into definitive information about the heterogeneity in the test series.

To be able to derive the average series, different factors must be considered (Mitchell, 1961) namely, the density of reporting stations; the length of the record being investigated; the relative incidence of station relocations; the climate uniformity over the area; e.t.c. Details of these methods are found in WMO (1986).

One example of absolute homogeneity test is the use of double mass curves. The basic concept of mass curves was discussed in section 2.3.3. In this method however, several stations situated within the same climatic zone and whose record is known to be homogeneous, are chosen. A plot of corresponding cumulative data of the station whose homogeneity is being tested and the homogeneous record is made. A straight line indicates homogeneity, otherwise the record is declared heterogeneous.

Heterogeneous records can be adjusted using the slopes of the graphs of the curves. Details may be found in WMO (1966, 1986) and Ogallo (1981, 1987).

2.3.6 MARONNA AND YOHAI METHOD

This method is an extension of the double mass curve but with a quantitative measure of the limits within which the series may be declared homogeneous. A major requirement of the method is that the data must be normally distributed, serially independent and stationary except for the shift in the mean of the series under test Details of the method can be found in Maronna and Yohai (1978) and Basalirwa (1991).

A major disadvantage of the method is the requirement of a normal distribution as this is not always possible especially with meteorological records.

The cumulative mass curve method was used in this study to test the homogeneity of the minimum and maximum temperature records. Double mass curves were used to adjust heterogeneous records.

The following section discusses the methods used for the temporal analysis of the extreme temperature records

2.4 TEMPORAL ANALYSIS

The temporal characteristics of the extreme temperatures that were investigated in this study include trend, seasonal variations, and periodic fluctuations.

2.4.1 TREND ANALYSIS

Trend is the long term behaviour of the time series. It indicates whether the series is stationary or non-stationary. Both statistical and graphical methods may be used to examine trend in a time series as discussed in the following sections.

2.4.1.1 GRAPHICAL METHODS

Graphical methods involve the plot of the time series on a linear graph paper. Several smoothing functions may be used to smooth the time series. In the smoothed time series, the trend at any point is represented by a weighted average of the observed values near that point. Regression analysis is often used to give the best mathematical equation for the observed trend. Details of this are presented in the next section.

The most commonly used smoothing method has been the use of Binomial coefficients (WMO, 1966; Tyson, 1975, Rodhe and Virji, 1976; Ogallo, 1977, 1979, 1980; and others).

The disadvantages of the graphical method for trend analysis are that the methods are highly subjective as they depend very much on individual visual judgements. Some data sets are also lost by some smoothing techniques, and fluctuations that were not in the original series introduced by the smoothing techniques (WMO, 1966, Kendall, 1961).

The moving average method of smoothing alters amplitude, and often the phase, of the fluctuations in a time series. The frequency response function, $R(\lambda)$, is used to measure the variations after smoothing relative to those before smoothing. It is therefore, a measure of the dynamic response of the filter for any given frequency of variation, λ.

Details on the determination of smoothing weights have been discussed by the WMO (1966), Shapiro (1970), Hermann (1971), Rabiner *et al* (1975), Ogallo (1980), and others

2.4.1.2 POLYNOMIAL APPROACH FOR TREND ANALYSIS

The method involves the approximation of the trend pattern with a mathematical polynomial function of time of the form:

$$X_t = f(t) \qquad (5)$$

where, f(t) is the best function for the trend and X_t the time series being investigated.

This method has a weakness in that often the trend will be an unknown function of time, which will gradually shift with time, making it difficult to represent it with a polynomial function

2.4.1.3 STATISTICAL METHODS FOR TREND DETERMINATION

The Analysis of Variance (ANOVA) is one of the most commonly used methods for trend tests Other methods include non parametric statistics like the Mann-Kendall rank and Spearman rank statistics. Details of the statistical methods can be obtained from WMO (1966). A brief account of some of the methods is given in the following section

2.4.1.3.1 ANALYSIS OF VARIANCE TECHNIQUES

One of the simplest ways of using ANOVA to search for climatic trends is for the period of study to be divided into subgroups of at least 30 years record each and the means of the subgroups found. The sub-group means are then compared using the students' t-test or any other appropriate tests of significance, depending on the frequency distribution of the time series (WMO, 1966; Parthasarathy and Dhar, 1973; Jones, 1975; Granger, 1976; Ogallo, 1980).

The major disadvantage of this method is that it requires a very large data sample since the normal period recommended by WMO (1967) is 30 years for each subgroup. Most climatic records are not that long.

Non-parametric statistics like those based on rank correlations are therefore widely used. Such methods do not normally require the frequency of the time series to be a normal distribution. Rank correlation methods, for example, use a non-parametric measure of correlation based on ranks. Detailed descriptions of the methods may be found in Siegel

(1956), Kendall (1961), and WMO (1966). Below is a brief discussion of two of the most commonly used methods.

2.4.1.3.2 MANN-KENDALL RANK STATISTIC, τ

This is among the most popular methods for testing for trend against randomness. It considers the relative values of all terms in the series X_i, under analysis. The series X_i is replaced by the ranks k_i, such that each X_i is assigned a number n_i, where, $1<n_i<N$; and n_i is the number of observations preceding X_i with magnitudes greater than that of X_i.

The statistic τ, can then be computed from the following formula:-

$$\tau = 4\{\frac{\sum_{i=1}^{N-1} n_i}{N(N-1)}\} - 1 \quad \text{.......} \quad (6)$$

where N is the total number of observations.

If the distribution is nearly Gaussian normal for all N>10, and has an expected value of zero and variance approximately equal to (4N+10)/[9N(N-1)], then τ can be used to assess the significance of trend by comparing with the statistic τ_g, where,

$$\tau_g = \pm_{t_g}\sqrt{\frac{(4N+10)}{9N(N-1)}} \quad \text{.......} \quad (7)$$

and t_g is the ordinate corresponding to the desired probability of the standard normal distribution for a two-tailed test. For routine application, the 95% probability point of t_g (i.e. $t_g = 1.96$) is recommended (WMO, 1966).

2.4.1.3.3 SPEARMAN RANK CORRELATION METHOD

This method is used to test for linear or non-linear trend in a time series against alternative randomness (WMO, 1966). The Spearman rank correlation coefficient, r_s, is defined as:

$$r_s = 1 - 6\left\{ \frac{\sum_{i=1}^{N} (d_i)^2}{N(N^2 - 1)} \right\} \qquad \text{.........(8)}$$

where, $d_i = k_i - i$, and k_i is the rank of the series X_i;

N is the total number of observations. For N>8, the significance of r_s can be tested using the statistic t_g, defined by:

$$t_g = r_s \sqrt{\frac{N-2}{1-r_s^2}} \qquad \text{.........(9)}$$

The statistic t_g is compared with the probability of the Students' t-distribution for (N-2) degrees of freedom.

In this study both statistical and graphical methods were used to examine the trend of the time series. In the graphical approach, the rate of change of the slope of the time series was used to describe trend of the time series. A positive slope would indicate an increasing trend and vice-versa The significance of the trend was tested using the standard methods like the Student's t-test and the Spearman rank correlation method

2.4.2 CYCLICAL VARIATIONS

Recurrences of cold and warm events are common in all locations Attempts were made here to investigate the cyclical nature of the recurrences of the warm and cold events using the method of spectral analysis. Three approaches of spectral analysis are known to exist, namely, the Fourier transformation of the auto-correlation function or auto-covariance function, the Fast Fourier Transform (FFT), and the Maximum Entropy Method (MEM)

A brief description of the methods is given below

2.4.2.1 AUTO-COVARIANCE/AUTO-CORRELATION FUNCTION

This is the most fundamental method of spectral analysis It computes the spectral estimates directly . The power spectrum, $F(\lambda)$, is expressed as a Fourier transform of the auto-covariance function, $R(k)$, or the auto-correlation function, $r(k)$ which can be estimated using equation 4 Power spectral density estimates based on auto-covariance function may be expressed as:

$$F(\lambda) = \sum_{k=-N}^{N} R(k) e^{-i2\pi\lambda k} \quad \text{...}(10)$$

where, $\lambda = 1,2,\ldots\ldots\ldots,m$, and m is the maximum time lag; N is the sample length and $i = (-1)^{1/2}$

The spectral density function, F(λ), can similarly be defined as the Fourier Transform of the auto-correlation function, r(k), as:

$$r(k) = R(k)/R(0) \quad \text{...}(11)$$

But $R(0) = S^2$, the variance. Hence $R(k)/R(0) = R(k)/S^2$ Thus,

$$F'(\lambda) = \sum_{k=-N}^{N} \frac{R(k)e^{-i2\pi\lambda k}}{S^2} \quad \text{...}(13)$$

where, S^2 is the variance of the time series.

If the series is normalised, then it has an expected value of 0 and variance, $S^2 = 1$. Hence

$$F'(\lambda) = \sum_{k=-N}^{N} r(k)e^{-i2\pi\lambda k} \quad \text{...} (14)$$

Various methods can then be used to smooth the spectral estimates derived from equation (14) in order to obtain 'mean smoothed' spectral values. The smoothed spectral estimates may be given by the spectral density function, f(λ), where:

$$f(\lambda) = F'(\lambda)W(k) = \sum r(k)w(k)e^{-i2\pi\lambda k} \quad \text{....................................} (15)$$

W(k) is a weighting function called the lag-window, and the weights w(k), expressed in terms of λ, are called spectral windows. The most commonly used spectral windows are those by Parzen, Tukey, Bartlett, and Hanning and Daniell (WMO, 1966; Ogallo, 1980).

The spectral density function, f(λ), is expressed using only positive values of λ as it is symmetrically distributed about λ = 0. The smoothed spectral estimates can be expressed as:

$$f(\lambda) = 2[1 - 2\sum_{k=1}^{m} r(k)W(k)\cos(2\pi\lambda k)] \quad \text{.............................} \mathbf{(16)}$$

for $0<\lambda<1/2$, where m is the maximum time-lag.

The major shortcomings of the Fourier Transform methods include the fact that they depict inadequate frequency resolution, i.e, they are not able to distinguish between two signals that are close in frequency. The problem is worse when very short time series are considered as the resolution is proportional to the data length. There is also often some leakage of power from the main lobes into the side lobes, masking weaker signals. This gives a 'smeared' look to the spectrum, which can be minimised by 'pre-whitening'.

Details of the auto-covariance method can be found in Blackman and Tukey (1958), Priestly (1962), Granger and Hatanaka (1964), Cooley and Tukey (1967), Helms (1967), Jenkins and Watts (1968), Fishman (1969), Ogallo (1980) and Anyamba (1990) among others.

2.4.2.2 THE MAXIMUM ENTROPY METHOD (MEM)

The MEM is based on the principle of fitting an auto-regressive process of order p expressed as:

$$X_t = \phi_1 X_{t-1} + \phi_2 X_{t-2} + \ldots\ldots\ldots\ldots + \phi_p X_{t-p} \quad \text{..} \mathbf{(17)}$$

where, p is the order of the auto-regressive process, and ϕ_1,, ϕ_2,..,ϕ_p are coefficients which may be estimated using the Yule-Walker equations.

Any stationary time series X_t may be expressed as an auto-regressive process of order p, AR(p), where,

$$X_t = \sum_{k=1}^{p} \phi_k X_{(t-k)} + W_t \quad \text{.......... (18)}$$

where, t= 0,1,2,......N-1; ϕ_k is the filter coefficient at time lag k, and W_k the zero mean white noise with variance σ^2.

Equation (18) may further be simplified to:

$$W_t = \sum_{k=0}^{p} a_k X_{(t-k)};\ a_0 = 1;\ a_k = -\phi_k;\ k = 1,2,....,p \quad \text{.......... (19)}$$

where W_t is now expressed as a linearly filtered version of X_t, a_k's are the filter coefficients.

The frequency response function, R(λ), of the filter is then given by:

$$R(\lambda) = \sum_{k=1}^{p} a_k e^{-2i\pi\lambda k};\ -\frac{1}{2} \leq \lambda \leq \frac{1}{2} \quad \text{.......... (20)}$$

It can be shown that the MEM or AR power spectral density can then be expressed as:

$$f(\lambda) = \frac{\sigma^2}{\left| 1 - \sum_{k=1}^{p} \phi_k e^{-2\pi i\lambda} \right|} \quad \text{.......... (21)}$$

Equation (21) reduces the spectrum estimation problem to one of determining the AR model of order p, filter coefficients ϕ_k, and error variance σ^2.

The major disadvantage of the method is its poor performance for signals with high levels of noise. The criteria for maximum time lags (i.e., the number of coefficients to be used) is also difficult to choose. The Akaike's criterion has been found to give fewer coefficients (Akaike, 1970).

This method however, has two major advantages in that it has good resolution and is therefore used for analysing short time series and for detecting weak signals. It can be used even when the wavelength, λ, is of the same size as the length of the series being investigated (Currie, 1974a, b; Bolt and Currie, 1974; Ogallo, 1980). The method also gives unbiased spectral estimates as no fixed smoothing window is applied (Currie, 1974; Lacoss, 1971; Ogallo, 1980).

Details of the AR process can be found in Granger and Hatanaka (1964) and Anyamba (1990), whilst those of the MEM approach are in Burg (1968, 70, 72), Akaike (1970), Lacoss (1971), Currie (1974a, b), Bolt and Currie (1974), Jenkinson (1977), Ulrych and Bishop (1975), Kay and Marple (1981), and Shumway (1988).

This method was adopted for use in this study because of its superiority over the Fourier transform methods when dealing with closely separated frequencies and short time series. Periodic fluctuations appear as peaks in the time plots of the smoothed spectral density function

2.4.2.3. TEST OF SIGNIFICANCE OF SPECTRAL PEAKS

Significance of the observed peaks can be tested by assuming either a null 'white noise', or a null 'red noise' hypotheses. For a 'white noise' hypothesis, the generating process in the time series is assumed to be random and the first order auto-correlation function, R_1, is used to test this. Methods of computing confidence limits for R_1 are found in Anderson (1942). For a random time series, R_1 is approximately normally distributed with mean, $\mu = [-1/(N-1)]$ and variance, $S_R^2 = (N-2)/(N-1)^2$. The significance of R_1 is tested using the statistic $(R_1)_t$, defined as

$$(R_1)_t = \frac{-1 + t_g\sqrt{N-2}}{N-1} \quad \text{...} \quad \textbf{(22)}$$

where t_g is the standard normal variate corresponding to the desired level of significance. The 95% confidence level is normally used and from tables of Gaussian distribution, the corresponding value of t_g for a one tailed test is found to be 1.645. If R_1 is not significantly different from 'zero', the 'null' continuum hypothesis is that of white noise as the series is then assumed to be free of persistence, thus a horizontal straight line whose value is everywhere equal to the average of the values of all m+1 'raw' spectral estimates in the computed spectrum. If R_1 is significantly different from 'zero', and the coefficients of the first one or two lags greater than 1 approximate to the exponential relation,

$$R_2 \approx R_1^2,\ R_3 \approx R_1^3,\ e.t.c. \quad \text{...} \quad \textbf{(23)}$$

the appropriate 'null' continuum is then that of the Markov 'red-noise' (WMO, 1966). The 'red noise' hypothesis assumes a high degree of persistence within the time series. Details of the different tests of significance of spectral peaks are found in WMO (1966) and many statistical books.

'White noise' hypothesis was used in this study to test the statistical significance of the spectral estimates. It should however, be noted that not all physically realistic spectral peaks are always statistically significant and vice versa. The physical significance of the cycles derived from spectral analysis is therefore one of the major issues which should be faced while searching for realistic cycles in any time series.

2.4.3 SEASONAL VARIATIONS

Seasonal characteristics of temperature are closely linked to the seasonal patterns of all temperature-dependent activities. Any shift in the traditional seasonal patterns would therefore have far-reaching socio-economic consequences. Harmonic analysis was used in this study to examine seasonal changes in the extreme temperature patterns within the period of study.

2.4.3.1 HARMONIC ANALYSIS

In this method, any time series may be expressed mathematically as a sum of simple trigonometric functions. The frequencies of these functions are multiples of the fundamental frequency, λ. For a time series, Y_t, with N data points, and represented by m cosine and sine sums (or harmonics),and which is equally spaced in the interval $(0, 2\pi)$, then the mathematical expression for the function is:

$$Y_t = \overline{Y} + \sum_{k=1}^{m} \left(a_k \cos\frac{2\pi kt}{N} + b_k \sin\frac{2\pi kt}{N}\right) \text{..............................} \quad \textbf{(24)}$$

where, $\overline{Y}$ is the arithmetic mean of Y_t. a_k and b_k are constants for each harmonic. The fundamental frequency, $f = 1/N$ for unit time interval, and the maximum value of k, $m = N/2$, where N is even

Equation (24) may further be reduced to

$$Y_t = \overline{Y} + \sum_{k=1}^{m} A_k \sin\left(\frac{2\pi kt}{N} + \theta_k\right) \text{..} \quad \textbf{(25)}$$

where, $A_k = (a_k^2 + b_k^2)^{0.5}$ where $k = 1, 2, \ldots\ldots, m$; and $\theta_k = \tan^{-1}(b_k/a_k)$. Hence

$$a_k = \sum_{t=1}^{N} Y_t \cos\frac{2\pi kt}{N}, \quad b_k = \sum_{t=1}^{N} Y_t \sin\frac{2\pi kt}{N} \quad \textbf{(26)}$$

The phase angle, θ_k, is the time interval between the first and the k'th harmonic and can be used to give the time of maximum or minimum for each harmonic. A shift in θ_k would indicate a shift in the seasonal peak time of the time-series

The ordinate distance from the mathematical mean to the maximum or minimum point is called the amplitude, A_k, and $(A_k)^2$ gives the contribution of each harmonic, k, to the total variance, where total variance, S^2, is given by:

$$S^2 = \frac{1}{2}\sum_{k=1}^{m} (A_k^2) \quad \textbf{(27)}$$

Details of harmonic analysis may be found in Jenkins and Watts (1968) and Kendall (1961) among many others.

In this study, temporal changes in the phase angle and amplitude were used to examine if there has been a shift in the seasonal temperature characteristics.

2.5 CAUSES OF THE OBSERVED COLD AND WARM SPELLS

Temperature anomalies are closely linked to anomalies in the net radiation received at any location. The factors which influence the net radiation reaching any surface are the prevailing cloudiness, atmospheric humidity, atmospheric transparency, and surface albedo. Atmospheric humidity and cloudiness have the highest space-time variability. Their space-time variabilities are controlled by the patterns of the atmospheric circulation at the global, regional, and local levels.

In this study, OLR data were used to represent grid-point cloudiness values Factors which may be associated with the extreme temperatures were examined here by investigating the relationships between the observed extreme temperatures and OLR anomalies Relationships between the observed temperature anomalies and both ENSO and QBO were also tested. ENSO phases were represented in the study by the positive and negative phases of the Southern Oscillation Indices (SOI), defined as the normalised pressure difference between Tahiti and Darwin

The QBO, which is a representation of the stratospheric shifts in the easterly/westerly wind phases, was quantified using the Nairobi stratospheric winds (Ogallo *et al*, 1994). Two methods which were adopted in this study in searching for relationships between pairs of variables were Simple Correlation analysis for the actual observations, and χ^2-tests for grouped data

2.5.1 SIMPLE CORRELATION ANALYSIS

Simple correlation analysis was used to investigate relationships between the observed temperature anomalies and both OLR and ENSO In this method, the Simple Correlation coefficient, r, between the temperature and both the Southern Oscillation index and OLR were computed The mathematical expression for r was given in equation (4).

Two variables are correlated if r is significantly different from 'zero', otherwise the relationship is not significant The students' t-test is used to test the statistical significance of the computed r values at the 95% confidence level using the statistic t_g as described in equation (9).

2.5.2 USE OF CHI-SQUARE TESTS

Some studies have observed that some complex relationships between variables may not be revealed by the use of the Simple Correlation coefficient, r. Grouping of data into certain categories has been used in many studies to generalise complex relationships between variables Contingency tables have often been used to categorise the characteristics of such variables into specific classes

In this study, the observed temperature, OLR, ENSO, and QBO values were grouped into three classes of 'normal', 'above normal' values, and 'below normal values'. The respective contingency tables were then generated and χ^2-tests used to examine the relationship between the observed groups of temperature anomalies and OLR, ENSO and QBO phases The results of the χ^2 -tests were used to determine the systems that could be associated with the extreme temperature anomalies which were observed over the study region

The results which were attained with the various analyses are the subject of the next section

CHAPTER THREE

3.0 RESULTS AND DISCUSSION

As stated in section 1.3, the objectives of this study were to examine the space-time characteristics of the extreme temperature values over the tropical Eastern Africa in order to identify any organized trends in the temperature records. To achieve the above objectives, various analyses were performed on the data, including trend analysis, seasonal analysis, cyclical analysis, and analyses to determine the causes of the observed extreme temperature anomalies. This chapter is devoted to presenting the results of the various analyses.

3.1 MISSING DATA

The data that were missing were estimated using correlation methods as were described in section 2.2.3. All the estimated records were subjected to quality-control tests before they were used in any analysis. The quality-control of the estimated records will be presented in the next section. It should however be noted that only a maximum of 10% of the total data at any station was estimated

3.2 DATA QUALITY CONTROL

Typical examples of the results obtained from the quality-control tests are given in Figures 6 (a) and (b). Most of the mass curves were almost linear, signifying that the temperature records were not heterogeneous. The minimum/maximum temperature records were therefore declared of high quality, and hence suitable for climatological analysis. This corroborates the findings of Ogallo and Aliba (1994), who found temperature records within the SADCC region to be generally homogeneous.

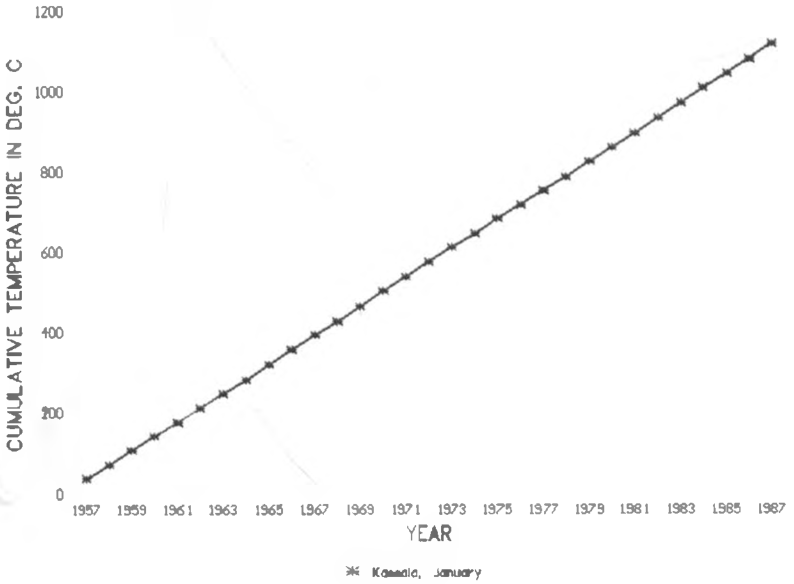

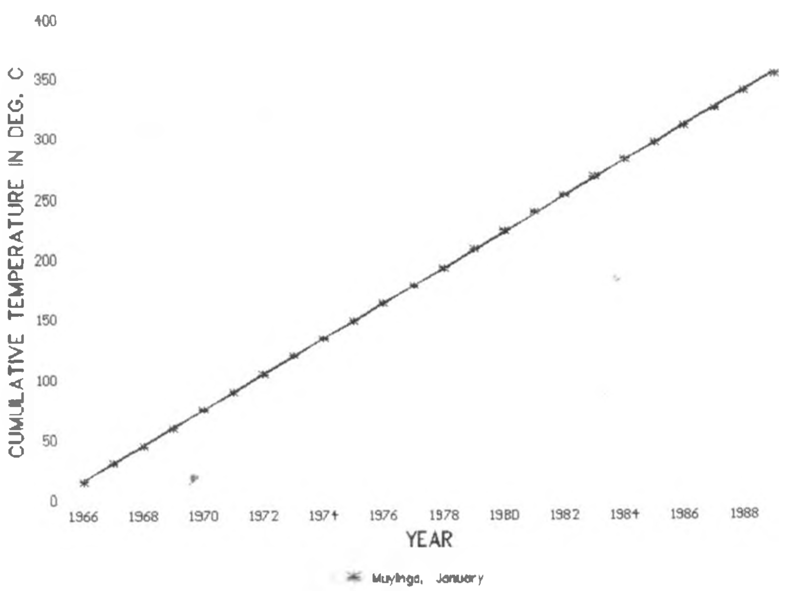

Figure 6: Cumulative temperature for Kassala, Sudan (top), Muyinga, Burundi (bottom)

The results of the trend analysis follow in the next section.

3.3 TREND ANALYSIS RESULTS

Typical examples of the results of graphical analysis of trend are shown in Figures 7 (a) to (h). The data were first normalised by subtracting the long term mean and dividing by the standard deviation before they were used in the analysis. These results show significant decadal variations in the mean patterns of the minimum and maximum temperature with the global scale warming signals of the 1980's clearly discernible at most locations. Significant geographical and seasonal differences were however observed in the minimum and maximum temperature trend patterns. The decadal differences between the mean temperatures of the decades of the 1950's to 1960's and the 1970's to the early 1990's introduced significant linear trends on the inter-annual patterns of minimum and maximum temperature values at most locations. Most of these trends were positive especially for minimum temperature to the north of the eastern Africa region. Typical examples are Dagoretti in Kenya and Debremarcos in Ethiopia (Figures 7 a to 7 d) which are shown to have experienced significant minimum temperature increases and no significant change in maximum temperature.

Coastal and island locations, and some other locations to the south of the study region showed significant decreasing minimum temperature trends. The 1980's experienced the lowest minimum temperature values at these locations. Typical examples are Lamu and Pemba (Figures 7 e to 7 h). More examples are given in appendix (ii)

It is apparent from these time series therefore, that whilst some areas have experienced warming trends in recent years, cooling trends were also observed at some locations whilst at others, no significant temperature changes could be delineated. Similar observations have been made by the IPCC (1990a, 1992a, 1992b). It should however be noted that most of the trends delineated from this study seem to have been induced by the inter-decadal scale variations. Whilst the decades of the 1950's to the early 1970's were relatively cool at many locations, the late 1980's to the early 1990's

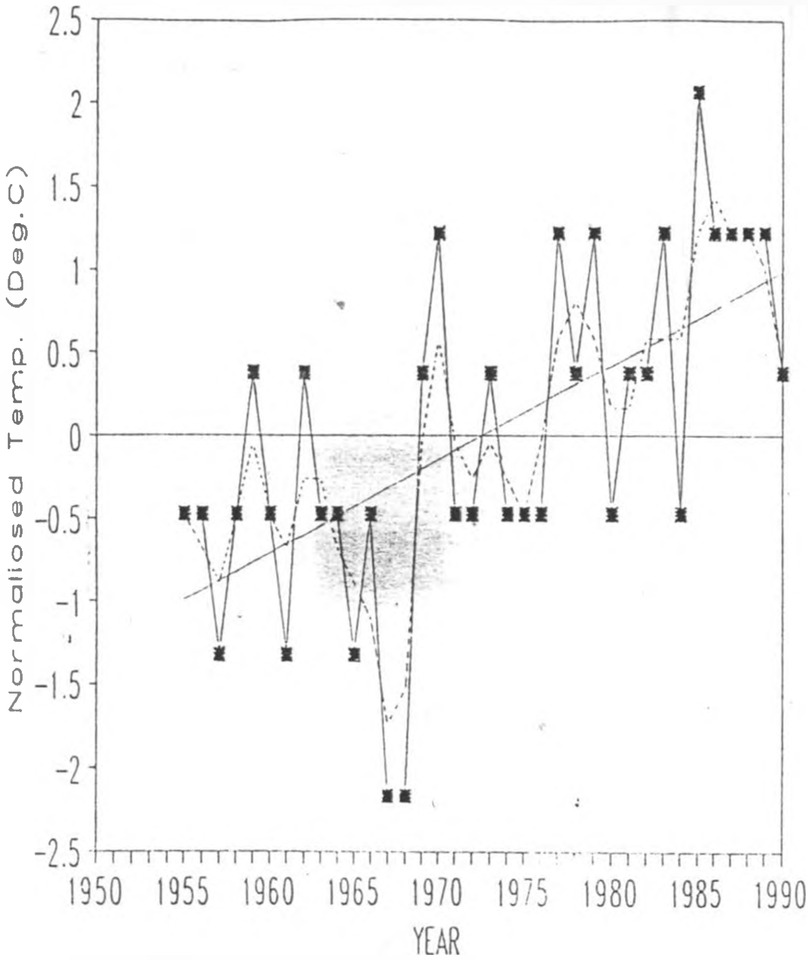

FIG 7 (a): Dagoretti, Min temp(Jan).

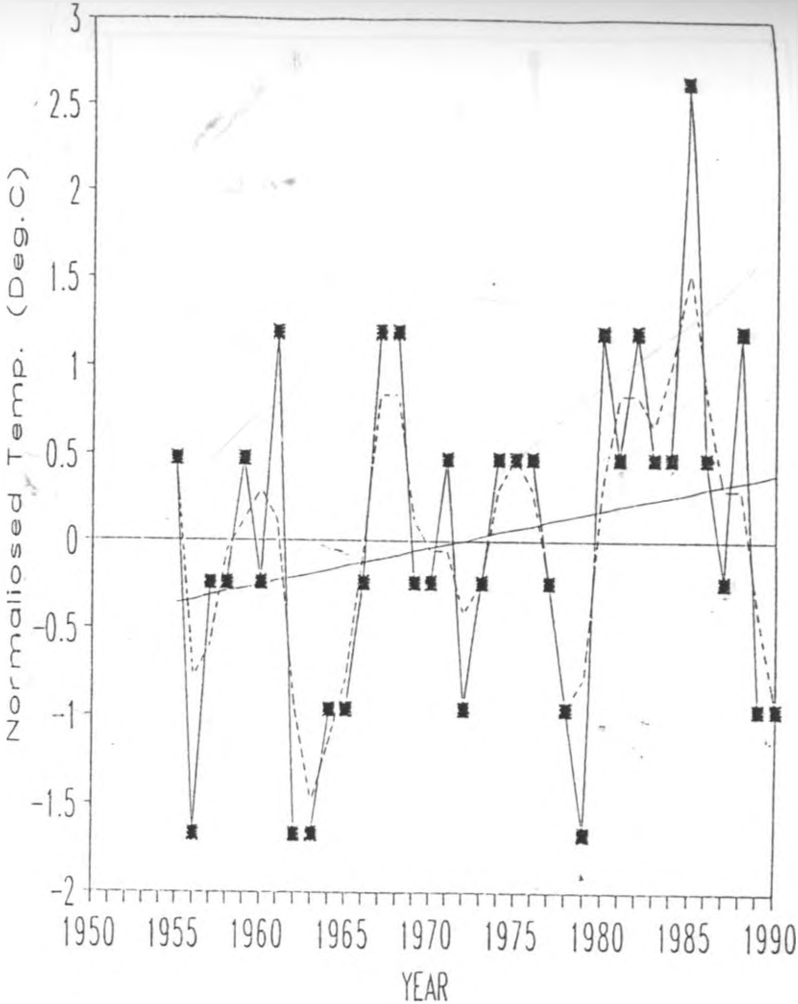

Fig 7(b): Dagoretti, Max temp(Jan).

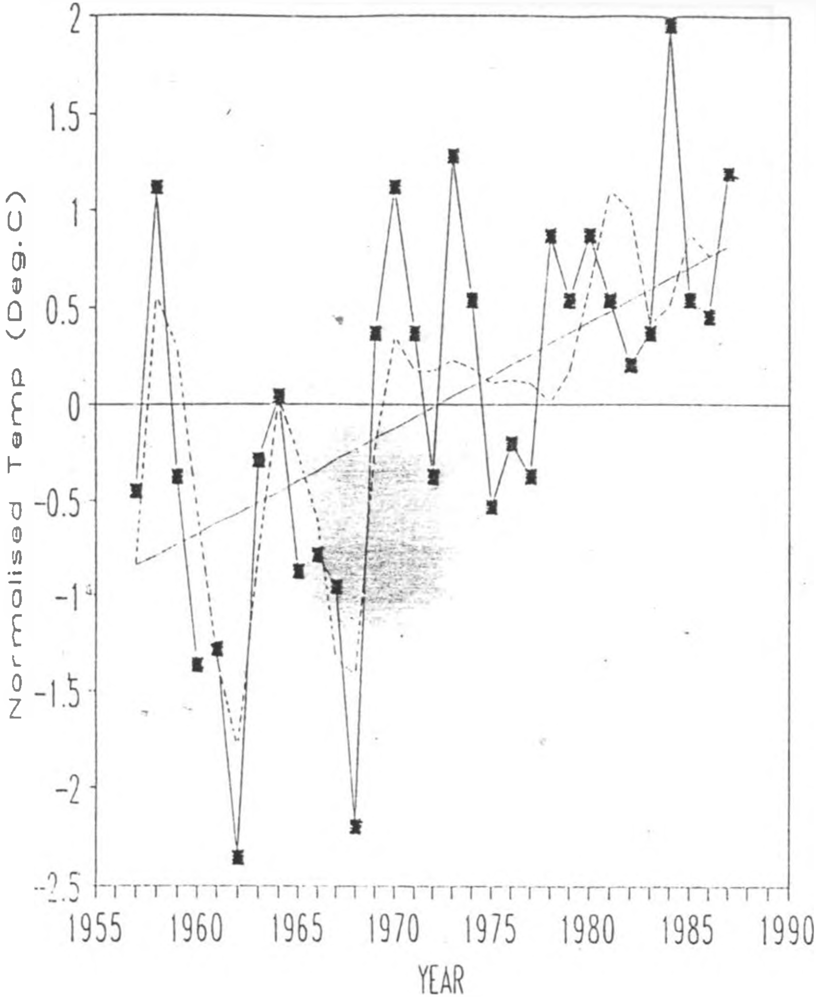

Fig 7(c): Debremarcos, Min temp-Apr.

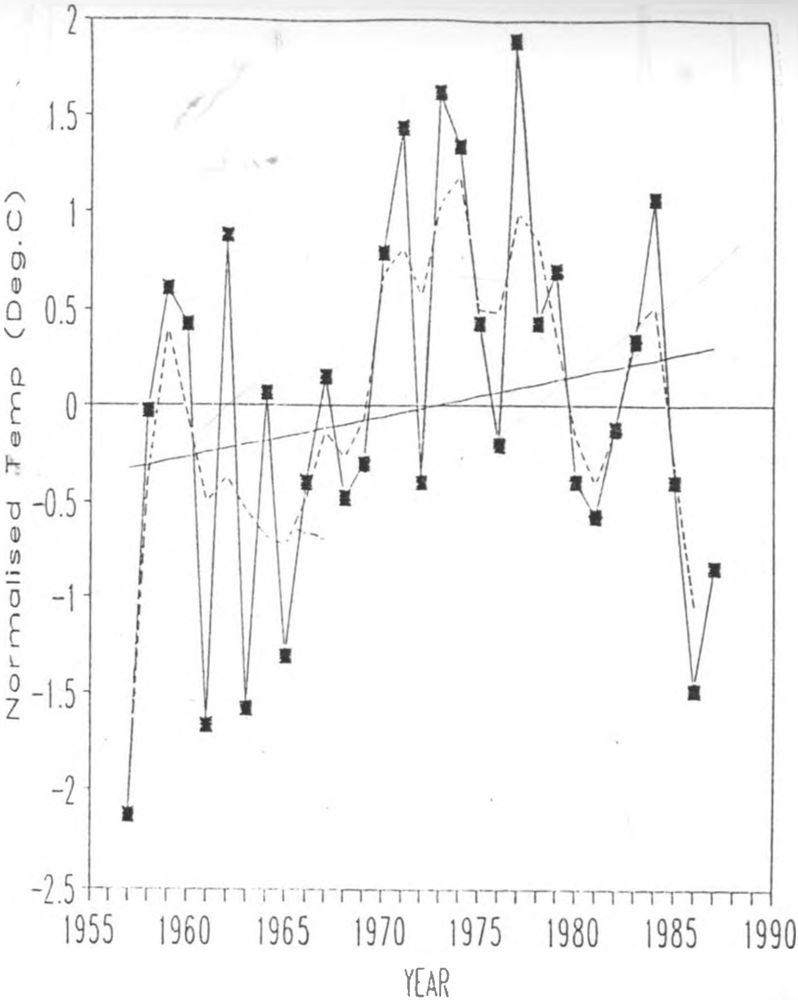

Fig 7(d): Debremarcos, Max temp-Apr.

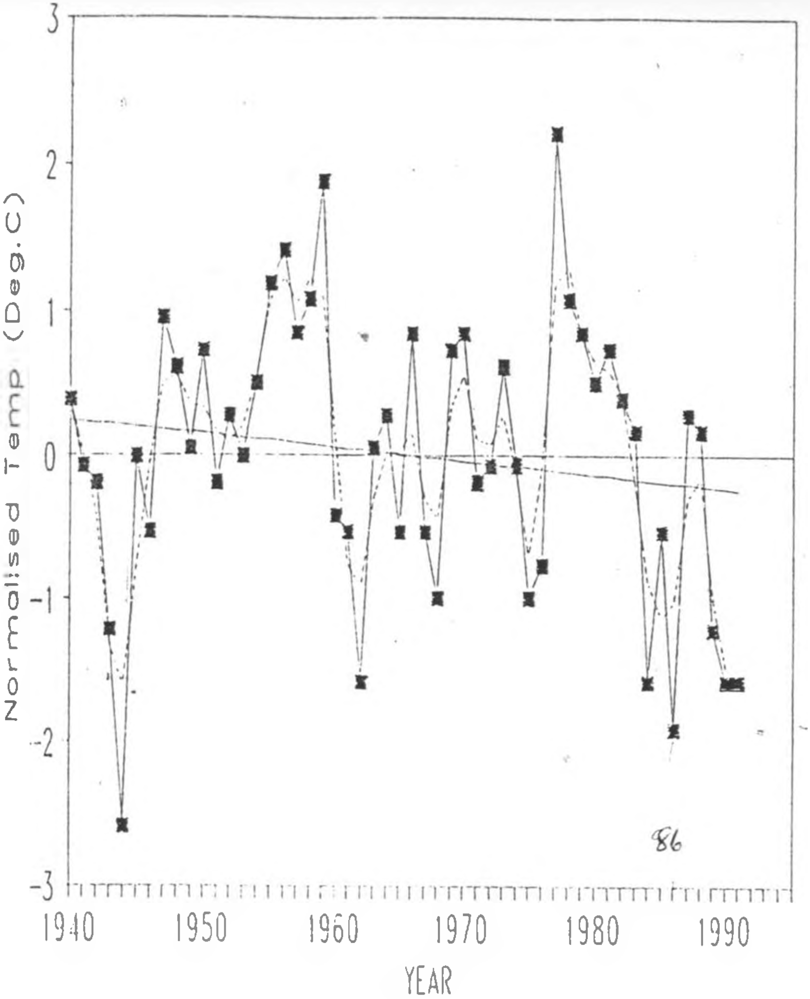

Fig 7(e): Lamu, Min temperature-Jan.

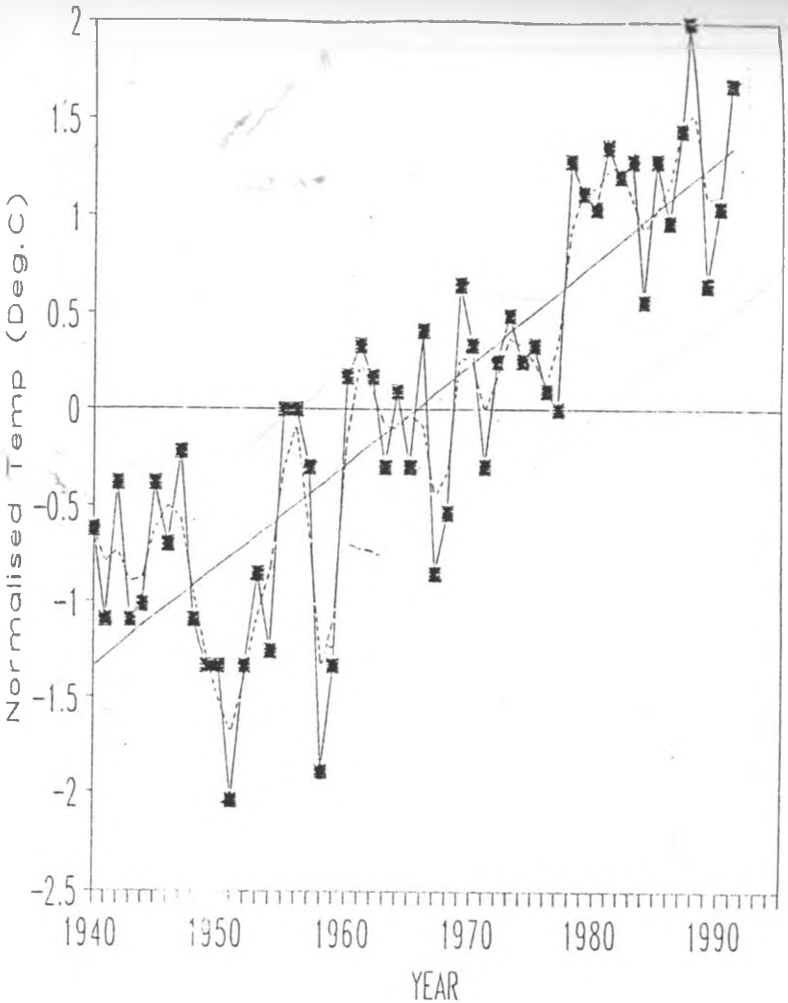

Fig 7(f): Lamu, Max temperature-Jan.

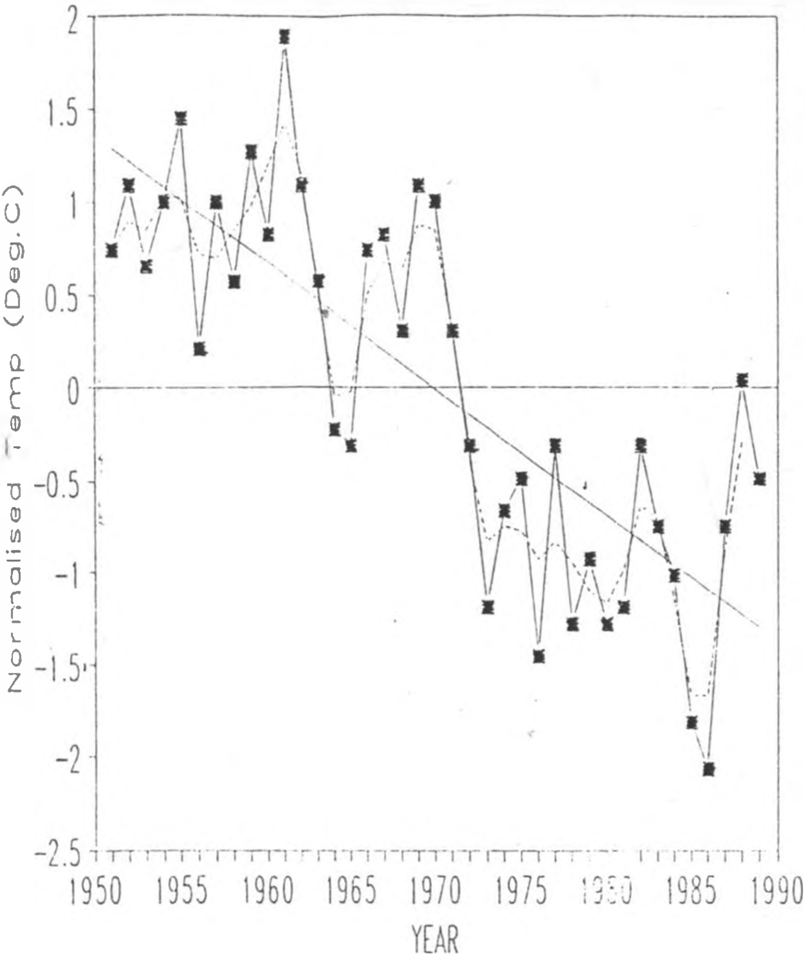

Fig 7(g):Pemba, Min temperature-Jul.

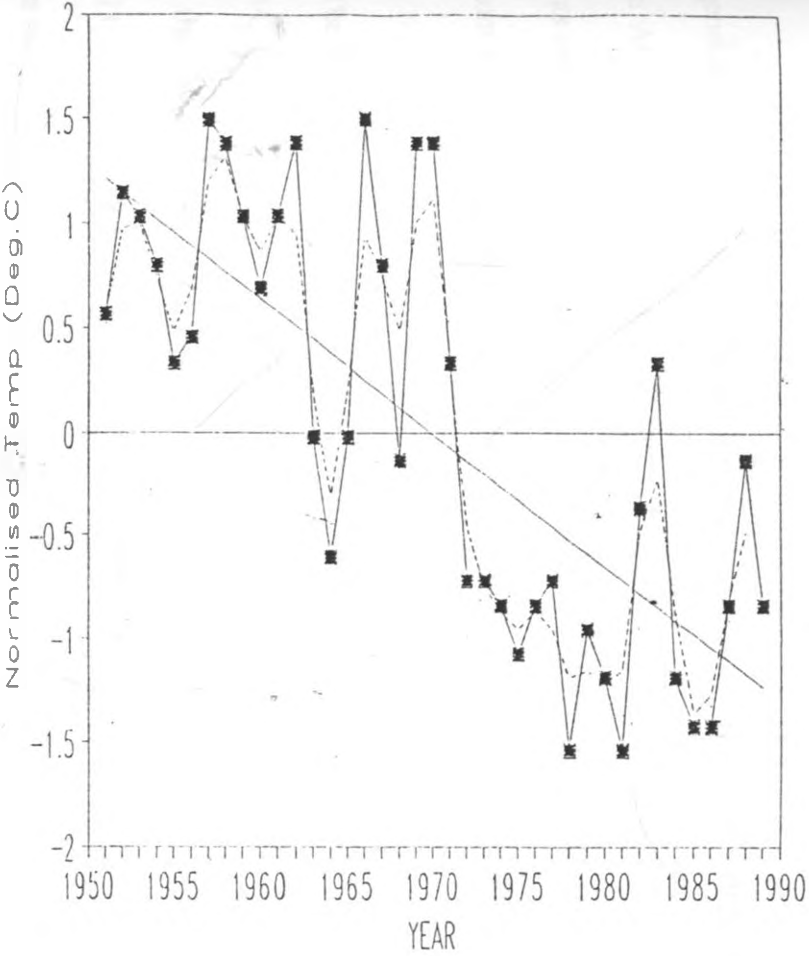

Fig 7 (h):Pemba, Max temperature-Jul.

were generally warm. The decade of the 1960's coincides with one of the wettest periods in the Eastern Africa region. The decades of the 1970's and early 1980's were dominated by severe droughts over most of eastern Africa. One of the main features of the observed minimum and maximum temperature patterns was however the recurrences of extremely high/low temperature values.

The lowest values of the minimum and maximum temperature records were observed in 1943/44, 1952, 1956, 1958, 1961/62, 1965, 1972, 1974, 1976, 1978, 1986, and 1990/91 years whilst the highest values were recorded in 1940/41, 1947, 1955/56, 1959, 1966/67, 1969/70, 1972/73, 1977/78, 1983/84, 1989, and 1991/92. Most of the years observed to have registered the highest minimum and maximum temperature values are known to coincide with **El-Niño** years like 1962/63, 1965, 1967, 1972, 1974, 1976, 1978, and 1983/84, whilst most of those that registered the lowest temperature values were **La-Nina** years. The above observed recurrence patterns also show recurrences of extremely high/ low temperature values every 2- 3 years, which falls within the period of the QBO. It is possible therefore that most of the observed recurrences of extremely high/ low minimum and maximum temperature values may be indicative of both ENSO and QBO signals inherent in the inter-annual temperature characteristics.

The results of the statistical analysis of the observed trends are summarised in Table 1. These results generally agree with those of the graphical approach in as far as the sign of temperature change is concerned. Many temperature changes that were apparent from the graphical analysis were, however, found not to be statistically significant from the statistical tests. The results, like those of the graphical approach, show significant seasonal and geographical variations in warming/cooling over the tropical Eastern Africa region in recent years. It is worth noting here, that some of the island, coastal, and lake stations like Kisumu, Mombasa, Lamu, Moroni, Xai-Xai,

TABLE 1: OBSERVED RATES OF TEMPERATURE CHANGE

Stn.	Temperature change rate in Degrees C per decade							
	JAN		APR		JUL		NOV	
	Min T	Max T	Min T	Max T	Min T	Max T	Min T	Max T
KASS	0.29+	-0.07	0.35	-0.17	0.47*	0.50+	0.66*	-0.16
KADU	0.08	-0.48+	0.49	-0.12	-0.16	-0.37#	-0.25+	0.49*
ELFA	0.21	-0.37	0.06	-0.22	0.25+	0.50+	-0.24	-0.45
KHAR	-0.31	-0.08	0.02	-0.22	0.35+	0.30	0.27+	-0.01
ATBA	0.10	-0.32	0.02	-0.21	-0.32	0.85+	0.17+	0.08
PORS	0.04	-0.07	0.12	0.15+	0.14	-0.41#	0.40*	-0.44
ASMA	-1.00*	0.32	-1.30*	-0.12	-0.97*	0.52	-0.84*	0.34#
COMB	-0.66	0.06	-0.63+	0.19+	-0.67	0.12	-0.51*	0.37#
DEBR	0.65*	0.06	0.74*	0.19	0.34+	0.12	0.53*	0.10
ADDS	-0.04*	0.10+	0.48	-0.16*	-0.22*	0.17*	0.08	0.59#
DIRE	0.25	-0.25	0.70*	-0.31	0.14*	0.23	0.34	-0.06
NEGH	-0.21+	0.13	0.14	-0.09	-0.18*	-0.11	-0.25#	0.27
LODR	-0.02	0.23	0.04	0.15	0.12*	0.12+	0.03	0.23*
MOYA	-0.01	0.13+	0.18*	0.14	0.25*	0.13+	0.08	0.05
WAJI	0.34*	0.26*	0.27*	-0.05	0.36*	0.05	0.38*	-0.06
KSMU	0.01	-0.11	0.04#	0.04	-0.06	0.22*	-0.08	-0.09
GARI	0.18*	0.07	-0.05	-0.14+	0.02#	-0.06	0.02	-0.11
DAGO	0.70*	0.27+	0.34*	0.03	0.86*	0.22	0.60*	0.09
MADU	0.20#	0.03	0.07*	0.00	0.21*	-0.09	0.23#	0.09
LAMU	-0.10#	0.54*	-0.10+	0.37*	0.16	0.03	-0.17*	0.55
MOSA	-0.03	-0.11	0.02	-0.08	0.02	-0.01+	0.08	-0.05
MBAR	0.35#	0.55+	0.25*	0.55*	0.78*	0.47#	0.35#	1.10*
BUJU	0.33*	0.04	0.41*	0.16	0.04	0.09	0.64*	0.06
MUYI	-0.11	-0.07	-0.31*	0.05	-0.14	0.29	-0.12	0.32
MORO	0.19	0.25	0.45	0.16+	0.24	0.19	0.28*	0.52+
KARI	0.31*	0.70*	0.41*	0.42	0.15	0.11	0.32	0.54+
MUTO	0.19*	0.50*	0.05	0.26+	0.09	0.32*	0.09	0.28#
MWIN	0.04	0.20#	-0.08	0.23	0.25+	0.23	0.07	0.35#
KASA	0.00	0.33*	-0.11	0.37*	-0.02	0.34*	-0.24+	0.00
ZAMB	-0.18	0.14*	-0.31#	0.07	-0.61*	0.42*	-0.36*	0.25*
NDOL	0.31*	0.38*	0.29*	0.31#	0.47*	0.54*	0.18+	0.32*
CHIP	0.33#	0.32*	0.24+	0.03	0.17+	0.26#	0.00	0.02
LUSA	0.35*	0.69*	-0.42*	0.23	-0.61*	0.25*	-0.18	0.49*
LIVI	0.22	0.40*	-0.08	0.10	-0.30*	0.11	0.22+	0.44*
PEMB	-0.07*	-0.38*	-0.90*	-0.51*	-0.01*	-0.65*	-0.71*	-0.59*
LICH	-0.27+	0.07	-0.04	0.07	0.17+	0.01	-0.27+	-0.19#
NAMP	0.65*	0.14	0.50*	0.02	0.36*	0.20	0.37*	-0.18
QUEL	-0.35*	-0.08	-0.30*	-0.33*	-0.36*	-0.16	-0.55*	-0.18
INHA	-0.37*	0.22	-0.43*	0.03	-0.40*	0.05	-0.37*	-0.14
XAI-	0.22	0.14	0.21+	0.03	0.48*	0.00	0.13	-0.05
MAPU	0.19	0.34*	0.19	0.18	0.35*	0.27*	0.03	-0.07
AGAL	-0.07	0.05	-0.05	0.13	-0.12	0.07	-0.43*	0.23
SBRA	0.08	-0.12	0.17+	-0.20+	0.17	-0.23#	-0.05	-0.29
RODR	0.08	0.22	0.14	0.40*	0.30*	0.47*	0.11	0.26
PLAI	0.17*	0.06	0.28#	0.20*	0.23*	0.20*	0.43*	0.25#
VACO	-0.17	0.11	0.27+	0.14	0.21+	0.34*	0.31#	0.11+
FRAN	-0.11	0.63	-0.72	0.19	-0.62	0.57	-0.37	0.24
MAHA	0.34+	0.30	0.26	0.82	0.30	0.98	0.18	0.30
TSHA	0.22+	0.22	0.36	0.18	0.28	0.43*	0.10	0.04+
TSAB	0.05	-0.30	0.89*	0.32	0.09	0.41	-0.56*	0.00
BIGB	0.12	0.21	0.08	0.45#	0.04	0.21	-0.11	0.05

LEGEND: *, # and + imply Confidence levels of 97.5%, 95%, and 90% respectively.

Agalega, Plaisance and others, have experienced opposite temperature trends to those of the mainland stations. Such stations have local moisture sources and are therefore not often affected by the many droughts that significantly affected the observed minimum and maximum temperature patterns over the rest of the study region.

The observed spatial patterns of warming/cooling trends for the four major seasons of the year are given in Figure 8. The isopleths represent the sign of the temperature change and its statistical significance. Confidence levels greater than or equal to 95% are shaded.

Figure 8 (a) shows that a greater part of tropical Eastern Africa has experienced night-time (minimum temperature) warming during the January season as indicated by positive trends with confidence levels ³95%. Significant negative minimum temperature trends (cooling) are shown to be confined only to the south of 10°S between longitudes 20°E and 35°E. The maximum temperature trends for the same season are given in Figure 8 (b). The day-time temperature values are shown to have either remained constant or decreased over most of the Eastern Africa region. The only area of significant maximum temperature rises is to the west of 35°E and south of 5°S.

Similar patterns of night-time temperature trends are maintained for the April and July seasons (Figure 8 c and e). The area between 5°S and 15°N is shown to have predominantly experienced higher than normal minimum temperature values in recent years. Opposite signals are however discernible over the area to the south of 5°S between longitudes 20° and 35°E. Negative trends in the minimum temperatures are also evident over the northern margins of Ethiopia and Sudan, but the patterns are not as well maintained as those for the eastern coast of southern Africa.

The day-time temperature change patterns for January are maintained for the April season (Figure 8 d), with the only area of significant increases remaining to the west of 35°E between 5° and 25°S. The pattern is slightly altered for July (Figure 8 f), with the south eastern part of the

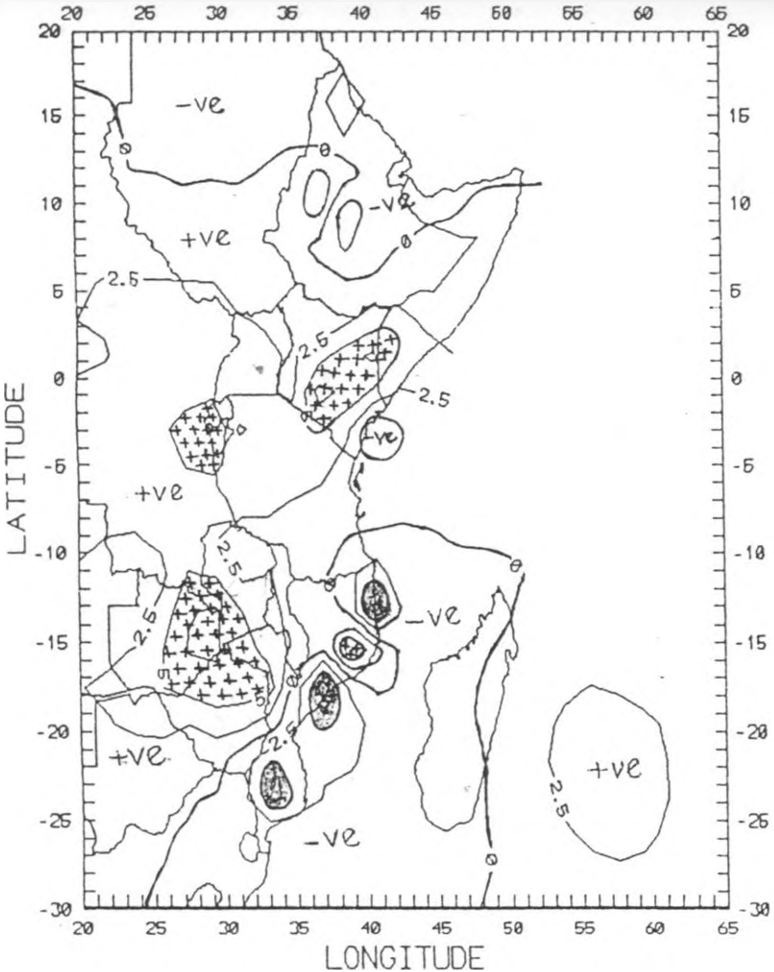

Figure 8a: Observed minimum temperature trend patterns for January

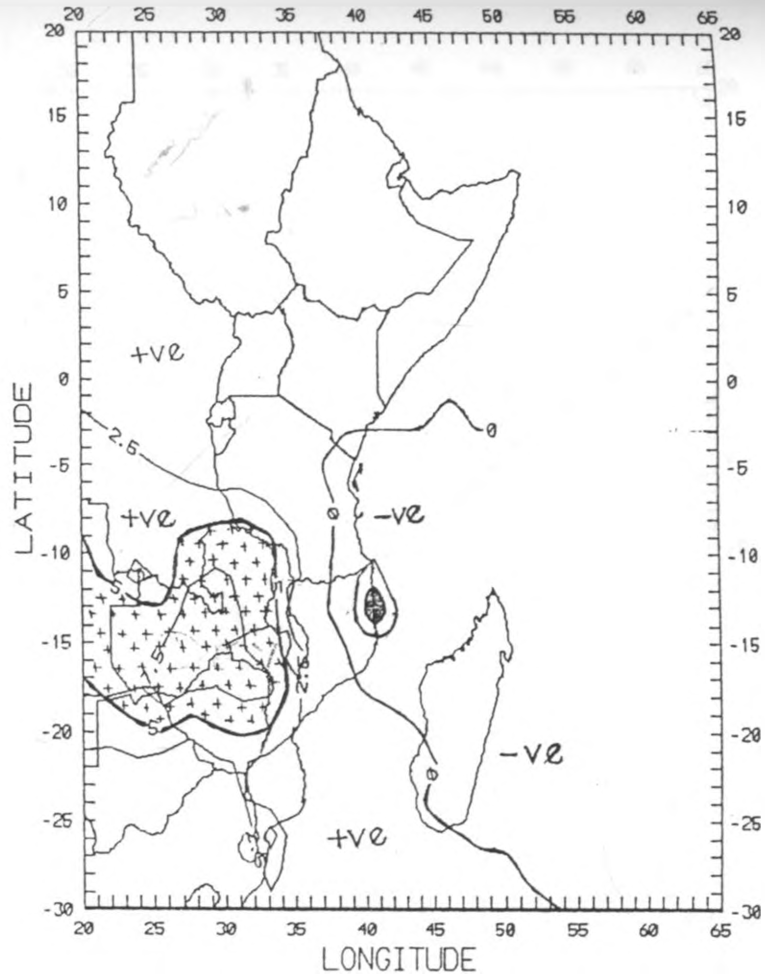

Figure 8b: Observed Maximum temperature trend patterns for January

NOTE: Isopleths represent both the sign and confidence levels of change: e.g. an isopleth of -5/+5 implies a negative/positive trend at the 95% c.l.; '0' implies either negative or positive trends at ≤90% c.l. Confidence levels ≥95% have been shaded.

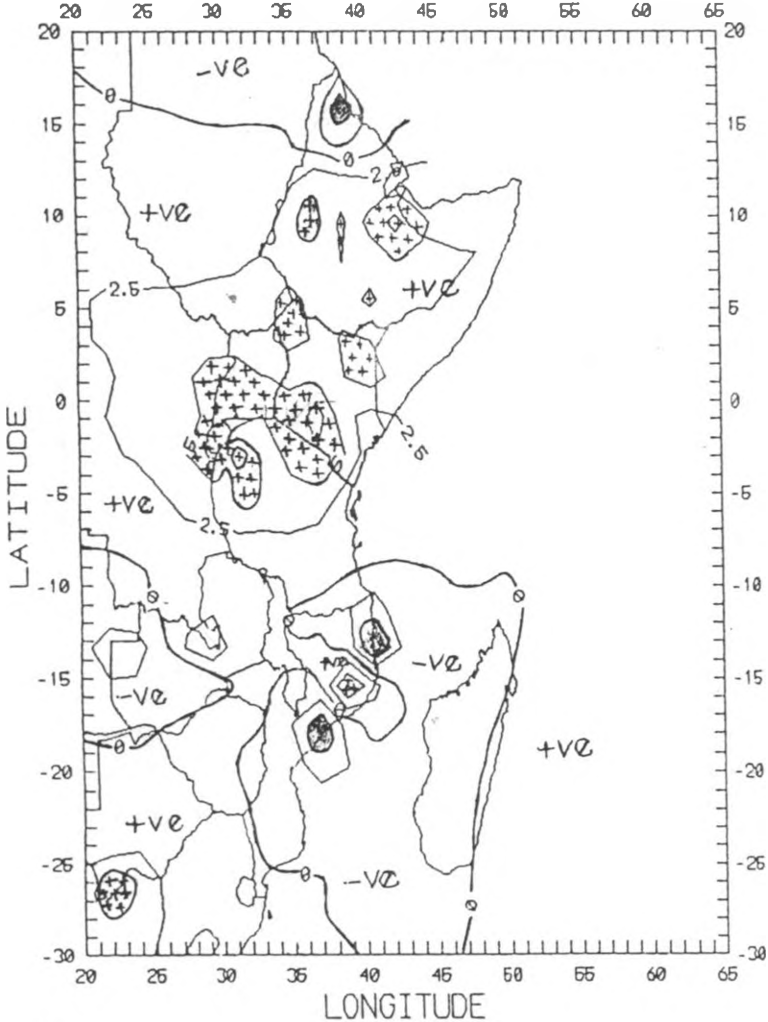

Figure 8c: Observed minimum temperature trend patterns for April

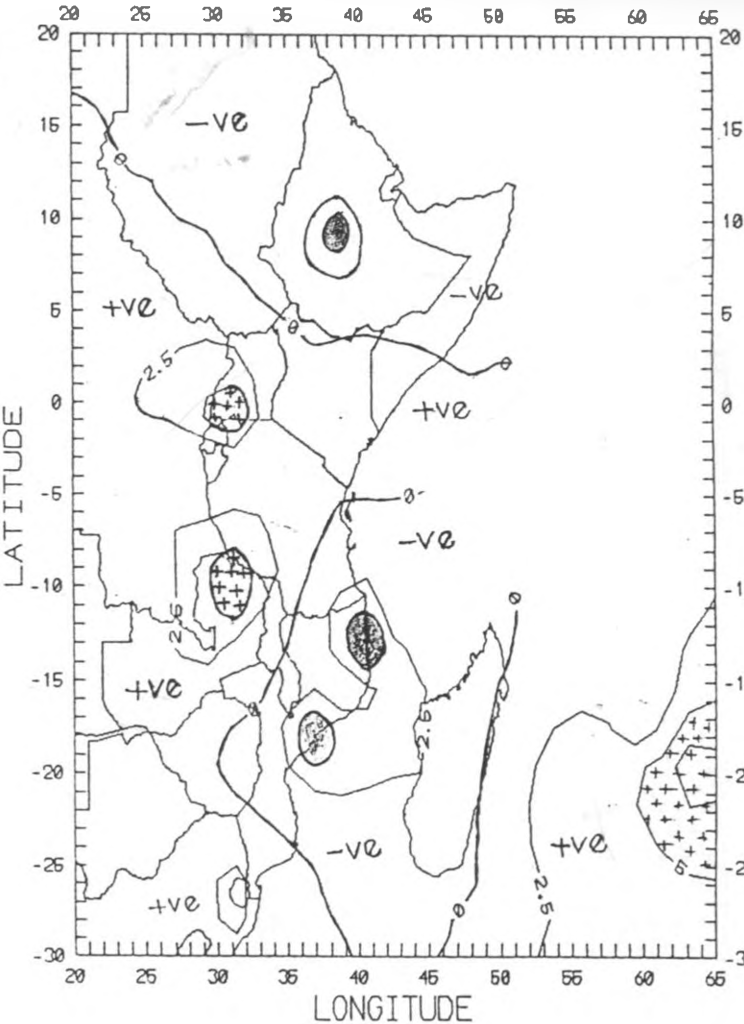

Figure 8d: Observed maximum temperature
trend patterns for April

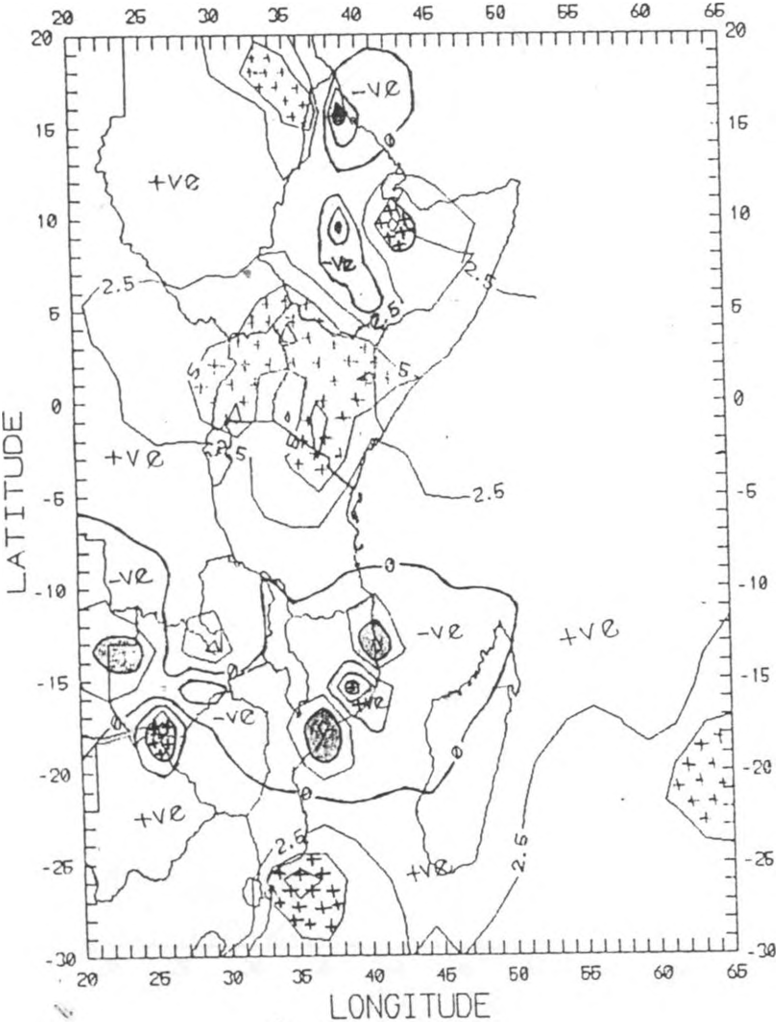

Figure 8e: Observed minimum temperature trend patterns for July

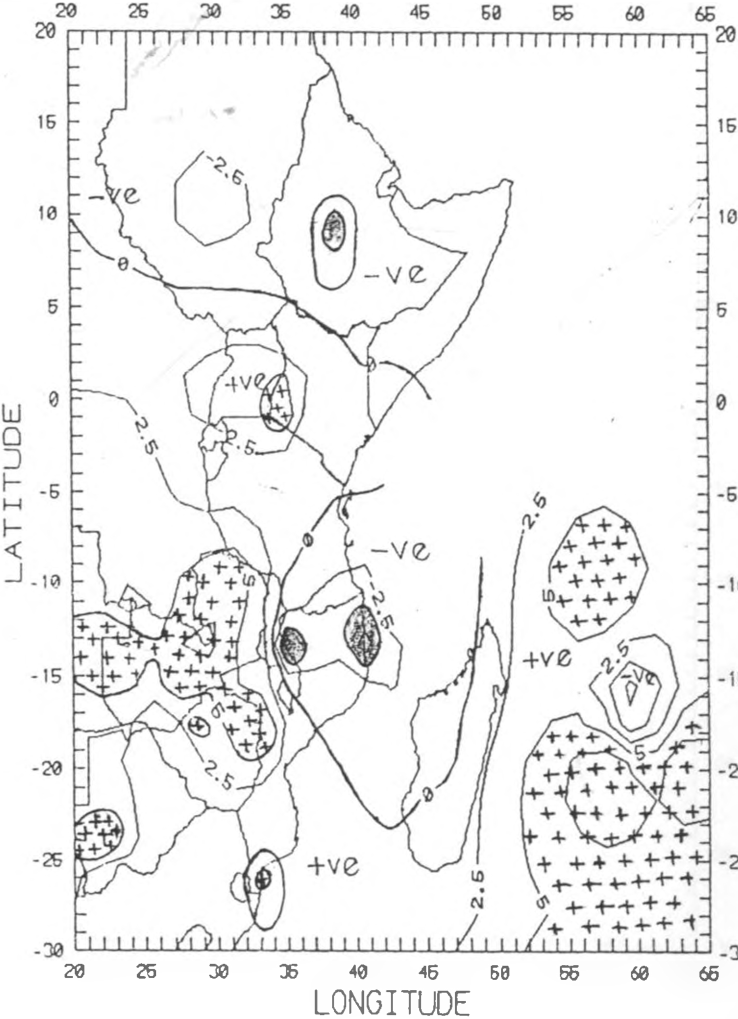

Figure 8f: Observed maximum temperature trend patterns for July

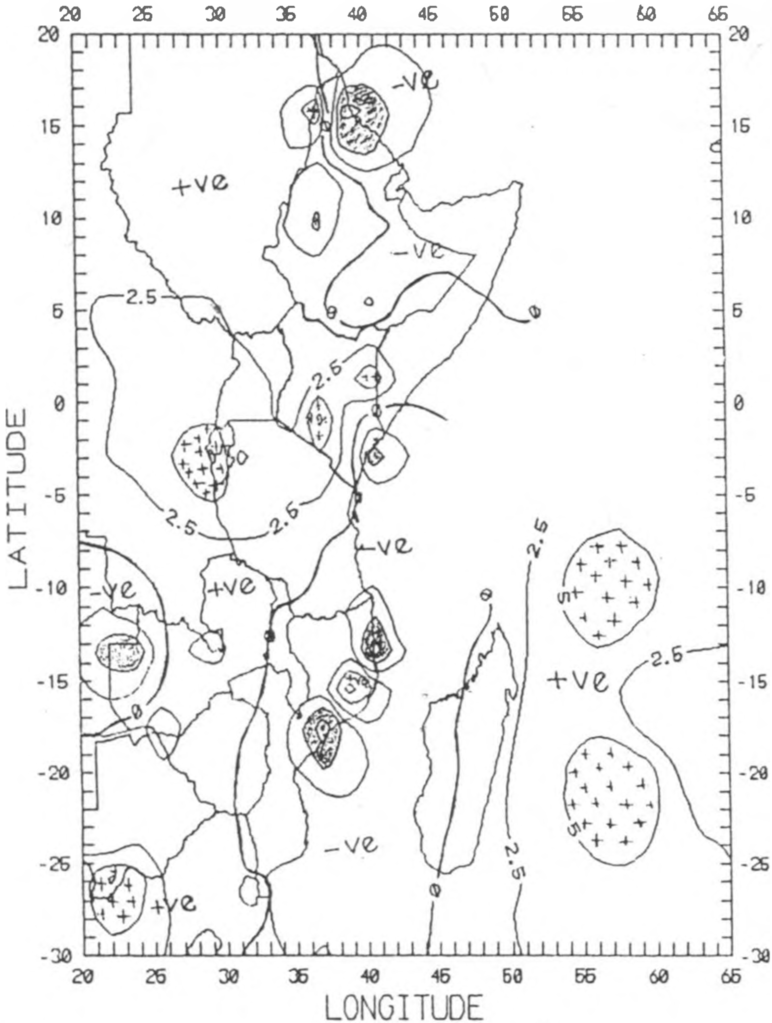

Figure 8g: Observed minimum temperature trend patterns for November

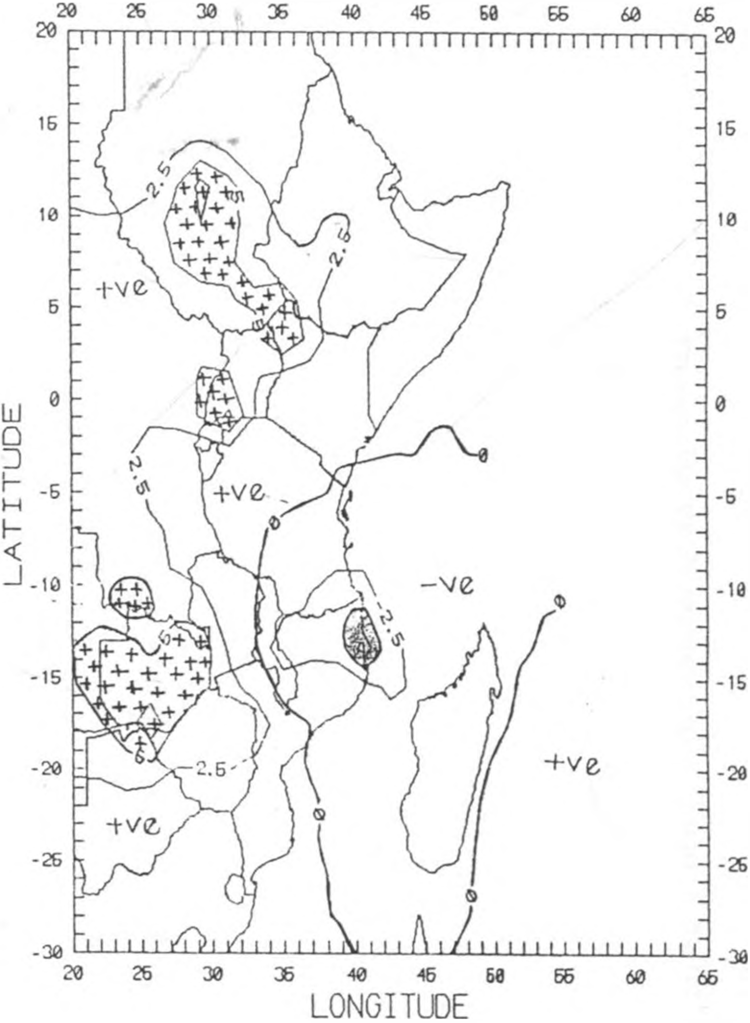

Figure 8h: Observed maximum temperature trend patterns for November

Indian ocean showing significant increases. For the November season (Figure 8 h), the pattern shows a meridional alignment with positive trends confined to the west of 35°E and negative ones to the east.

An important feature of the spatial distribution patterns is the area between 15°N and 5°S, which is shown to have been dominated by positive trends in the minimum temperature values and either no change or negative trends in the maximum temperature for all the four seasons of the year. Figure 9 gives a typical example of the observed temperature range series from this region. In general, the results indicate that the range between the diurnal minimum and maximum temperature values within 5°S and 15°N has been decreasing in recent years. This is as indicated by the observed relatively higher rates of increase in the minimum temperature values than the corresponding rates in the maximum temperature values. These patterns compare well with the observations by Karl *et al* (1988), Karl (1991), and Kukla and Karl (1992), who found that the gap between the minimum and maximum temperature values has been decreasing over the U.S.A., the U.S.S.R., and the Peoples' Republic of China (PRC) in recent years.

Urbanization has been cited as the main cause of warming at local scales, especially where the minimum temperature values are rising whilst those of the maximum temperature are constant or falling (Karl *et al*, 1991; Kukla and Karl, 1992). Karl *et al* (1988) found that urbanization decreases the daily maximum temperature in all seasons apart from winter, decreases the diurnal temperature range in all seasons, and increases the diurnal minimum temperature in all seasons.

No comprehensive analysis was performed in this study to delineate urbanisation effects. Preliminary investigations using population estimates for the 1980's, when peak warming signals were observed in most of the Kenyan stations however, showed that small urban centres with populations of less than 2,000 inhabitants like Moyale, Wajir, Garissa, and Makindu showed

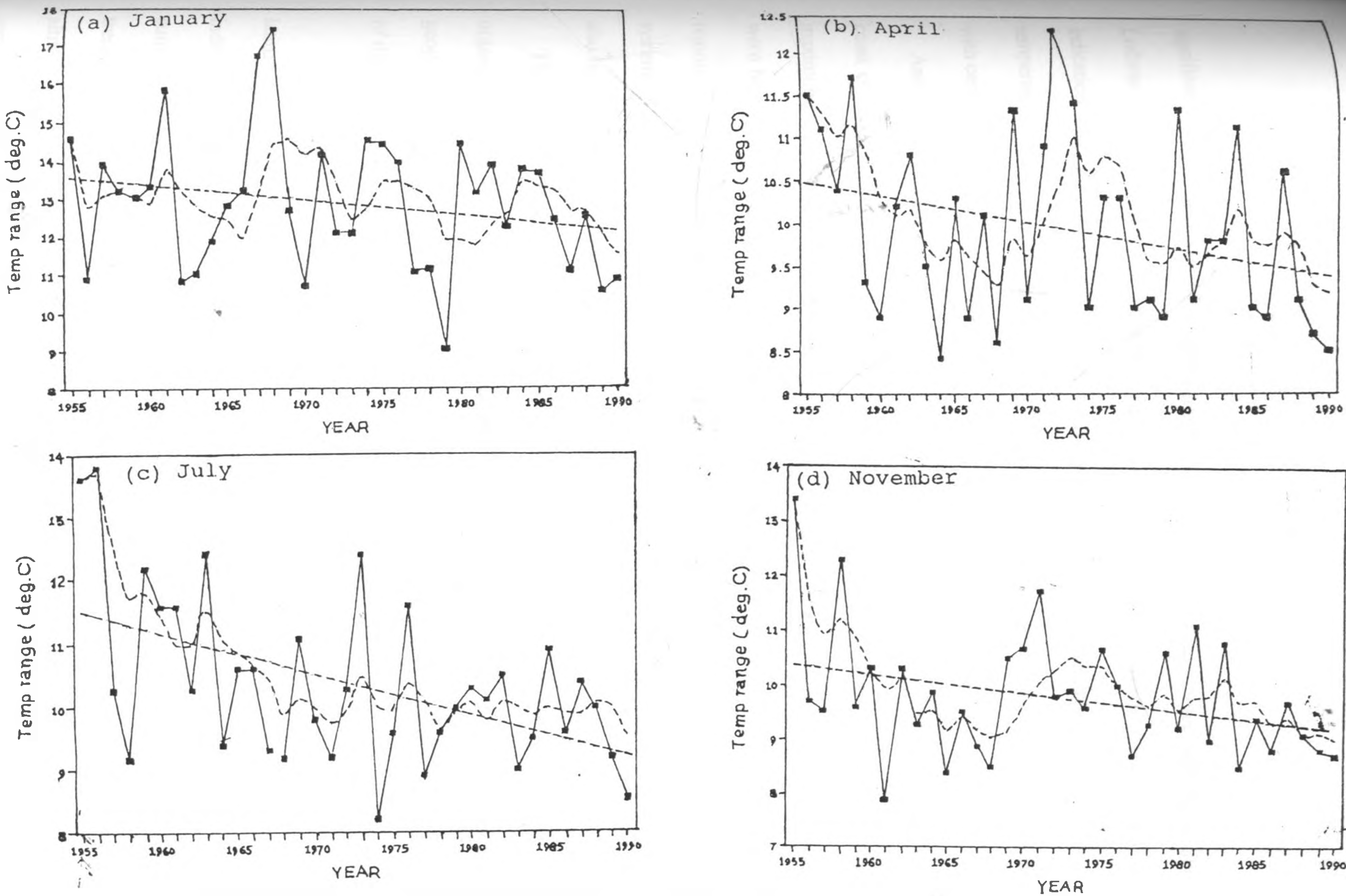

Figure 9: Observed temperature range time series for Dagoretti, Kenya.

significant positive minimum temperature trends whilst other centres with larger populations like Lodwar, Lamu, Kisumu, and Mombasa did not show any significant trends. This may be an indication that apart from urbanisation, other systems may be responsible for the observed temperature trends. A more elaborate approach would however be required in order to delineate with certainty the impacts of urbanisation on the observed temperature trends.

Another important feature of the spatial distribution of warming/cooling is the area around the coast of Mozambique which seems to have experienced decreasing trends in both minimum and maximum temperature values. Extremely high/low minimum and maximum temperature values were however recurrent within the period of study. Most of the temporal variability around this region has been found to be closely related to variability in ENSO and other rainfall generating systems (Ogallo, 1993a, 1993b). Lower temperature values over the Mozambique channel may also be indicative of a weakening of the Agulhas warm current (Hastenrath, 1985).

The spatial distribution of the temperature trends over the southern Africa region is not as well organized as that of the area to the north of 5°S. Over southern Africa, there are significant geographical variations from one location to the other. This is however in line with the observations of the IPCC (1990, 1992a, 1992b).

Correlation coefficients between the observed temperature trends and the station altitude, latitude and longitude were computed to examine if the physical and geographical position of individual stations may have had significant influence on the observed trends. The results are summarised in Table 2(a). The simple correlation coefficients between the observed temperature trends and both altitude and longitude were generally not statistically significant. The station altitude and latitude therefore, did not seem to play any significant contribution in the observed temperature trends.

Table 2 (a): Correlation between the observed temperature values and altitude, Latitude, and Longitude

	January		April		July		November	
	Min.T	Max.T	Min.T	Max.T	Min.T	Max.T	Min.T	Max.T
Altit.	0.060	0.172	0.106	-0.047	-0.176	-0.047	-0.095	0.167
Latit.	-0.039	-0.275 *	0.076	-0.097	0.052	-0.310 *	0.050	-0.028
Longi.	-0.039	-0.340 **	0.022	0.165	0.138	0.066	0.119	-0.219

LEGEND: * , ** imply confidence levels of 95%, and 99% respectively.

Table 2 (b): Correlation between the observed minimum and maximum temperature trends for January, April, July, and November.

	January		April		July		November
	Min T	Max T	Min T	Max T	Min T	Max T	Min T
Jan Max T	0.396*						
Apr Min T	0.571*	-0.017					
Max T	0.493*	0.256#	0.325*				
Jul Min T	0.501*	0.023	0.659*	0.500*			
Max T	0.353*	0.540*	0.055	0.567*	0.147		
Nov Min T	0.632*	0.016	0.671*	0.325*	0.596*	0.143	
Max T	0.298#	0.539*	0.054	0.296#	0.143	0.363*	0.132

LEGEND: * and # imply confidence levels of 99% and 95% respectively.

The observed maximum temperature trends for both January and July were however found to have statistically significant negative correlation with the station latitude at the 95% confidence level. This implies that as one moves towards the south within Eastern Africa, the maximum temperature trends become dominantly positive whilst towards the north, negative maximum temperature trends dominate

The results of the study further showed that Simple correlation coefficients between the January minimum temperature trends and those for April, July, and November were all positive and significant at the 99.9% confidence level (Table 2b). This implies that those areas that showed significant nigh-time warming/cooling for January had high chances of showing similar trends for all the other seasons of the year.

The following section presents the results of seasonal characteristics on the minimum and maximum temperature values as derived from harmonic analysis.

3.4 SEASONAL VARIATIONS

The results of harmonic analysis indicated the dominance of the annual and semi-annual cycle on the seasonal temperature characteristics. The two cycles accounted for more than 85% of the seasonal temperature variation at most locations, with the annual cycle accounting for more than 50% of the total variation. The dominance of the bi-modal and uni-modal distribution of seasonal temperature peaks at equatorial locations and those locations further away from the equator respectively, are reflective of the seasonal passage of the over-head sun. This is attributable to the earth's revolution around the sun and the tilt of its axis of rotation about its orbital plane. It is however worth noting that, even at equatorial locations, the annual temperature cycle seems to dominate over the semi-annual one.

The harmonic analysis results further showed that although there were significant inter-annual variations in the amplitude of the oscillations, no statistically significant changes were detected in the inter-annual patterns of the time of occurrence of temperature maximum. Figure 10 (a) gives the typical patterns of the observed inter-annual characteristics of the amplitudes for Zambezi in Zambia (13°32'S, 23°07'E, 1077 m a.m.s.l.) and Garissa in Kenya (00°28'S, 39°38'E, 138 m a.m.s.l.). Zambezi has a uni-modal temperature distribution with peak temperature observed in February, whilst Garissa has a bi-modal distribution with a major peak in March and a minor one in October (Figure 10a iii). Both stations show significant inter-annual variability in the amplitudes. Similar characteristics were reflected in the observed inter-annual variations of the minimum and maximum temperature values (Appendix iii).

Figure 10(a) shows that the annual temperature cycle may have been amplified during **El-Niño** and anomalously dry years like 1965/66, 1969, 1973, 1977, 1980, 1982/83, and 1989/90. During La-Nina and anomalously wet years like 1947, 1951, 1957, 1961/62, 1967/68, 1970, 1981, 1985/86, and 1991, the cycle was apparently less amplified. The temperature distribution

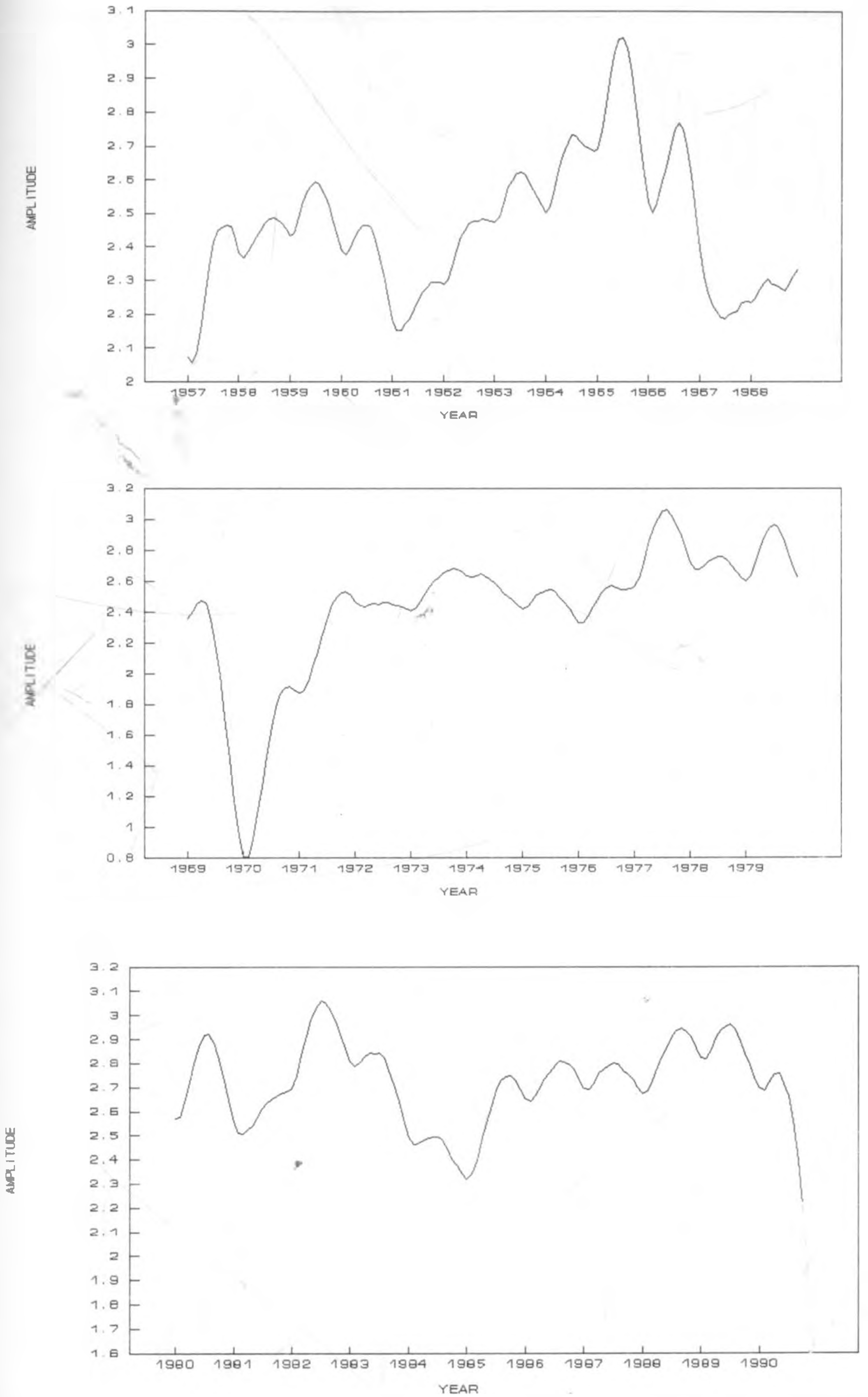

Figure 10 a(i): Interannual fluctuation of the first minimum temperature amplitude at Zambezi (Zambia), 1957-1990

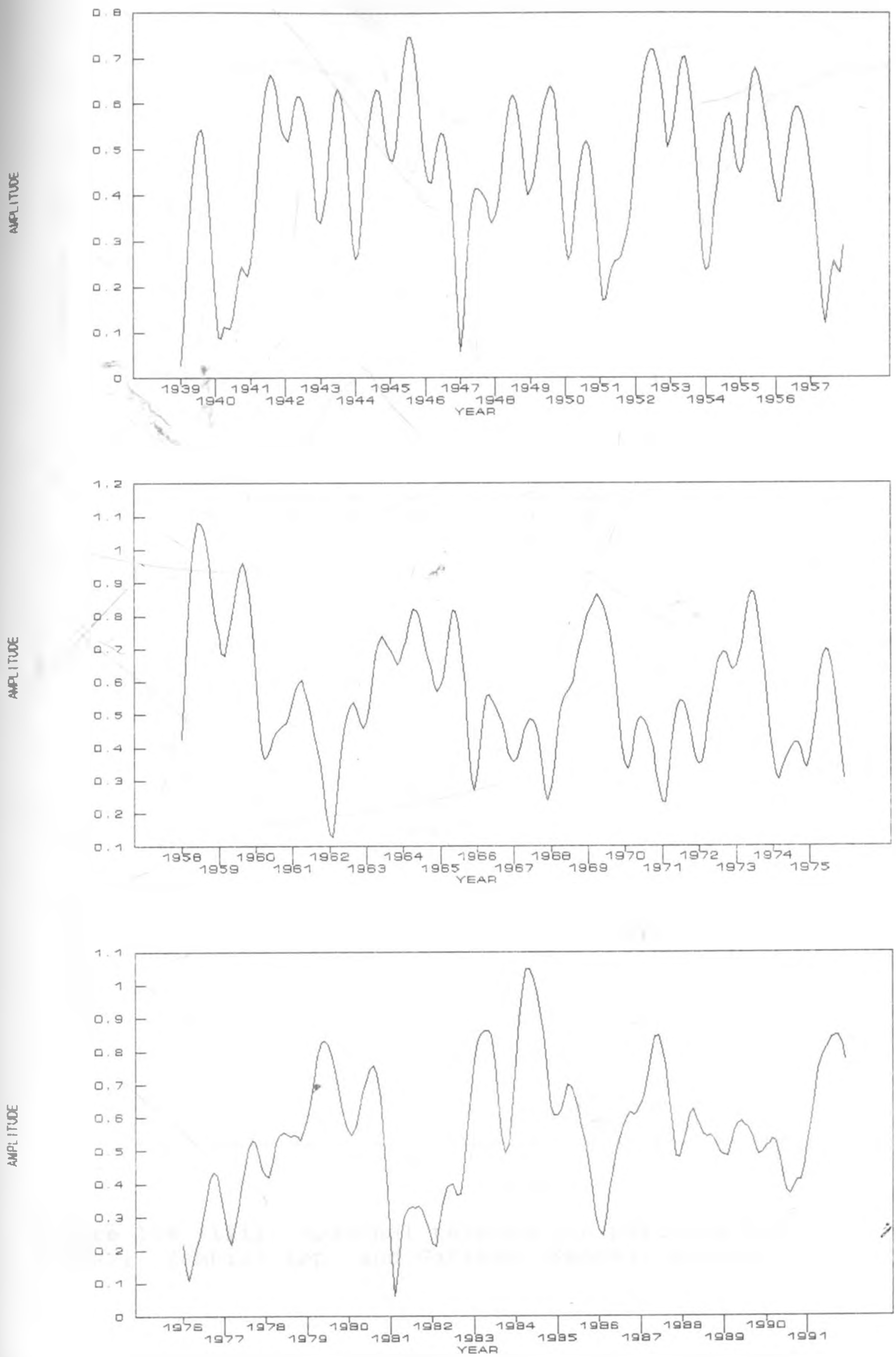

Figure 10a (ii): Interannual fluctuation of the first maximum temperature amplitude at Garissa (Kenya), 1939-1991

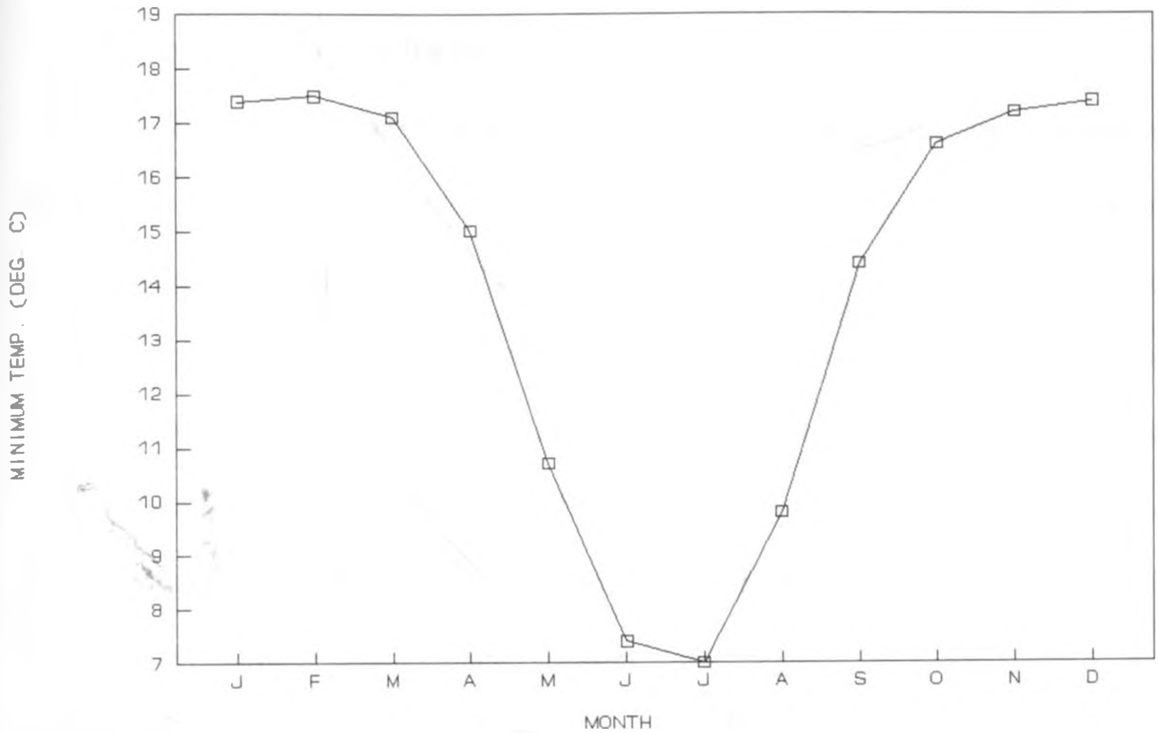

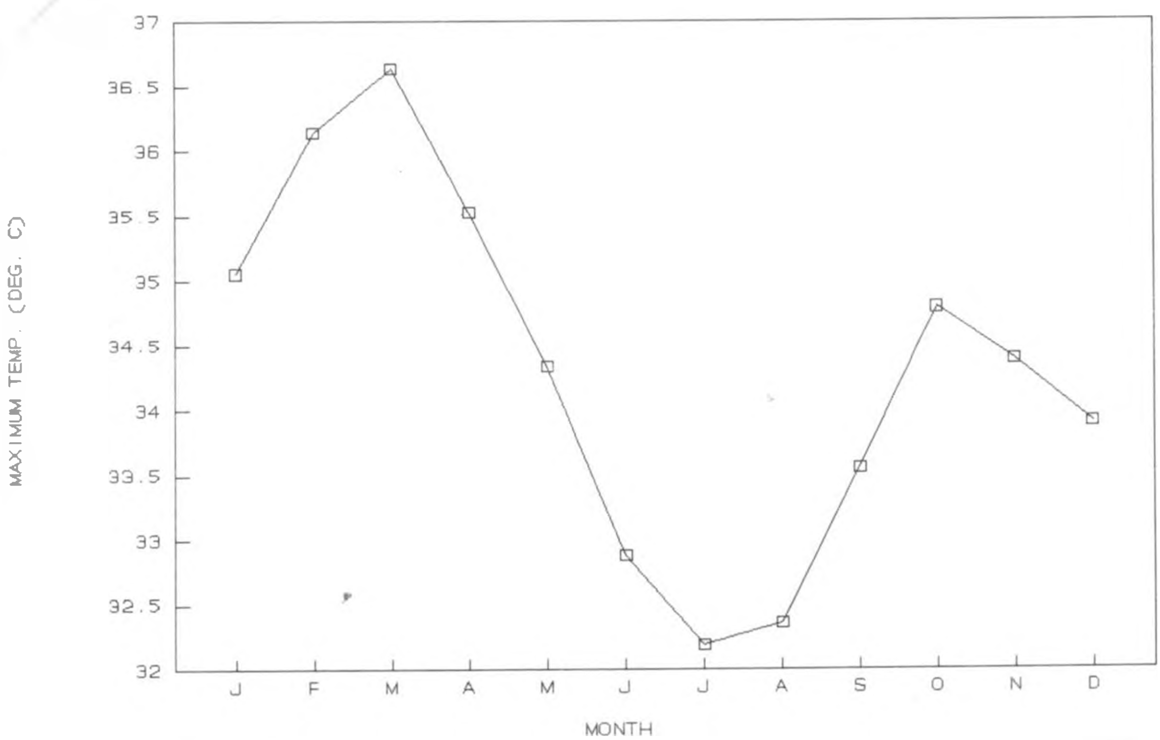

Figure 10a (iii): Seasonal temperature patterns for Zambezi (Zambia),top, and Garissa (Kenya), bottom for Zambezi is skewed, with a greater part of the year recording above normal temperature values as can be seen in Figure 10a (iii).

The patterns of the observed time of occurrence of temperature maximum is shown in Figure 10 b. The inter-annual patterns of the time of occurrence of temperature maximum reflect the inter-annual changes in the temporal location of seasonal temperature peaks. The results from this study however indicated significant inter-annual variations in the patterns of the time of occurrence of temperature maximum of the two dominant cycles. No statistically significant seasonal shifts could however be detected from the study. Late or early occurrences of cold and warm spells are quite common in the region as reflected in the inter-annual patterns of the time of occurrence of temperature maximum.

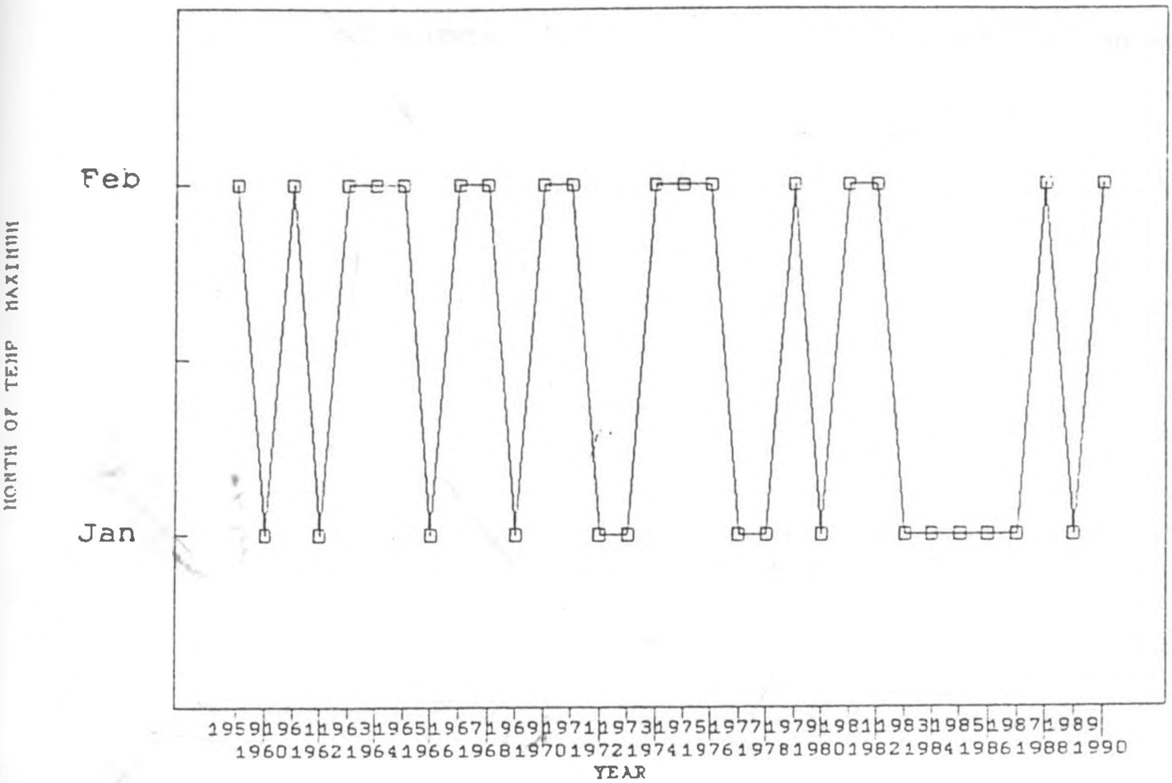

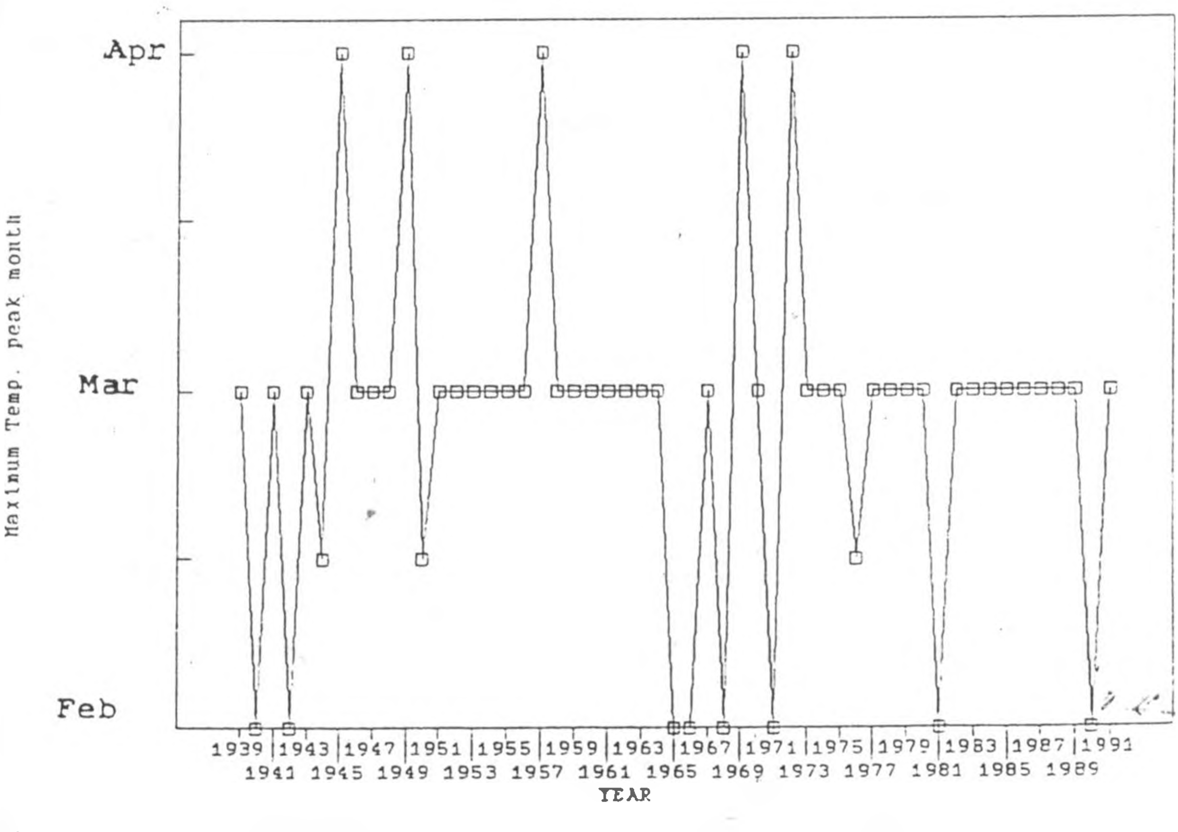

Figure 10 b: Interannual fluctuation in the time of occurence of temperature maximum at Zambezi in Zambia (top) and Garissa in Kenya (bottom)

3.5 CYCLICAL VARIATIONS

Results of spectral analysis revealed the existence of various quasi-periodic fluctuations in the inter-annual patterns of the extreme temperature records. Most of the stations showed the dominance of periodicities of 2.0 - 2.9 years. Other quasi-periodic fluctuations that were common in most of the series are 3.0 - 4.0 years, 4.5 - 6.5 years, and 10 - 12.5 years. Figures 11 (a) and (b) show typical patterns of the Spectral density functions which were observed when the minimum and maximum temperature values were subjected to the Maximum Entropy Method of spectral analysis. The spectral peak centred around 10 - 12.5 years was not statistically significant at the 95% confidence level at most locations when the White noise hypothesis was used. Such spectral peaks have been observed in many other weather parameters over East Africa (Rodhe and Virji, 1976, Ogallo, 1982, 1988; Nyenzi, 1992).

The first three quasi-periodic fluctuations accounted for the highest proportions of the total inter-annual temperature variance. There were however significant geographical and seasonal variations in the variance explained by each of the observed spectral peaks. The total variance accounted for by all the spectral peaks was however less than 50%. This indicates that quasi-periodic fluctuations cannot account for most of the inter-annual variance of the minimum and maximum temperature values. The predictability of the inter-annual variations of the minimum and maximum temperature values using periodic fluctuations would thus have low skill.

The 2 - 2.9 year spectral peak has been associated with the reversal of easterly/westerly phases of the tropical stratospheric winds (QBO). Relationships between East African rainfall and QBO has been discussed by Ogallo *et al* (1994) whilst correlations between the observed minimum and maximum temperature values and QBO will be discussed in the following section.

(a)

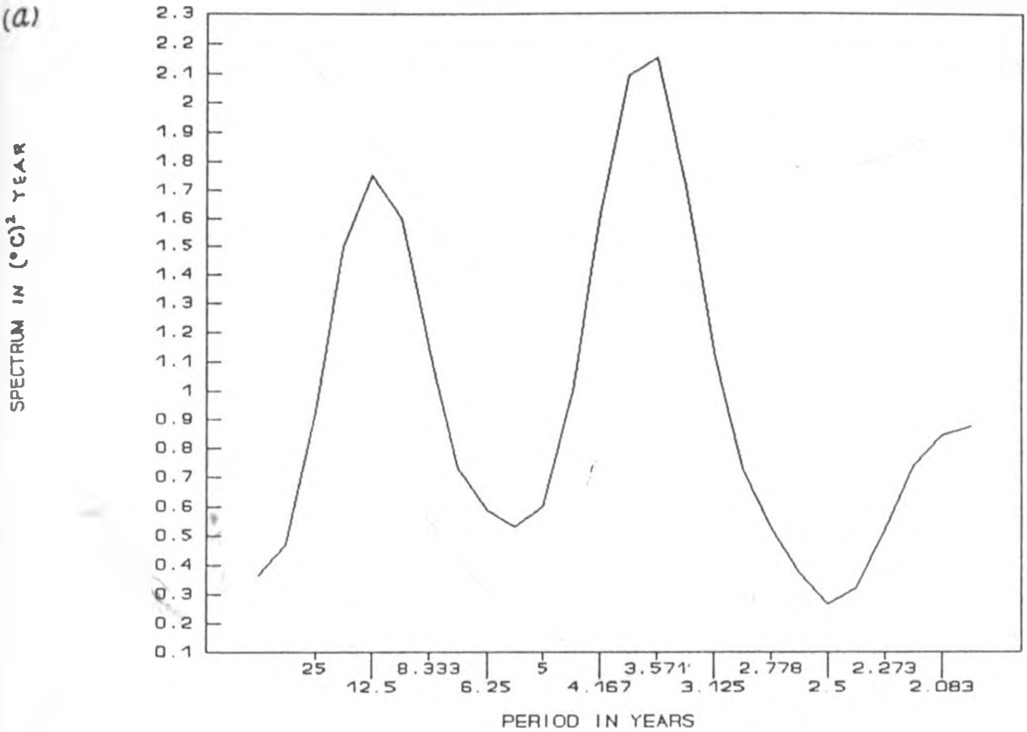

(b)

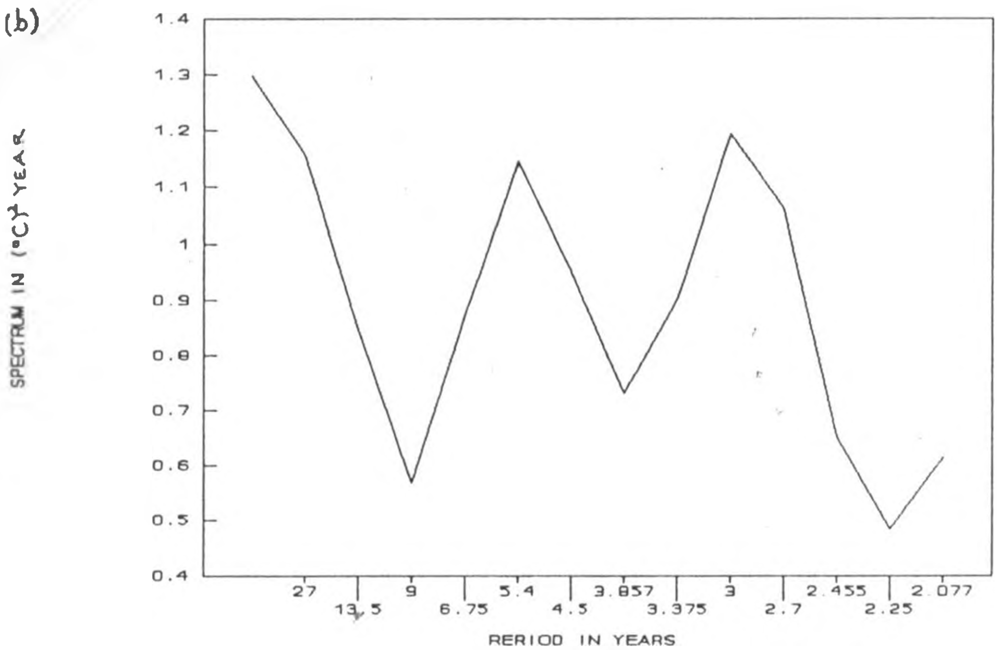

Fig. 11: Spectral cycles (a) Lamu, Kenya (b) Kariba, Zimbabwe

The 3 - 4 and 4 5 - 6.5 years periodicities fall within ENSO cycles. Ogallo (1993a, 1993b) observed that most of the periodicities in the temperature series are closely related to the recurrences of anomalously cold (high)/warm (low) ENSO events. Relationships between ENSO and the observed minimum and maximum temperature values will be discussed in the following section.

The 10 - 12.5 years spectral peak falls within the solar variability cycle. Although this peak was not statistically significant at most of the locations, many authors have discussed its association with the solar variability cycle (Newell *et al,* 1989; Wood and Lovett, 1974; Jagannathan, 1973). Another issue that has been addressed by various authors is whether or not the lower periods are just harmonics (multiples) of the 10 - 12.5 years cycle, which would have the effect of masking the actual variance accounted for by the cycle in the observed data.

Methods are available for filtering out individual spectral bands in order to study them independently This approach was not adopted for use in this study as the study of individual peaks was outside the objectives of the present study. The following section discusses the physical significance of the first three peaks.

3.6 RELATIONSHIPS BETWEEN THE OBSERVED MINIMUM AND MAXIMUM TEMPERATURE VALUES AND GENERAL CIRCULATION ANOMALIES

The general circulation parameters that were used to investigate the relationships between the observed minimum and maximum temperature values and regional/global general circulation anomalies include SOI, QBO, OLR records, and actual cloudiness data for some stations Both correlation analysis and χ^2- tests were used in the study. The next section presents a discussion of the results

3.6.1 RELATIONSHIP BETWEEN THE EXTREME TEMPERATURES AND CLOUDINESS DATA

As indicated in section 3.4, OLR data were used in this study as a proxy for cloudiness and precipitation When OLR data were correlated with the observed minimum and maximum temperatures, only a few stations showed statistically significant simple correlation coefficients. One would generally expect that increased night-time cloudiness would lead to more OLR trapped below the cloud (i.e. less OLR reaching the satellite level) and hence to higher mean surface temperatures and vice versa Thus the negative correlation coefficients between the observed minimum (night-time) temperature and OLR data

Lower/higher cloudiness during the day would lead to more/less incoming solar radiation reaching the surface and the lower atmosphere and consequently to increased/reduced surface and lower atmosphere warming. This would lead to increased/ reduced mean surface maximum temperatures Thus the positive correlation coefficients between the observed maximum temperature and OLR data These results are presented in Table 3(a).

Actual cloudiness data for Nairobi (Dagoretti Corner) and Lamu were also correlated with the observed minimum/maximum temperature data The results of this analysis for Nairobi are

Table 3(a): Correlation coefficients between OLR and Temperature.

STATION	JANUARY		APRIL		JULY		NOVEMBER	
	MINT	MAXT	MINT	MAXT	MINT	MAXT	MINT	MAXT
COMB	-.428	0.714#	.060	.454	.357	.560#	-.469	.347
ELFA	.004	.308	.004	.277	.478	.858*	.026	.249
KADU	.111	.251	-.224	.184	.191	.565#	-.115	.597#
KASS	.327	.219	-.182	-.039	.818#	.113	.315	.406
KSMU	-.062	.759#	-.293	.478	.122	.678#	.198	.306
MOYA	-.345	.816#	.390	.871*	.147	.648#	-.090	.340
MOSA	.009	.219	.155	.311	-.095	.085	.356	.207
MBAR	-.346	-.139	-.758#	.248	.438	-.062	.563#	.365
KASA	-.520	.124	-.536	.243	.340	.492	-.550#	.164
XAI-	-.321	.122	.048	.245	-.067	.168	.266	.551#
NAMP	-.421	.752#	-.122	-.039	-.118	.601#	-.164	.255
TSHA	.685#	.756#	.551	.400	.305	.054	.105	.147

LEGEND: * and # imply confidence levels of 99% and 95% respectively.

Table 3(b): Correlation between the observed temperature and cloudiness data for Dagoretti Corner (Kenya).

	0800GMT cloudiness		1200GMT cloudiness	
	Simple corr,r	C.L./%	Simple corr,r	C.L./%
Min Temp.	-0.353	99.9	-0.335	99.9
Max temp	-0.620	99.9	-0.069	<90
Temp range	-0.344	99.9	0.201	95

summarised in Table 3(b). The results show that morning cloudiness was negatively correlated with the observed minimum and maximum temperature and the subsequent temperature range. Increased cloud cover would lead to less incoming solar radiation reaching the surface, and hence less surface and lower atmospheric warming. This would lead to lower maximum temperatures, and subsequently lower temperature ranges, hence the inverse relationship between the prevailing cloudiness and both the maximum temperature and temperature range.

The χ^2-tests also showed significant relationships between the observed grouped temperature values and the corresponding OLR data at many locations. The results from the grouped records generally agree with those of the simple correlation analysis as derived from the individual observations. An interesting feature of these results is that locations to the north of the study area showed statistically significant relationships between grouped records of OLR and maximum temperature, whilst no significant relationships were found between the former and minimum temperature. These results are summerised in Table 4 (a).

The observed OLR and cloudiness data were also subjected to trend analysis to test if the observed temperature trends could be explained using trends in the cloud cover. Results of this analysis are presented in Table 4 (b). Some locations showed no significant trends in the observed cloudiness. Other locations however, showed statistically significant observed cloudiness (and OLR) trends in recent years. For locations like Kadugli, Kassala, Moyale, Mbarara, Xai-Xai, and Kampala, the observed increasing/decreasing minimum/maximum temperature trends may be explained using positive trends, with the converse also being true.

The following section discusses the relationship between the extreme temperature values and the QBO.

TABLE 4(a): χ^2- TEST BETWEEN TEMPERATURE AND OLR DATA

STATION	MINIMUM TEMP			MAXIMUM TEMP		
	χ-sq	DF	% C.L.	χ-sq	DF	% C.L.
COMB	1.24	1	73.0	6.09	1	97.5
ELFA	4.63	4	67.5	9.87	4	97.5
KADU	4.85	4	67.5	14.81	4	99.0
KASS	2.10	1	85.3	4.67	1	97.0
KSMU	2.94	4	40.0	21.42	4	99.9
MOYA	1.49	4	15.0	20.26	4	99.9
MOSA	4.80	4	67.5	5.25	4	87.5
MBAR	0.43	1	48.0	0.95	1	68.0
KASA	0.42	1	48.0	0.87	1	68.0
XAI-	2.64	1	90.0	1.69	1	81.0
NAMP	3.14	1	92.2	5.41	1	98.0
TSHA	3.51	4	67.5	3.47	4	67.5

TABLE 4(b): Observed trends in the cloudiness and OLR data

Station	OLR/Cloudiness trend January	April	July	November
COMB	0.65*	-0.80**	0.43	-0.07
ELFA	0.46	-0.45	0.02	-0.02
KADU	0.71**	-0.41	-0.02	0.44
KASS	0.66*	-0.90**	0.32	-0.17
MOYA	0.47	-0.49	-0.29	-0.39
MBAR	-0.05	-0.76**	0.06	-0.82**
KASA	-0.66*	0.36	0.31	-0.88**
XAI-	-0.12	0.09	-0.54#	-0.54#
NAMP	-0.43	0.16	0.20	-0.86**
TSHA	0.46	0.43	0.37	-0.42
DAGO	-0.43**	-0.12	-0.16	-0.28
LAMU	0.15	0.30#	0.34*	0.25

LEGEND: **, *, # imply confidence levels of 99%, 95%, and 90% respectively.
NOTE: For Dagoretti and Lamu, actual cloudiness data was used whilst for the rest of the stations, OLR data was used.

3.6.2 RELATIONSHIP BETWEEN EXTREME TEMPERATURE VALUES AND THE QBO

As stated elsewhere, the Nairobi upper air zonal wind phases were used to represent the QBO as have been used in other studies (Ogallo *et al*, 1994). The contingency tables for both grouped minimum and maximum temperature are presented in Table 5. The results show that the associations between maximum temperature and the QBO are much stronger than those between the latter and minimum temperature. This is indicated by the confidence levels of the χ^2-test of greater/less than 95% for maximum/minimum temperature values respectively.

The easterly/westerly phases of the QBO was shown to coincide with below/above normal maximum temperature values. Ogallo *et al* (1994) observed that the westerly QBO phase coincided with wet atmospheric conditions due to moisture inflow from the Indian ocean and the Congo air whilst the easterly phase coincided with dry weather conditions. Warm and wet atmospheric conditions are often associated with moist convective activities whilst dry and cold conditions are associated with subsidence. The results from this study may therefore be indicative of the association of the easterly/westerly QBO phases with subsidence/moist convective activities over the study region.

The following section discusses the relationship between the observed temperature values and the **El-Niño**/Southern oscillation.

Table 5(a): Chi-Square analysis between QBO and min Temp.

		MIN.T ANOMALY			
		cold	normal	hot	Total
QBO PHASE	E	32	6	87	125
	W	48	5	97	150
	Total	80	11	184	275

χ^2 = 1.57 DF = 2 C.l. <95%

Table 5(b): Chi-Square analysis between QBO and max Temp.

		MAX.T ANOMALY			
		cold	normal	hot	Total
QBO PHASE	E	68	4	67	139
	W	51	10	76	137
	Total	119	14	143	276

χ^2 = 5.55 df = 2 C.l. > 99.5%

3.6.3 RELATIONSHIP BETWEEN EXTREME TEMPERATURE VALUES AND ENSO

The computed Simple correlation coefficients between the observed temperatures and the SOI were statistically significant only for some locations at zero time lags. When temperature and SOI were lagged however, most of the computed Simple correlation coefficients were statistically significant. The observed time lags for significant correlations ranged from 2 to 9 months with peak correlations at time lags of 3 - 6 months. Most of the coefficients were negative/positive over locations that are often wet/dry during positive/negative ENSO phases. These findings corroborate those of Pan and Oort (1983), who showed that maximum global temperatures tend to occur 3-6 months after the peak warmth of ENSO. The heat absorbed in the warm tropical Western Pacific during a warm episode is first redistributed to other tropical oceans and later released into the global atmosphere, warming it, hence the time lag. Some of the results are presented in Table 6.

The results of the χ^2- test between the grouped temperature and SOI records are given in Table 7. These results agree very well with those of the Simple correlation analysis.

Typical inter-annual temperature patterns were shown in Fig 7. Anomalies in maximum temperature during the anomalously cold years of 1962/63, 1972, 1988, and 1990 are quite evident in the maximum temperature series for Nairobi (Figure 7). Significantly high minimum and maximum temperature values during the warm ENSO events of 1955, 1966, 1973, 1977, and 1983/84, are also evident.

It may therefore be concluded from these results that the temporal characteristics of the daily minimum and maximum temperature over eastern Africa are closely related to anomalies in the local, regional, and global scale systems like those that have been linked with OLR, cloudiness, ENSO, and QBO. Similar observations have been made by other authors world wide (Ogallo, 1983, 1992, 1993a, 1993b; Nyenzi,1992; Pan and Oort, 1983; Tyson 1993, and others).

The following section gives the summary and conclusions from this study.

Table 6: LAGGED CORRELATION BETWEEN THE OBSERVED TEMPERATURES AND ENSO

STATION	VARIABLE/ MONTH	SOI MONTH	TIME-LAG/ months	Simple corr. r	C.L./ %
MOSA	Min 10	10	0	-0.46	99.5
	MAX 10	10	0	+0.40	99.5
	MIN 7	10	9	-0.42	99.5
KSMU	MIN 10	7	3	-0.44	99.9
	MIN 10	4	6	-0.41	99.5
	MIN 1	1	0	-0.39	99.0
MADU	MIN 7	1	6	-0.33	95.0
	MIN 10	10	0	-0.42	99.5
	MAX 10	4	6	-0.42	99.9
ASMA	MAX 4	1	3	+0.42	97.5
	MIN 10	7	3	-0.45	97.5
	MAX 7	4	3	-0.35	99.9
KHAR	MIN 7	7	0	-0.39,-0.47	98.0,99.9
	MAX 1	1	0	+0.33	99.0
	MIN 7	4	3	-0.43	99.9
SBRA	MIN 1	10	3	-0.50	99.9
	MAX 10	7	3	+0.29	95.0
	MAX 11	11	0	+0.34	97.5
FRAN	MIN 1	4	8	-0.36	97.5
	MIN 1	7,10	6,3	-0.53	99.9
	MIN 7	4,7,10	3,0,9	<-0.30	>95.0
TSAB	MIN 1	7	6	-0.52	99.0
	MIN 4	10	6	-0.40	99.0
	MAX 1	10,11	6,5	-0.65	99.9
AGAL	MIN 1	10,11	6,5	-0.51	99.0
	MIN 7	10	9	-0.43	99.5
	MAX 4,7	11	5,6	-0.43	99.9
MAHA	MIN 1	7,10,11	6,3,2	-0.45	99.9
	MIN 4	11	5	-0.38	99.0
	MAX 1	7,10,11	6,3,2	-0.38	99.9
BUJU	MIN 1	11,10	2,3	-0.38	>99.0
	MIN 4	10,11	6,5	-0.36	>97.5
	MAX 1	10,11	6,5	-0.60	99.9
LODR	MIN 7	4	3	-0.50	97.5
	MIN 4	1	3	-0.34	97.5

Table 7: Confidence levels of the χ^2- test between SOI and the observed minimum and maximum temperature values.

REGION	MIN TEMP VS SOI C.l./%	MAX TEMP VS SOI c.l./%
SUDAN	99.0	95.0
ETHIOPIA	99.9	67.5
KENYA	99.9	37.5
UGANDA	98.0	81.0
BURUNDI	99.5	92.5
ZAMBIA	99.9	99.9
MOZAMBIQUE	92.6	97.0
COMOROS	97.5	99.5
ZIMBABWE	84.0	91.0
BOTSWANA	99.9	99.5
MAURITIUS	99.9	99.5
SWAZILAND	99.5	95.0

3.7 SUMMARY AND CONCLUSIONS

This study showed that minimum and maximum temperature records which were used in the study were of high quality. Heterogeneity has been detected in instrumental records world-wide due to changes in instrument types, changes in observational schedules and methods, and changes in the station environment These data were subjected to several analyses which included trend, cyclical, and seasonal analyses, and analysis to determine the causes of the observed temperature anomalies.

The inter-annual patterns of the minimum and maximum temperature records showed distinct decadal variability signals. The decades of the 1950's and 1960's were relatively cold at most locations whilst those of the late 1970's to the early 1990's were generally warm The 1980's decade was shown to have been the warmest in record The observed inter-decadal patterns were however reversed at some ocean, island, and lake locations

The inter-decadal differences between the mean temperatures of the 1950's to the 1960's and those of the late 1970's to the early 1990's introduced statistically significant linear trends in the inter-annual patterns of minimum and maximum temperature at most locations when the records were subjected to trend analysis Most of the locations to the north of the study region showed statistically significant positive minimum (night-time) temperature trends and either no significant trends or negative trends in the maximum temperature Most locations within this region hence showed decreasing trends in the diurnal temperature range. These results agree with the observations by Karl *et al* (1988), Karl (1991), Kukla and Karl (1992), and Kinuthia *et al* (1991).

Most coastal, island, and lake locations however showed either opposite trends or no statistically significant trends The observed minimum and maximum temperature trend patterns therefore showed a lot of geographical and seasonal variations. These observations are however in agreement with the expectations of the IPCC (1990, 1992).

Results of harmonic analysis showed the dominance of the annual and semi-annual cycles on the seasonal minimum and maximum temperature characteristics. The two cycles explained more than 85% of the total seasonal variation with the annual cycle alone explaining more than 50% of the total seasonal temperature variation. This is indicative of the dominance of the uni-modal and bi-modal seasonal temperature distribution attributable to the double seasonal passage of the ITCZ and the overhead sun

The harmonic analysis results further revealed no significant changes in the amplitude and the time of occurrence of temperature maximums of the first two harmonics. A large degree of inter-annual variations were however revealed. No significant shifts could however be delineated from the seasonal temperature characteristics. The amplitude of the annual cycle seems to have been amplified during **El-Niño** and anomalously dry years.

Results of spectral analysis on the extreme temperature values revealed recurrences of warm/cold episodes centred around 2.0- 2.9, 3.0- 4.0, 4.5- 6.5, 10.0- 12.5. Few spectral peaks with longer periods also appeared but these were not statistically significant at most locations. The 2.0- 2.9 years peak was associated with the QBO whilst those of 3.0- 4.0 and 4.5- 6.5 years were associated with ENSO. The 10- 12.5 years peak was attributed to the solar variability cycle. These quasi-periodic oscillations have been observed in other climate parameters within the region of study (Ogallo, 1988, 1993a, 1993b, Newell *et al*, 1989). The cycles however explained only a small proportion of the total inter-annual minimum and maximum temperature variation.

Simple Correlation analysis revealed statistically significant correlation between OLR data and the observed minimum and maximum temperature records only at some locations. The results generally showed positive/negative correlation between OLR and the observed minimum/maximum temperature values. These results were confirmed by those of c^2-tests. Locations to the north of the study area showed statistically significant relationships between OLR and minimum temperature whilst no significant relationships were observed between the former and maximum temperature. It was also observed that both morning and afternoon cloudiness had significant negative correlations with the observed minimum and maximum temperature and the subsequent diurnal temperature range.

c^2-tests further revealed significant relationships between the observed maximum temperature records and the QBO and no significant relationships between the latter and the observed minimum temperature values. The easterly/westerly phase of the QBO was found to coincide with low/high maximum temperature values. This may be indicative of the coincidence of dry/moist atmospheric conditions with the easterly/westerly QBO phases.

Only few locations showed statistically significant Simple Correlation coefficients between the observed minimum and maximum temperature and ENSO at 'zero' time lag. Most of the locations however showed statistically significant time-lagged correlations, with peak correlations centred around the time lags of 3-6 months.

It can be concluded from the results of this study that some parts of the Tropical eastern Africa region have experienced minimum/maximum temperature warming/cooling in recent years. Preliminary investigations also showed that apart from urbanisation, a larger scale system may be responsible for the observed temperature trend patterns. The prevailing cloudiness, rainfall, QBO, and ENSO were found to have influenced the observed temperature trend patterns.

The findings of this study are of importance to planners and managers of food, agriculture, water, socio-economic, and other climate dependent natural resources. The spatial distribution of these resources is determined by that of climatic parameters, amongst them temperature. These findings will also complement the current global search for models that can incorporate climate change and variability at the regional and local levels.

3.8 SUGGESTIONS FOR FUTURE WORK

As stated in section 3.7, some locations within tropical eastern Africa experienced minimum/maximum temperature warming/ cooling in recent years. Further work needs to be done to ascertain the extent and cause of this warming/cooling. A more elaborate approach is also required in order to delineate the actual effects of urbanisation on the observed inter-annual patterns of the minimum and maximum temperature records. For this to be attained, a better data net work will be necessary. It may be necessary to use Micro-wave Sounding Unit (MSU) records, especially over areas where data were missing in the current study.

It will be necessary also to investigate in more details the nature and cause of the observed inter-decadal temperature variability. Further analysis will also be necessary to establish the exact relationship between the observed minimum and maximum temperature characteristics and human activities like urbanisation, and the effect of the large-scale circulation systems like the QBO, ENSO, rainfall, and the prevailing cloudiness, in order to refine such relationships at the regional and local levels. This will help establish which of these systems is causing warming/ cooling at particular locations. It is only then that proper mitigation steps can be taken.

It may also be important to investigate the cause of the negative temperature trends over the Mozambique channel, with a view to establishing if the Agulhas current may have weakened in recent years.

4.0 ACKNOWLEDGEMENTS

I am greatly indebted to my two supervisors, Prof. L. A. Ogallo and Dr E.K Anyamba for their invaluable guidance during the course of this study. This thesis would not have been what it is without their counsel and correction.

I wish also to acknowledge the part played by the Director of the Kenya Meteorological services, Mr E. Mukolwe, through whose help this scholarship was provided. I am grateful too to all those members of the Kenya Meteorological department whose criticism and encouragement helped shape this study.

I wish also to register my appreciation to the manager and staff of the Drought Monitoring Centre, Nairobi, who availed their computer facilities for data extraction and analysis.

Lastly, I wish to acknowledge the encouragement and other support I received from my wife, Dorothy, and our children through out the course of the study. Their prayers and understanding gave me the required impetus to go on.

There are many other friends and colleagues who helped me in one way or the other at some stage of this study, but who I am not able to mention by name due to limitation of space. To all those I register my gratitude.

APPENDIX i: LIST OF STATIONS USED IN THE STUDY

COUNTRY	CODE	STN.NAME	WMO/No.	LATI.	LONG.	ALT.	RECORD
SUDAN	KASS	KASSALA	62730	15 28 N	36 24 E	500	1957-87
	KADU	KADUGLI	810	11 00 N	29 43 E	499	1957-87
	ELFA	EL-FASHER	760	13 37 N	25 20 E	730	1957-87
	KHAR	KHARTOUM	721	15 36 N	32 33 E	380	1957-87
	ATBA	ATBARA	680	17 42 N	33 58 E	345	1957-87
	PORS	PORT SUDAN	641	19 35 N	37 13 E	2	1957-87
ETHIOPIA	ASMA	ASMARA	63021	15 17 N	38 55 E	2325	1957-87
	COMB	COMBOLCHA	333	15 05 N	39 43 E	1916	1957-87
	DEBR	DEBREMARCOS	334	10 21 N	37 43 E	2440	1957-87
	ADDS	ADDIS-ABABA	450	8 59 N	38 48 E	2324	1957-87
	DIRE	DIRE DAWA	471	9 36 N	41 52 E	1146	1957-87
	NEGH	NEGHELLE	533	5 17 N	39 45 E	1455	1957-87
DJIBOUTI	DJIB	DJIBOUTI	63125	11 33 N	43 09 E	19	
KENYA	LODR	LODWAR	63612	4 07 N	35 37 E	515	1951-90
	MOYA	MOYALE	619	4 32 N	39 03 E	1097	1951-90
	KITA	KITALE	661	1 01 N	35 00 E	1875	1951-90
	WAJI	WAJIR	671	1 45 N	40 04 E	244	1942-91
	KSMU	KISUMU	708	0 06 S	34 45 E	1157	1951-90
	GARI	GARISSA	723	0 28 S	39 38 e	138	1939-91
	DAGO	DAGORETTI	741	1 18 S	36 45 E	1798	1955-90
	MADU	MAKINDU	766	2 17 S	37 50 E	1000	1951-90
	LAMU	LAMU	772	2 16 S	40 50 E	6	1940-91
	MOSA	MOMBASA	820	4 02 S	39 37 E	57	1951-90
UGANDA	MBAR	MBARARA	63702	0 37 S	30 39 E	1413	1960-92
BURUNDI	BUJU	BUJUMBURA	64390	3 19 S	29 19 E	782	1959-89
	MUYI	MUYINGA	397	2 50 S	30 20 E	1755	1966-89
COMOROS	MORO	MORONI	67001	11 42 S	43 14 E	6	1971-90
ZIMBABWE	KARI	KARIBA	67761	16 31 S	28 53 E	718	1963-89
	MUTO	MUTOKO	781	17 25 S	32 13 E	1244	1951-89
ZAMBIA	MWIN	MWINILUNGA	67441	11 45 S	24 26 E	136	1951-89
	KASA	KASAMA	475	10 13 S	31 08 E	1382	1951-88
	ZAMB	ZAMBEZI	531	13 32 S	23 07 E	1077	1956-89
	NDOL	NDOLA	561	13 00 S	28 39 E	1269	1951-89
	CHIP	CHIPITA	581	13 33 S	32 35 E	1028	1951-88
	LUSA	LUSAKA	665	15 19 S	28 27 E	1152	1951-88
	LIVI	LIVINGSTONE	743	17 49 S	25 49 E	985	1951-88
MOZAMBIQUE	PEMB	PEMBA	67215	12 58 S	40 30 E	49	1951-89
	LICH	LICHINGA	217	13 17 S	35 15 E	1364	1951-89
	NAMP	NAMPULA	237	15 06 S	39 17 E	438	1957-90
	QUEL	QUELIMANE	283	17 53 S	36 53 E	10	1951-89
	INHA	INHAMBANE	323	23 03 S	33 38 E	4	1951-89
	XAI-	XAI-XAI	335	25 52 S	35 23 E	14	1951-89
	MAPU	MAPUTO	341	25 55 S	32 34 E	39	1951-90
MAURITIUS	AGAL	AGALEGA	61974	10 26 S	56 45 E	2	1961-90
	SBRA	ST. BRANDON	986	16 27 S	59 37 E	2	1961-90
	RODR	RODRIGUES	988	19 41 S	63 25 E	58	1961-90
	PLAI	PLAISANCE	990	20 26 S	57 40 E	55	1951-90
	VACO	VACOAS	995	20 18 S	57 30 E	423	1961-90
BOTSWANA	SHAK	SHAKAWE	68024	18 22 S	21 51 E	1032	1959-89
	FRAN	FRANCISTOWN	54	21 13 S	27 30 E	1001	1958-89
	MAHA	MAHALAPYE	148	23 05 S	26 48 E	991	1961-89
	TSHA	TSHANE	226	24 01 S	21 53 E	1118	1959-89
	TSAB	TSABONG	328	26 03 S	22 27 E	960	1959-80
SWAZILAND	BIGB	BIGBEND	68396	26 32 S	31 18 E	641	1960-89

Appendix (ii): Observed trends of minimum and maximum temperature.

MIN TEMP

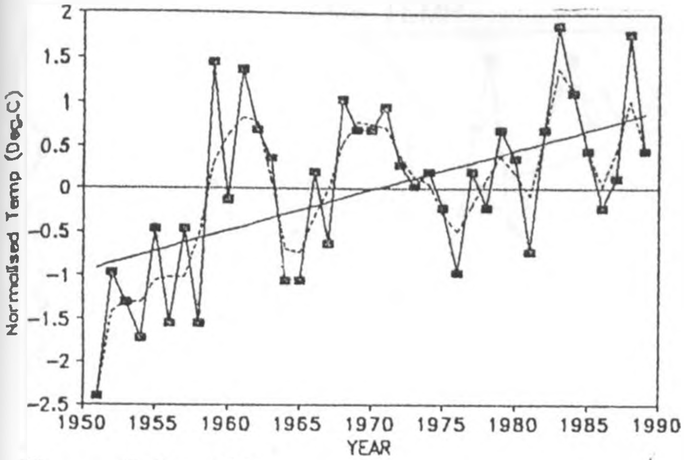

MAX TEMP

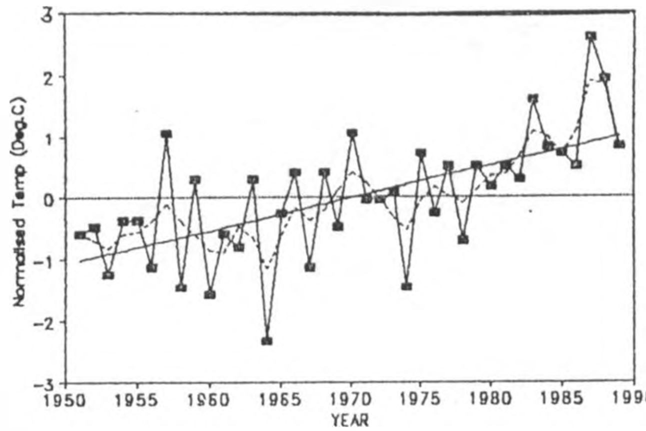

a: NDOLA JULY

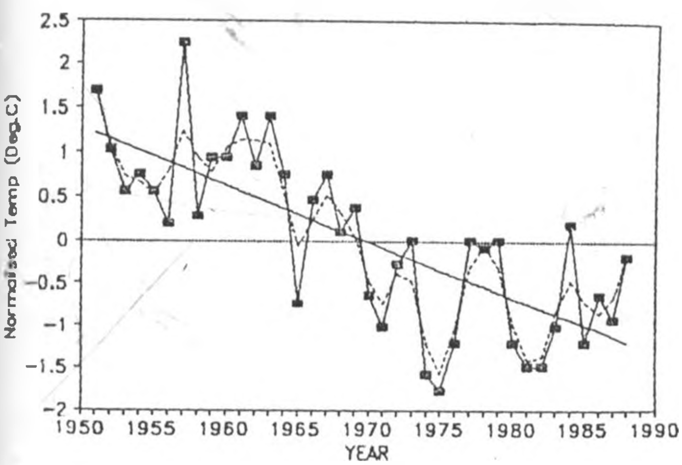

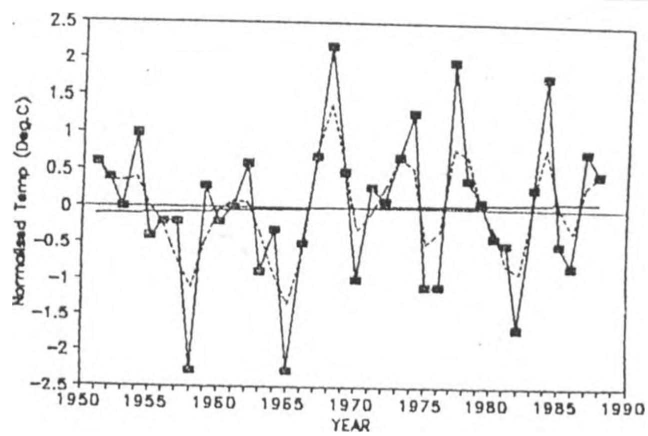

b: LUSAKA **OCT**

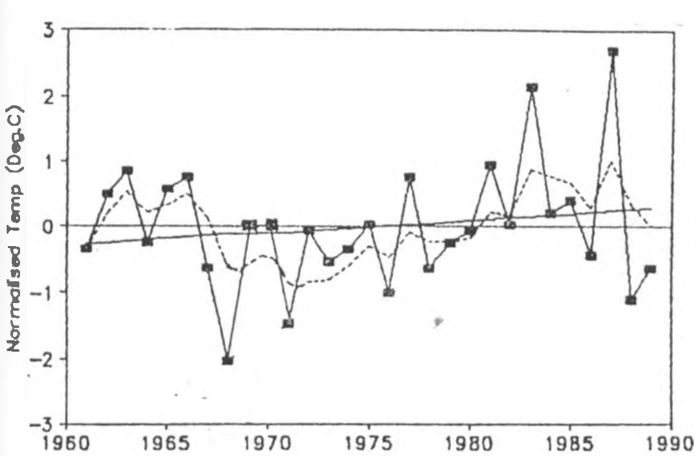

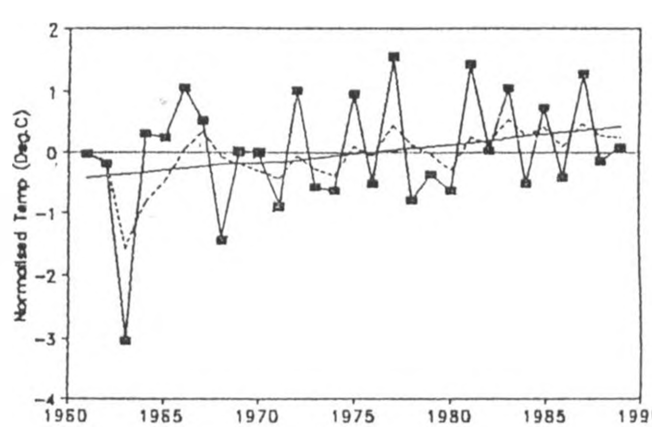

c: MAHALAPYE NOVEMBER

Appendix (ii) continued

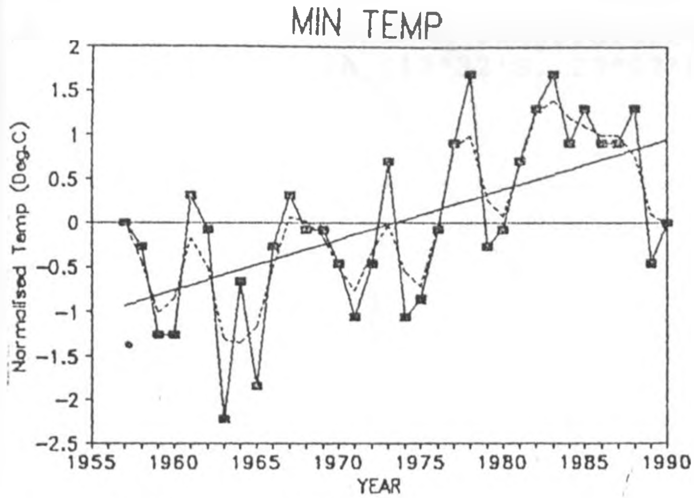

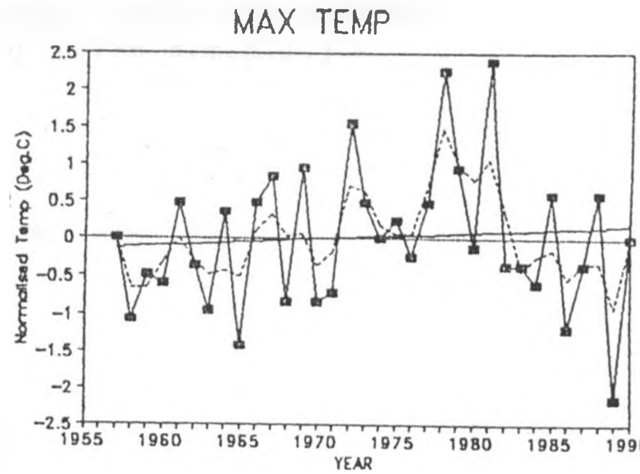

d: NAMPULA JANUARY

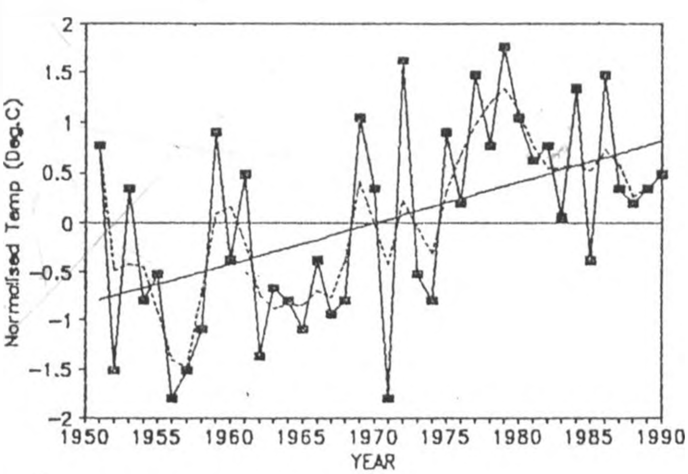

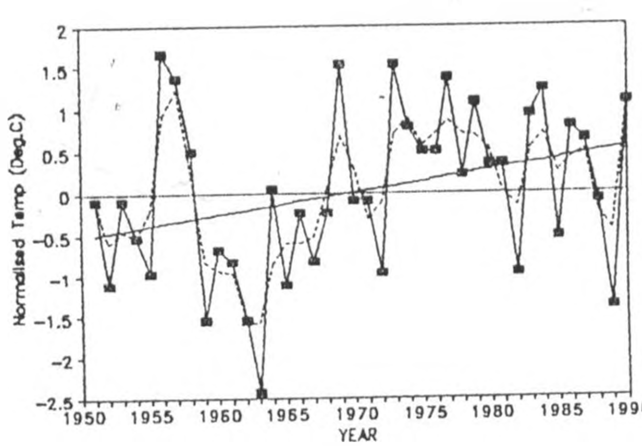

e: PLAISANCE NOVEMBER

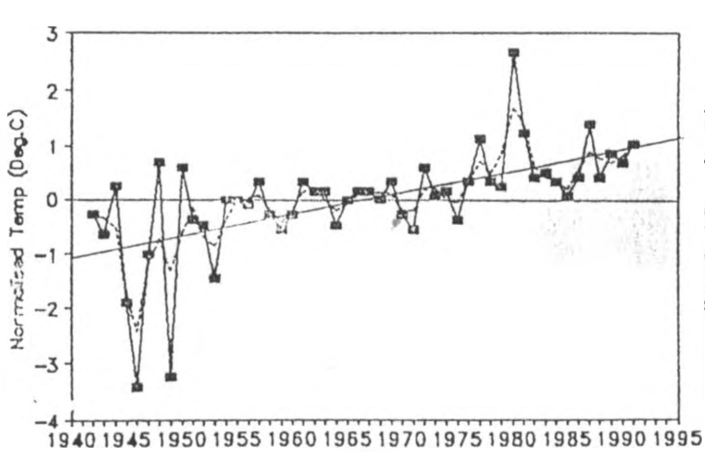

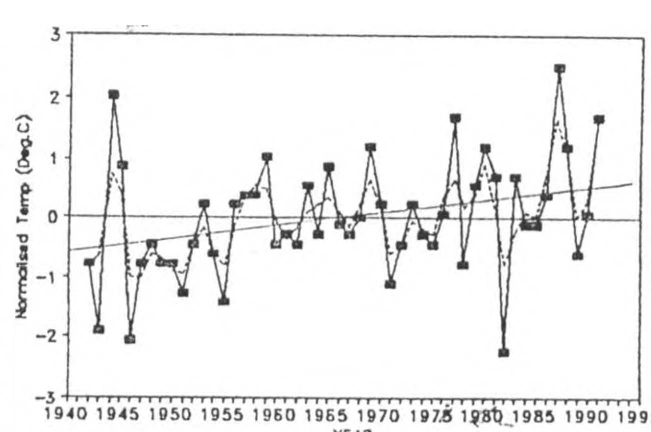

f: WAJIR NOVEMBER

Appendix ii: Minimum temperature time series for Zambezi in Zambia (13°32'S, 23°07'E; 1077m a.m.s.l.)

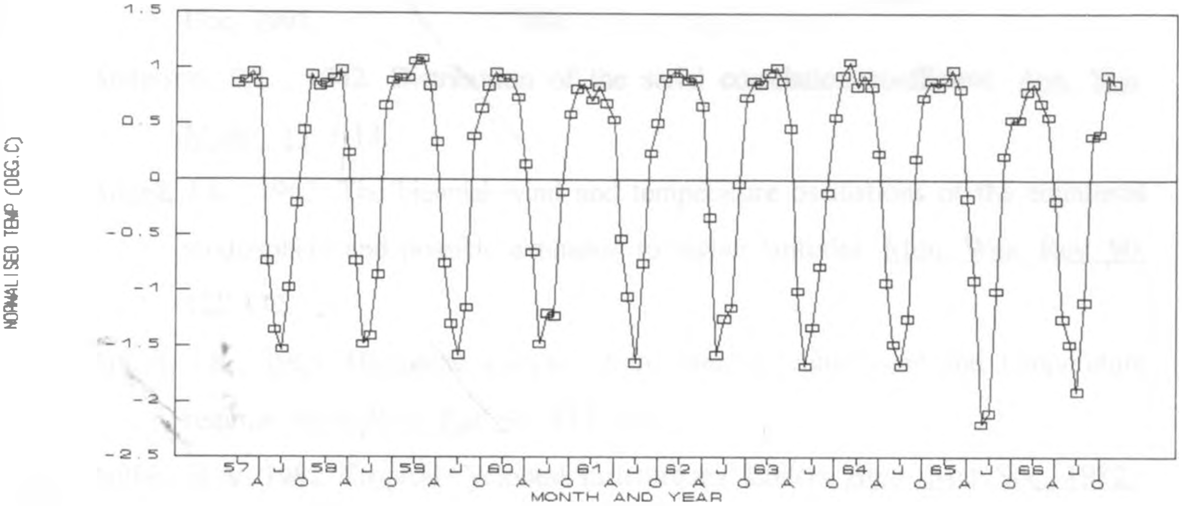

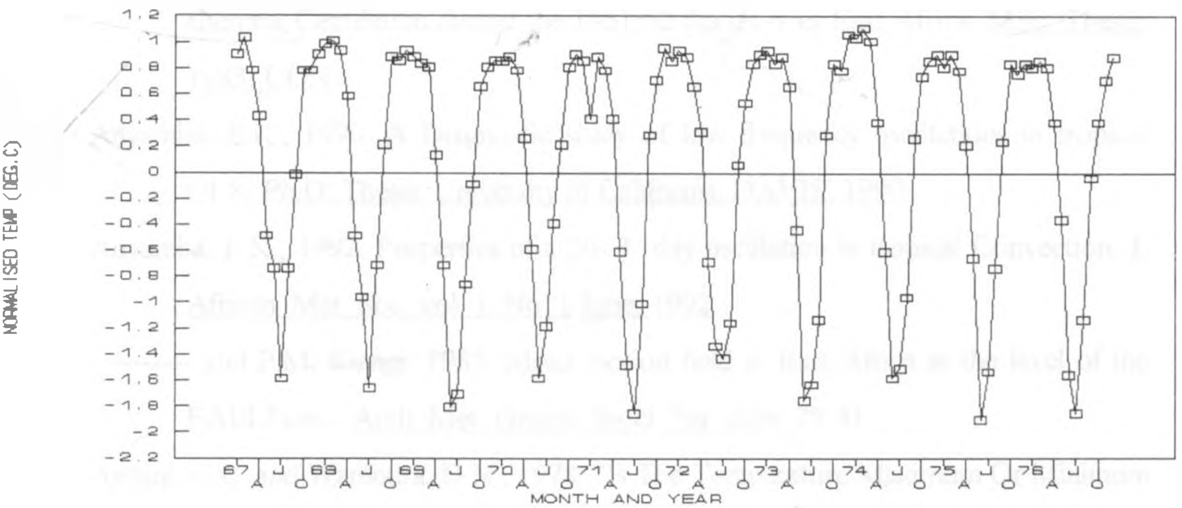

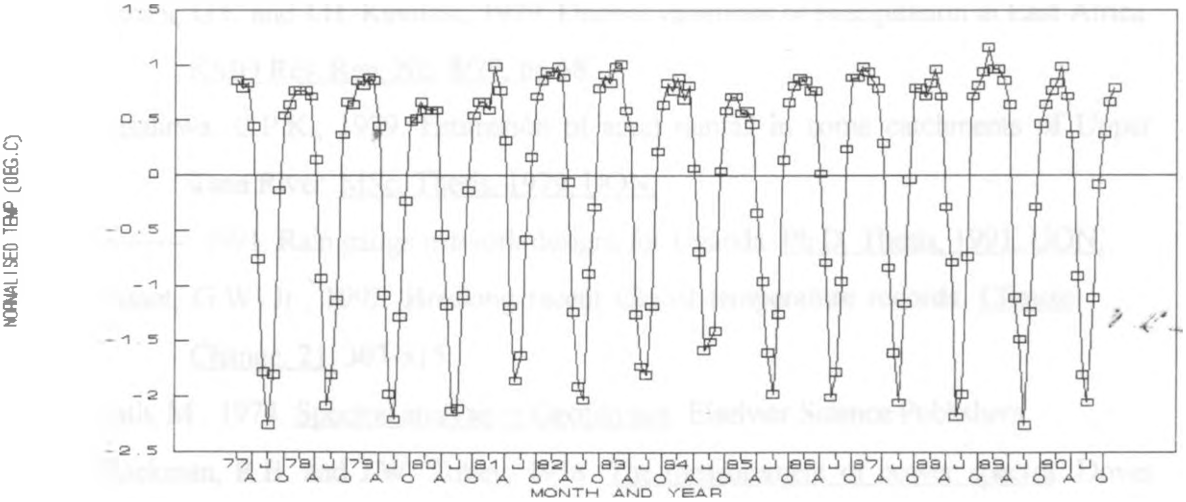

REFERENCES

Akaike, H., 1970. Statistical predictor identification. Ann. Stat. Math. 22, 203-17.

---------, 1974. A new look at the statistical identification. IEEE. Ac. 6, 661-75.

Alusa, A. and M. Allen, 1991. The role of the Tropics in climate change. Impact No. 3, Dec, 1991.

Anderson, R.L., 1942. Distribution of the serial correlation coefficient. Ann. Stat. Math. , 13, 1-13.

Angell, J.K., 1962. The biennial wind and temperature oscillations of the equatorial stratosphere and possible extension to higher latitudes. Mon. Wea. Rev. 90. 127-132.

Angell, J.K., 1963. Harmonic analysis of the biennial zonal wind and temperature regimes. Mon. Wea. Rev. 91, 537-548.

Anthes, R.A., 1982. Tropical Cyclones- structure and Effects. Amer. Met. Soc., 1982.

Anyamba, E.K., 1983. On the monthly mean lower tropospheric Circulation and the aberrant Circulation during the 1961/62 floods over East Africa. MSc. Thesis. 1983. UON.

Anyamba, E.K., 1990. A Diagnostic study of low frequency oscillations in tropical OLR. Ph.D. Thesis. University of California. DAVIS. 1990.

Anyamba, E.K., 1992. Properties of a 20- 3- day oscillation in tropical Convection. J. African Met. Soc. vol. 1. No. 1 June. 1992.

---------- and P.M. Kiangi, 1985. Mean motion field in East Africa at the level of the EALLJ core. Arch. Met. Geoph. Biocl. Ser. B36, 29-41.

Asnani, G.C. and Wambura, D.N., 1978. "Is The Temperature Maximum Or Minimum Over The Equator ?". EAMD Research Report No: 4, 1978.

Asnani, G.C and J.H. Kinuthia, 1979. Diurnal variations of precipitation in East Africa. KMD Res. Rep. No. 8/79. pp 58.

Basalirwa, C.P.K., 1979. Estimation of areal rainfall in some catchments of Upper Tana River. MSc. Thesis. 1979. UON.

---------, 1991. Rain gauge network designs for Uganda. Ph.D. Thesis. 1991. UON.

Basset, G.W. Jr., 1992. Breaking recent Global temperature records. Climate Change. 21, 303-315.

Bath, M., 1974. Spectral analysis in Geophysics. Elselvier Science Publishers.

Blackman, R.B. and J.W. Tukey, 1958. The measurement of power spectra. Dover publ. 190 pp. N. York.

Bolt, B.A., R.G. Currie, 1974. ME estimates of the earth's torsional eigen periods. Geoph. J. Roy. Astron. Soc. 40, 107- 114.

Box, G.E.P. and Jenkins, G.M., 1976. Time series analysis: Forecasting and control. Holden- Day, 5785pp.

Brower, R.L, H.S Gohrband, W.G. Pichel, T.L. Sigmore and C.C. Walton, 1976. Satellite derived SST from NOAA space- craft. NOAA Tech. memo NESS 78, 74pp.

Budyko, 1990. Predictions Based on Past and Current Analogues- 2nd World Climate Conference Proceedings. Geneva Switzerland, 1990.

Bunker, A.F., 1965. Interactions of the summer monsoon air with the Arabian sea. Symp. on met. Results of the Indian ocean exp. Bombay, 7-9. Indian Met. Dept. New Delhi.

Bunting, A.H., 1975. Rainfall Trends In The West African Sahel. Quart. J. Roy. Met. Soc. 102, 59-64.

Burg, J.P., 1970. New concepts in power spectra estimation. Soc. Explo. Geoph. New Orleans.

-----, 1972. The relationship between ME and maximum likelihood spectra. Geoph. 37, 375-6.

Burpee, R.W., 1972. The Origin and Structure of Easterly Waves in the Lower Troposphere of west Africa. J. Atm. Sci. 29, 77- 90.

Burpee, R.W., 1974. Characteristics of the North African Easterly waves during summers of 1968 and 1969. J. Atm. Sci. 31, 1556-1570.

Cadet, D. and P. Olory-Togbe, 1977. The Propagation of Tropical Disturbances over the Indian Ocean During the Summer Monsoon. Mon. Wea. Rev. 105, 700-708.

Cadet, D. and G. Reverdin, 1981. Monsoons Over Indian Ocean during Summer 1975- Part I - Mean fields. Mon. Wea. Rev. 109, 143- 158.

Cadet D. and P. Daniel, 1988. Long-range forecasting of the break and active summer monsoon. Tellus, 40A, 133-150.

Callander, G.S, 1938. Artificial production of CO_2 and its effect on temperature. Quart. J. Roy. Met. Soc. 64, 223.

-------, 1961. Temperature Fluctuations and Trends over the Earth. Quart. J. Roy. Met. Soc. 87, 1-12.

Christy, J.R. and R.T. McNider, 1994. Satellite greenhouse warming. NATURE. 367. 325-326.

Chu, P.S. and R. Katz, 1985. Modeling and forecasting the southern Oscillation- A time Approach. Mon. Wea. Rev. 115. 1542-

Cooley, J.W. and J.W. Tukey, 1967. An algorithm for machine calculation of complex fourier analysis. Math. Comp. 19. 297-301.

Currie, R.G., 1974a. Solar cycle signal in surface air temp. J. Geoph. Res. 79. 5657-9.

-------, 1974b. Harmonic analysis of the geomagnetic annual variation. J. Geomag. Geoelect. 26. 319-28.

Davis, H.T., 1963. Analysis of econometric time series. The Principia Press. Trinity Uni., Texas.

Diggle, P.J., 1990. Time Series: A bio-statistical Introduction. Clareder Press- Oxford 1990.

DROUGHT, 1993. Drought Net-work News. News letter of the Int. Drought Info. centre. Vol. 4. No. 3. Oct. 1993.

Druyan, L.M., 1988. Advances in the study of the Sub-Saharan drought. Int. J. Clim., 9, 77-90.

Ellsaesser, H.W., 1986. Global Climate Trends as Revealed by Recorded Data. Rev. Geophysics. 24. 745-792.

Emmanuel, K.A., 1987. Dependence of hurricane intensity on Climate. Nature. 326. 483-485.

Findlater, J., 1968. The Month to Month Variation of winds at low Level over East Africa. EAMD Tech. Memo no. 12. 1968.

Findlater, J., 1969. A major low Level air Current near the Indian Ocean during the Northern Summer. Quart. J. Roy. Met. Soc. 95, 362-380.

Findlater, J., 1977. Observational aspect of the Low level Cross-equatorial Jet-stream of west Indian Ocean. Pure and Applied Geophysics 115. 1251-1262.

Findly, D.F. (Edit). Applied Time Series analysis II. University Of Tulsa, Tulsa, Oklohama.

Fishman, G.S., 1969. Spectral methods in economics. Havard University Press. Mass.

Folland, C.K., T.N. Palmer, and D.E. Parker, 1986. Sahel rainfall based on worldwide sea surface temperatures 1901-1985. NATURE. 320. 602-607.

Forsdyke, A.G., 1960. Synoptic models of the Tropics. Symposium on Tropical Met. in Africa (Proceedings). Munitalp foundation. Nairobi. Kenya. 14-23.

Fremming, D., 1970. Note on an easterly Distribution affecting East Africa, 5-7 Sept 1967. EAMD Tech. Memo No. 3 1970.

Gichuiya, S.N., 1970. Easterly Distribution Of East Africa. E. A. Agricultural For. Journal Volume 23, 179-185.

Glantz, M.H., 1990. Assessing winners and losers in the context of Global Warming. Report of workshop held 18-21 Jun. 1990 at St. Julians, Malta-Nat. Centre for Atm. Res. Boulder, CO.

---------, 1992. Global Warming and Regional Environmental Changes: Winners and losers in Africa. Nat. Cent. for Atm. Res., Boulder, CO. U. S. A.

Gordon, A., 1994. Weekends warmer than week days? NATURE, 367,6.

Granger, C.W.J., 1976. Aspects of analysis and interpretation of temporal and spatial data. Stat., 24, 197-211.

Granger and Hatanaka, 1964. Spectral analysis of economic Time-Series. Princeton University Press. Princeton.

Gray, W.M., 1984. Atlantic seasonal hurricane frequency: Pt. 1, El-Nino and 30 mb QBO influences. Mon. Wea. Rev., 112, 1649- 1683.

Griffiths, J.F., 1972. Climates of Africa. World Survey Of Climatology. Vol. 10. Edited by Landsberg, H.E. Elselvier Publishing Co. Amsterdam- London- New York.

Hansen, J.E. and S. Lebedeff, 1987. Global trends of measured air temps. J. Geoph. Res. 92, 13345- 13372.

______ and ____, 1988. Global air temperatures update through 1987. Geophys. Res. Letters, 15, 323 - 326.

Hastenrath, S., 1983. The glaciers of equatorial Eastern Africa. D. Reidel publ. co. Dordretch- Boston- Lancaster.

---------,1985. Climate and circulation of the Tropics. D. Reidel publ. co. Dordretch- Boston- Lancaster-Tokyo.

---------, 1986. On the climate predictability in the tropics. Bull. Amer. Met. Soc. 67, 696-702.

Helms, H.D., 1967. FFT of computing difference equations and simulating filters. IEEE, AU15, 45pp.

Herman, O., 1971. On the approximation problem in non-recursive digital filter design. Ibid, CT 18, 411-13.

IMPACT, 1992-5. Impact. Newsletter of the Climate Network Africa. No. 5, June 1992.

IPCC, 1990a. Climate Change - Scientific Assessment. WMO/UNEP.

IPCC, 1990b. Climate change: The IPCC impacts assessment-WGII final report. Edit. Teggart, W.J.M., G.W. Sheldon, and D.C. Griffith. WMO/UNEP.

IPCC, 1992a. Climatic Change: The Supplementary Report To the IPCC Scientific Assessment- WMO/UNEP.

IPCC, 1992b. IPCC Supplement: Scientific Assessment Of Climate Change- WMO/UNEP.

Jagannathan, P., 1973. Trends and Periodicities of Indian Rainfall. Mon. Wea. Rev. 101, 371-375.

Jenkins, G.M. and D.G. Watts, 1968. Spectral analysis and its applications. Holden-Day.

Jenkinson, A.F., 1977. A powerful elementary method of spectral analysis for use with meteorology.

Jianping, X., Z. Guangze, Q. Kangmu, F. Zongyi, X. Qianguang, W. Rongcheng, S. Ziyu, 1990. A course of the WMO workshop on satellite met. Edited by the Satellite Met. Centre, China Meteorological Press.

Johnson, D., 1962. Rain In E. Africa. Quart. J. Roy. Met. Soc. 88, 1-19.

Johnson, D.H. and H.T. Morth, 1960. Forecasting research in East Africa. Proc. of symp. on tropical Met. in Africa. Munitalp Foundation, Nairobi-Kenya.

Jones, R.H., 1975. Estimating the variance of time averages. J. Appl. Met. 14, 159-163.

Jones, P.D., 1986a. Northern Hemisphere Surface Air Temperature Variations 1851-1984. J. Clim. Appl. Met. 25, 161-179.

________, 1986b. Southern Hemisphere Surface Air Temperature Variations 1851-1984. J. Clim. Appl. Met. 25, 1213- 1230.

Joseph, E.S., 1973a. Time Series Analysis of Annual Temperatures. Mon. Wea. Rev. 101, 501-504.

Joseph, E.S., 1973b. Spectral Analysis of Daily Maximum and Minimum Temperatures Series on the East Slopes of Col. Front Range. Mon. Wea. Rev. 101, 505-509.

Jury, and Pathack, 1991. A study of climate and weather variability over Tropical south west Indian ocean. Met. and Atm. Phys., 47, 37-48.

Karl, T.R., G. Kukla, J. Gavin, 1984. Decreasing Diurnal Temperature Range In The US and Canada 1941-1980. J. Clim. Appl. Met. 23, 1489-1504.

Karl, T.R., C.N. Williams, P.J. Young and W.M. Wendland, 1986. A model to Estimate the Time of Observation Bias associated with Monthly Mean Maximum Minimum and Mean Temperatures for the US. J. Clim. Appl. Met. 25, 145- 160.

Karl, T.R., H.F. Diaz and G. Kukla, 1988. Urbanization: Its detection and effect in the US climatic record. J. Clim. 1, 1099- 1123.

Karl, T.R., G. Kukla, V.N. Razuvayer, M.J. Changery, R.G. Quayle, R.R. Heim, D.R. Easterling and C.B. Fu, 1991. Global Warming: Evidence for asymmetric diurnal temperature change. Geoph. Res. Lett., 18, 2253-56.

Katz, R.W. and B.G. Brown, 1992. Extreme events in a changing variability is more important than averages. Clim. Change, 21, 289-302.

Katz, R.W. and R.H. Skaggs, 1981. On the Use of auto-regressive MA process to Model Meteorological time series. Mon. Wea. Rev. 109, 479-484.

Kay, S.M. and S.L. Marple, 1981. Spectrum analysis: A modern perspective. Proc. IEEE, 69, 1380-1419.

Kendall, M.A., 1961. The advanced theory of statistics-vol. 3. Design and analysis and time series. Charles Griffin and co. ltd.- London.

Kinuthia, J.H., 1991. Wind study in northern Kenya (Turkana channel). KMD Res. Rep. no. 1/91.

Kinuthia, J.H., P.D. Munah, C.K. Kahoro, 1991. Kenya warming since the mid-1960's. Impact, No. 3, Dec. 1991.

Krishnamurti, T.N., J. Molinari, and H.L. Pan, 1976. Numerical simulation of the Somali jet. J. Atm. Sci., 33, 2350-62.

Kukla, G. and T.R. Karl, 1992a. Recent rise in night-time temperatures in the N.H. Dept. Of Energy(DOE) Research Summary no. 14, Jan, 1992.

------ and -----, 1992b. Night time temps. in the N.H. CDIAC comms. 1992 summer issue.

Lacoss, R.T., 1971. Data adaptive spectral analysis methods. Geoph. 36, 661-75.

Landsberg, H.E., 1959. Power spectrum analysis of climatological data for Woodstock college-Maryland. Mon. Wea. Rev. 87, 283- 298.

--------, 1963. Surface signs of the biennial atmospheric pulse. Mon. Wea. Rev. 91, 549-556.

Malone, T.F., 1951. Compendium of Met.- American Meteorological Society. Edited by T.F. Malone. Boston, Massachusetts.

Maronna, R. and V.J. Yohai, 1978. Bivariate test for the detection of a systematic change in the mean. J. Atm. Ass., 73, p640.

Masaya, 1975. Spectral analysis of rainfall series in Kenya. Manuscript; Economics Dept. UON.

McClaim, E.P., W. Pichel, C. Walton, A. Ahmed and J. Sultan, 1982. Multi- channel improvements to satellite derived global SSTs. Report XXIV, COSPAR Ottawa, Canada, 22-29 May, 1982.

Medden, R.A., 1977. Estimation of auto-covariances and spectra of seasonal mean temps over N. America. Mon. Wea. Rev. 40, 1-2.

Mitchell, J.M., 1961. The measurement of secular temperature change in the US. Research paper no. 43, US weather bureau, 80pp. Washington D.C.

Morel, P., 1993. Climate Change Bulletin Vol. 1, Issue 1, 3rd Quarter, 1993.

Moura, A.D., 1993. Global Change News letter No. 13, March, 1993.

Nakamura, K., 1966. The city temperature of Nairobi. J. Geog. Jap. 75, 316-317.

-------, 1967. Climate of East Africa as related to equatorial westerlies. Rep. of Tokyo Metropolitan Uni. no. 2, pp 49- 69.

Newell, N.E, R.E. Newell, J. Hsiung, and Z. Wu, 1989. Global marine temperature variation and solar magnetic cycle. Geoph. Res. Lett., 16, 311-314.

Ngara, T. 1977. Some aspects of the EALLJ. MSc. thesis, UON.

Nichols, N., 1984. The SO, SST, and inter-annual fluctuations in Australian tropical cyclones activity. J. Clim., 4, 661 -70.

Nicholson, S.E., 1989a. Long term changes in African rainfall. Weather, 44, 46-55.

--------, 1989b. African drought: Characteristics, causal theories, and global teleconnections. Geoph. Monogr., 52, 79-100.

------ and D. Entekhabi, 1986. Rainfall variability in equatorial and southern Africa: Relationship with SSTs along the S.W. coast of Africa. J. Clim. Appl. Met., 26, 561-578.

Njau, L.N., 1982. Tropospheric wave disturbances in East Africa. MSc. thesis, Dept. of Met. UON, 1982.

Norquist, D.C., 1976. A diagnostic study of the energetics of African wave disturbances. MSc. thesis, Dept. of Atmo. Sci., Uni. of Washington, 1976.

------, E.E. Recker, and R.J. Reed, 1977. The energetics of the African wave disturbances as observed during Phase III of GATE. Mon. Wea. Rev., 105, 317-333.

Nyenzi, B.S., 1988. Mechanisms of East African rainfall variability. Ph.D. dissertation. 1988. FSU. Tallahassee. FL. U.S.A.

-------, 1992. Analysis of the inter-annual rainfall variability over E. Africa. J. African Met. Soc. vol 1. no. 1.

Ogallo, L.A.J, 1977. Periodicities and trends in the annual rainfall over Africa. MSc. thesis. 1977. UON.

Ogallo, L.A.J., 1979. Rainfall variability in Africa. Mon. Wea. Rev.. 107. 9. 1122-1139.

Ogallo, L.A.J., 1980. Time series analysis of rainfall in East Africa. Ph.D. thesis. 1980. UON.

Ogallo, L.A.J., 1983. Temporal fluctuations of seasonal rainfall patterns in E. A. MAUSAM 35. 2. 175-180.

Ogallo, L.A.J., 1992. Temperature and rainfall variability/ changes over the SADCC region. (Presented at the 1st SADCC conference on climate change; March, 2-6, Windhoek, Namibia).

Ogallo, L.A.J., 1993a. Dynamics of the East African climate. Proc. Indian Academy Sci. (Earth planet sc.) vol. 102. No. 1. March. 1993. 203- 217.

Ogallo, L.A.J., 1993b. Climate change signals over Eastern and southern Africa. (Presented at 3rd Technical conf. on Met. Research in East and Southern Africa, Feb, 1993).

Ogallo, L.A.J. and J.N. Aliba, 1994. Spatial and inter-annual patterns of the surface temperatures over East Africa. (Submitted for publication).

Ogallo, L.A.J., R.E. Okoola and D.N. Wanjohi, 1994. Characteristics of the QBO over Kenya and their predictability potential for the seasonal rainfall. MAUSAM. 1. 1. 57-62.

Okumu, A.M., 1985. Study of the features of the Somali current along the coast of East Africa. MSc. thesis. 1985. UON.

Okoola, R.E., 1979. The Nairobi heat island. Res. rep. no. 4. 1979. Kenya Met. Dept.

Okoola, R.E., 1983. Monsoon system over S.W. Indian ocean during northern summer of 1979. MSc. thesis. 1979. UON.

Pan, Y-H., and Oort, 1983. Global climate variations connected with sea surface temp. anomalies in the eastern equatorial Pacific ocean, 1958-1973 period. Mon. Wea. Rev. 111, 1244- 1258.

Panofsky, A.H. and G.W. Brier, 1958. Some applications of statistics to met. Pennsylvania State Uni., 1965.

Pant, G.B., K. Rupa, and N.A. Sontakke, 1993. Climate variability over India on century and longer time scales. Adv. Trop. Met., Tata McGraw-Hill, N. Delhi.

Parker, 1990. Effects of changing exposure of thermometers at land stations. Draft contribution to the IPCC WGI, section 7, IPCC, 1990.

Parsatharathy, B. and O.N. Dhar, 1973. Secular variations of regional rainfall over India. Quart. J. Roy. Met. Soc. 100, 245-257.

Polowchak, V.M., 1968. The spectrum of daily temperature as a climatic indicator. Mon. Wea. Rev. 96, 596-600.

Priestly, M.B., 1962. Basic considerations in the estimation of spectra. Technom., 4, 55pp.

Rabiner, L.R., C. McLellan, and T.W. Parks, 1975. FIR Digital filter design techniques using weighted Chebychev approximation. Proc. IEEE, 63, 593-610.

Rapper, S.C.B., 1990. Climate and sea level change: Observations. properties, Implications. R.A. Warrick and T.M.C. Wigley (Editors). Cambridge University Press.

Rasmusson, E.M., and T.H. Carpenter, 1982. Variations in tropical SST and surface wind fields associated with ENSO. Mon. Wea. Rev. 110, 354-384.

Rennick, M.A., 1976. The generation of the African waves. J. Atm. Sci. 33, 1955-1969.

Rodhe, H. and H. Virji, 1976. Trends and periodicities of East African rainfall. Mon. Wea. Rev. 104, 307-

Salinger, M.J., 1981. New Zealand climate: The instrumental record. Victoria Uni. Wellington. 327 pp.

---------, 1989. New Zealand climate: From ice-age to present. Environmental Monitoring in N. Zealand, 32-40.

Semazzi, F.H.M., V. Mehta, Y.C. Sud, 1988. An investigation of relation between Sub-Sahelian rainfall and global SSTs. Atm.-Ocean 26, 118-138.

Shapiro, R., 1970. Smoothing, filters, and boundary effects. Rev. Geoph. Space Phys., 8, 159-64.

Shumway, R.H., 1988. Applied Statistical Time series analysis. Prentice-Hall, 379 pp.

Siegel, S., 1956. Non-parametric statistics for the behavioral sciences. McGraw-Hill, 313pp.

Simpson, R., H. Riehl., 1951. The Hurricane and its impacts. Basil- Blackwell. Oxford.

Smith, W.L., P.K. Rao, R. Koffler, W.R. Curtis, 1970. Determination of SST from satellite HRIR window radiation measurements. Mon. Wea. Rev. 98, 604- 611.

Solow, A.R. and J.M. Broadus, 1989. On the detection of greenhouse warming. Climatic Change, 15, 5-37.

Sontakke, N.A., G.B. Pant and N. Singh, 1993. Construction of all India summer monsoon rainfall series for the period 1844-1991. J. Clim., 6, 1806-11.

Spencer, R.W., 1993. Global ocean precipitation from MSU during 1979-1991 and comparisons to other climatologies. J. Clim. 6, No. 7, 1301-20.

Stouffer, R.J., Manabe, S. Bryan, K. , 1989. Inter-hemispheric asymmetry in climate response to a gradual increase in CO_2. NATURE, 342, 660-662.

Tarleton, L.F. and R.W. Katz, 1993. Effect of urban heat island on temp. variability and extremes. Reprints 8th conf. Appl. Clim., Amer. Met. Soc. Boston.

Thomson, B.W., 1957. The diurnal variation of precipitation in British East Africa. EAMD Tech. memo. No. 8, 1957.

Troup, A.J., 1965. The southern oscillation. Quart. J. Roy. Met. Soc. 91, 490- 506.

Tyson, P.D., 1984. Climate change and variability in southern Africa. Univ. Press. Cape Town.

-------, 1993. Recent developments in the modeling of the future climate of South Africa. S. Afr. J. Sci. 89, 1993.

------, T.G.J. Dyer, and M.N. Mametse, 1975. Secular changes in South African rainfall. Quart. J. Roy. Met. Soc. 101, 817-833.

Ulrych, T.J. and T.N. Bishop, 1975. Maximum entropy spectral analysis and AR decomposition. Rev. Geoph. Space Phys., 13, 183-200.

UNEP, 1985. Environmental assessment of the Ozone layer modification. Bull. no. 9, Jan 1985-UNEP.

UNEP, 1987. The Ozone layer. UNEP/GEMS envir. lib. no. 2.

UNEP, 1989. Action on Ozone. UNEP, 1989.

UNEP, 1991. Climate Sys. Monitoring (CSM). Sept. 1991-UNEP/WMO.

UNEP, 1992a. Climate Sys. Monitoring (CSM)-ENSO Diagnostic Advisory -Special issue, Jan. 1992-UNEP/WMO.

UNEP, 1992b. Climate Sys. Monitoring (CSM). Feb. 1992-UNEP/WMO.

Valadon, Y., 1992. Variability of tropical cyclones over S.W. Indian ocean. J. Afr. Met. Soc., Vol. 1, No. 1, 45-51.

Van Loo and J. Williams, 1976. Connection between trends in mean temperature and circulation at surface. Pt. I- Winter. Mon. Wea. Rev. 104, 365-380.

Vinnikov, K.Ya, 1990. The empirical data on modern global climate changes. (temp. and precipitation). J. Clim., 3, 1990

............., P. Ya. Groisman, K.M. Lugina, and A.A. Golubev, 1987. Variations in northern hemisphere mean surface air temperatures over 1881-1985. Met. and Hydro. 1, 45-53.

Wald, A. and J. Walfowitz, 1943. An exact test of randomness in non-parametric cases based on serial correlations. Ann. Math. Stat. 14, 378-88.

Winstanley, D., 1973. Recent rainfall trends in Africa, Middle East, and India. NATURE 243, 464-465.

WMO, 1966. TECHNICAL NOTE NO. 79. Climate change. WMO-no. 195. TP. 100.

WMO, 1967. A note on climatological normals. TECHNICAL NOTE NO. 84.

WMO, 1981. Guidelines to hydrological practices. Data acquisition and processing. WMO No. 168.

WMO, 1985. Atm. Ozone. WMO Global O_3 Research and monitoring Project- Report no. 16. Vol. III.

WMO, 1986. Guidelines on quality control of surface climatological Data. WCP-85. WMO/TD, 56pp.

WMO, 1992. PRESS RELEASE-OZONE LEVELS IN THE ANTARCTICA. WMO No. 486 15-09-92.

WMO, 1992b. Global Climate Monitoring. December 1988 - May 1991. WMO.

WMO, 1993. WMO annual Report, 1993. WMO No. 800.

Wolter, K., 1989. Models of tropical circulation, SO, and Sahel rainfall anomalies. J. Clim., 2, 149-172.

Wood, C.A. and R.R. Lovett, 1974. Rainfall, drought and the solar cycle. NATURE, 251, 594-96.

Yasunari, T., 1980. A quasi-stationary appearance of 30-40 day period in cloudiness fluctuations during the summer monsoon over India. J. Meteo. Soc. Jap., 58, 225-9.

Zangvil, A., 1975. Temporal and spatial behaviour of large scale disturbances in tropical cloudiness deduced from satellite brightness data. Mon. Wea. Rev. 103, 904-920.